Democratic and Popular Republic of Algeria

Ministry of Higher Education and Scientific Research

University Mohamed Khider of Biskra

Faculty of Exact Sciences and Science of Nature and Life

Department of Material Sciences

Thesis

Presented to obtain the degree of

Doctorate

Speciality: Physics of thin films

Elaboration and characterization of thin layers of zinc oxide (ZnO) deposited by ultrasonic spray for photovoltaic and optoelectronic applications

Presented by:

BENKHETTA YOUCEF

Publicly defended on: / / 2019

To the Jury composed by:

M^{r}. N. Attaf	Professor	University of Cons1	President
M^{r}. A. Attaf	Professor	University of Biskra	Supervisor
M^{me}. H. Saidi	MCA	University of Biskra	Co-Supervisor
M^{r}. S. Rahmane	Professor	University of Biskra	Examiner
M^{r}.M. L. Benkhedir	Professor	University of Tebessa	Examiner

Acadymic year 2018-2019

Dedication

I dedicate this thesis

To my wife who supported me to make this work easier

To all my family

To all my friends

YOUCEF

Acknowledgements

It was for me a great chance to be able to prepare this thesis with laboratory of the thin films of our university, which I have to achieve it thanks to the contribution of a great number of persons, and that no matter what I say, I will never be able all as much them to thank. But before that I thank GOD the whole powerful for having agreed his infinite kindness, courage, the force and patience to complete this modest work. After that, I make a point of profoundly thanking to my director for thesis Mister **ATTAF Abdallah**, *Professor at the Department of sciences of matter at Faculty of Exact Sciences and Sciences of Nature and Life in Mohamed KHIDER University, Biskra, for his confidence that he testified to me during this work, for his support and its councils, accompanied me with the daily in the preparation by this work with greatest assiduity, and to devote necessary time to discussions and human remarkable qualities, and his daily presence was a major asset for the realization of this work, as well from a scientific point of view as moral, thanks to him my efforts was leaded. I express my deep gratitude has Mister* **ATTAF Nadhir**, *Professor at the Department of physics in Constantine.1 University for the honor that makes to me by accepting the presidency of this jury.*

My sharp thanks to:

M^me^ Hanane Saidi *Professor at the Department of sciences of matter in Med university of Biskra who agreed to agree to belong to the jury and to examine my work .***M´ Rahmane Saad** *Professor at the Department of sciences of matter in Med university of Biskra, who agreed to accept to belong to the jury and to examine my work.* **M´ Mohamed Lotfi Benkhedir** *Professor in university of Tebssa who agreed to agree to belong to the jury and to examine my work.*

I address to my sincere thanks to all the teachers of the department of sciences of matter especially the teachers of physics, everyone by his name, for all for their advised councils and their continuous encouragement. I to also thank my friends in the laboratory of thin films whom with them I have realized this work. To all my friends with whom I divided so many moments of life, content and difficult, and who helped me to cross certain tests during this period.

Contents

General introduction

Zinc oxide, with the formula ZnO, is an inorganic compound which presents in the earth's crust as the mineral zincite [1]. It is not a novel material for scientific study, and has been widely used in industry. ZnO can be found in numerous materials and products as an additive including plastics, ceramics, glass, cement, rubber, paint, adhesives, sealants and pigments [2]. In these traditional applications, ZnO is valued for its ultra-violet (UV) absorbance, piezoelectricity and luminescence at high temperatures. It is even added to food such cereals as the source of Zn nutrient.

As a semiconducting material, ZnO was first studied as early as 1930 [3], and research focused on bulk ZnO growth, characterizations and applications had rapidly grown since then. By the end of the twentieth century, ZnO had been widely used in semiconductor industry as varistors operated at elevated temperatures or high voltages [4], and as ultrasonic transducers in high-frequency regions [5].

The methods employed for thin oxide film deposition can be divided into two groups based on the nature of the deposition process. The physical methods include physical vapour deposition (PVD), laser ablation, molecular beam epitaxy, and sputtering. The chemical methods comprise gas phase deposition methods and solution techniques. The gas phase methods are chemical vapour deposition (CVD) [6,7] and atomic layer epitaxy (ALE) [8], while spray pyrolysis [9], sol-gel [10], spin- [11] and dip-coating [12] methods employ precursor solutions.

Spray pyrolysis is a processing technique to prepare dense and porous oxide films, ceramic coatings, and powders. Unlike many other film deposition techniques, spray pyrolysis represents a very simple and relatively cost-effective method, especially regarding equipment cost. Spray pyrolysis does not require high quality substrates or chemicals. The method has been employed for the deposition of dense films, porous films, and for powder production. Spray pyrolysis has been used for several decades in the glass industry [13] and in solar cell production to deposit electrically conducting electrodes [14].

Chapter one presents a review of thin films and growth modes. Then, we talk about zinc oxide (ZnO), the properties and their applications.

Chapter two presents a review of spray pyrolysis and the characterization techniques employed on the films are also described at the end of this chapter.

Chapter three contains an interpretation of the solution flow rate effect on ZnO thin films properties deposited using zinc acetate as precursor.

Chapter four talk about of the effect of substrate temperature on structural, optical and electrical properties of ZnO thin films.

We studied the influence of tin doping concentration and annealing temperature on ZnO thin films properties in chapter five. Finally we move general conclusion and future work.

The objective of this work is to study the structural, morphological, optical and electrical properties of ZnO thin films prepared by ultrasonic spray process (USP).

To this end, we want to fix the optimal parameters which are represented in solution flow rate, solution concentration, and annealing temperature. These parameters make the thin films of ZnO appropriate to optoelectronic and photovoltaic applications (gas sensors, solar cells…etc)

Chapter I

Review of thin films, Zinc Oxide Properties and their Applications

I.1. Introduction

This chapter includes a description of thin films growth at different modes. The different properties of zinc oxide such as structural, optical and electrical are reviewed in this chapter. Applications of zinc oxide are discussed towards the end of the chapter.

I.2 Thin films growth process

Thin films are deposited on a substrate by thermal evaporation, chemical decomposition, and/or the evaporation of source materials by the irradiation of energetic species or photons. Any thin-film deposition process involves three main steps:

1. Production of the appropriate atomic, molecular, or ionic species.
2. Transport of these species to the substrate.
3. Condensation on the substrate, either directly or via a chemical and/or electrochemical reaction, to form a solid deposit.

The unit species, on impacting the substrate, lose their velocity component normal to the substrate (provided the incident energy is not too high) and are physically adsorbed on the substrate surface.The adsorbed species are not, initially, in thermal equilibrium with the substrate initially and move over the substrate surface. In this process, they interact among themselves forming bigger clusters.

The clusters or the nuclei, as they are called, are thermodynamically unstable and may tend to desorb in time, depending on the deposition parameters. If the deposition parameters are such that a cluster collides with other adsorbed species before getting desorbed, it starts growing in size. After reaching a certain critical size, the cluster becomes thermodynamically stable and the nucleation barrier is said to have been overcome. This step involving the formation of stable, chemisorbed, critical-sized nuclei is called the nucleation stage.

The critical nuclei grow in number as well as in size until a saturation nucleation density is reached. The nucleation density and the average nucleus size depend on a number of parameters such as the energy of the impinging species, the rate of impingement, the activation energies of adsorption, desorption, thermal diffusion, and the temperature, topography, and chemical nature of the substrate. A nucleus can grow both parallel to the substrate by surface diffusion of the adsorbed species, and perpendicular to it by direct impingement of the incident species. In general, however, the rate of lateral growth at this stage is much higher than the perpendicular growth. The grown nuclei are called islands. The next stage in the process of film formation is the coalescence stage, in which the small islands

start coalescing with each other in an attempt to reduce the substrate surface area. This tendency to form bigger islands is termed agglomeration and is enhanced by increasing the surface mobility of the adsorbed species,

Larger islands grow together, leaving channels and holes of uncovered substrate. The structure of the films at this stage changes from discontinuous island type to porous network type. Filling of the channels and holes forms a completely continuous film [5].

I.3 Growth modes

In the early stage of research on thin films, it soon became clear that it was imperative to understand the mechanisms, which control and define the growth of thin films to achieve good control over these novel materials. Hence the huge effort of the scientific community to characterize, optimize and understand film growth.

Evidently, thin films are composed of atoms, which are their zero-dimensional building blocks. Extending this concept, nanoparticles (also termed 'nano-crystals') can also serve as zero-dimensional building blocks which by self-assembly may form two-dimensional thin films or three-dimensional crystals (so-called 'nanoparticle super-lattices'), analogous to atomic films and crystal lattices[15,16,17].

Atomic thin film growth is understood to occur in form of three basic growth modes, which result from competing energy terms during the film deposition, i.e. Frank van der Merwe, Stranski-Krastanov, and Volmer-Weber growth. Various processes occur when atoms arrive at a substrate during thin film growth. That is adsorption, desorption, diffusion, finding or leaving of equilibrium positions. These processes occur simultaneously averaged over the ensemble of arriving atoms [18, 19, 20].

As in the case of atoms, the interplay of various free energy terms determines the way on how the nanoparticles (NPs)films will grow. These are in detail [21]: an entropic contribution E_{TS}, an inter-particle energy term E_p, summing up all relevant types of interactions between NPs[22], and a NP-to-substrate interaction energy E_s. A further important factor is the diffusion energy barrier, E_d, which can be overcome by 'thermal' energy $k_B T_s$. Hereby T_s is a quantity comparable to a substrate 'temperature', which precise physical meaning still needs to be understood for NP systems.

Depending on the relative magnitudes of E_d and k_BT_s the NPs will either stay fixed at one place once they are attached to the substrate or move freely to seek energetically more favorable locations considering the two extreme cases.

From a comparison of these free energy terms one finds[20, 21] that three different growth modes follow: in the case where NP-to-substrate energy, Es, dominates a layer-by-layer growth is found, viz. the so-called Frank-van-der-Merwe growth mode (FvdM). This case is depicted in Fig.I.1. Once a stable cluster (or 'nucleus') of NPs is formed, the following NPs prefer to attach at the periphery of the nucleus in contact with the substrate.

Accordingly this leads to the advancement of planar film growth [21]. Depending on the ratio of Ed and k_BT_s (i.e. the mobility of NPs) one will either obtain polycrystalline or single-crystalline superlattices. In the first case, the immobility of NPs leads to the nucleation of many independent superlattice crystallites, while, in the other case, the large mobility enables the NPs to seek equilibrium positions and hence promotes single-crystal growth.

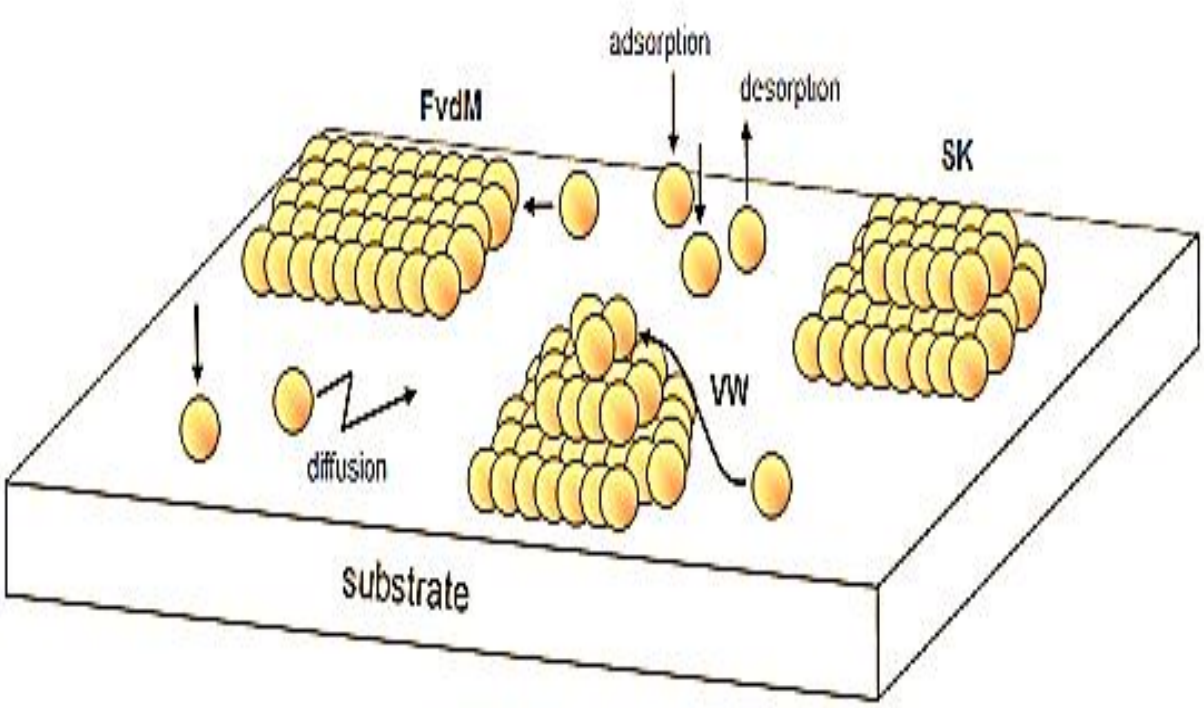

Fig.I.1. Schematic representation of the three known film growth modes[20].

I.4 Zinc oxide

Zinc Oxide is a II - VI compound semiconductor. It exists in natural form, under the name of "Zincite", but can also be synthesized artificially in solid form "ZnO bulk" with different colors depending to the impurities that it contains (Fig.I.2) [22].

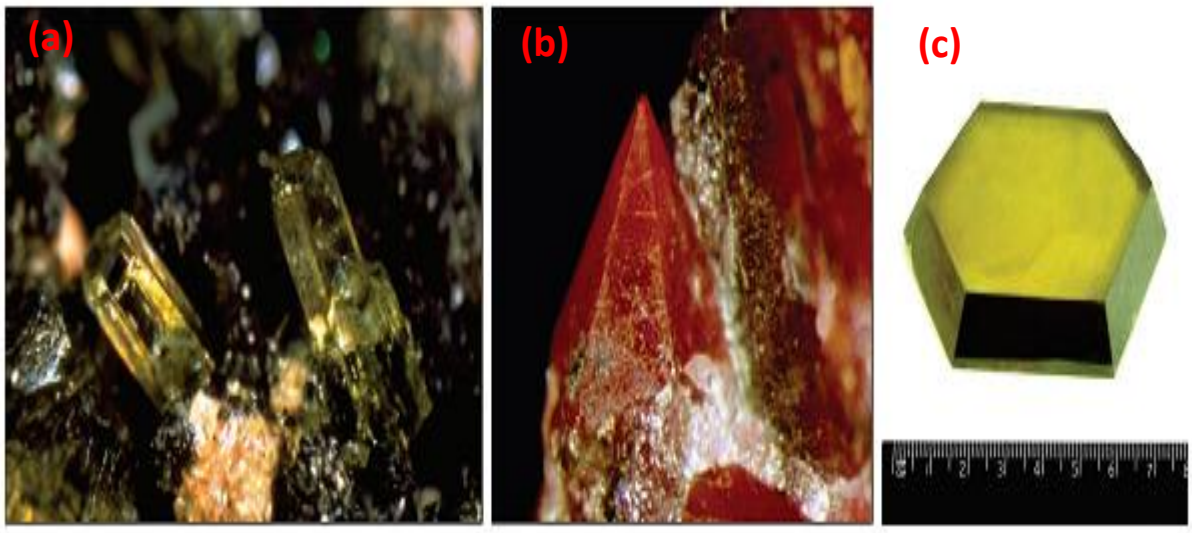

Fig.I.2.ZnO bulk in natural form (a) and (b) and from hydrothermal synthesis (c).

Most of the group II–VI binary compound semiconductors crystallize in either cubic zinc blende or hexagonal wurtzite (Wz) structure where each anion is surrounded by four cations at the corners of a tetrahedron, and vice versa. This tetrahedral coordination is typical of sp3 covalent bonding nature; but these materials also have substantial ionic character that tends to increase the band gap beyond the one expected from the covalent bonding [23].

I.4.1Structural properties

ZnO has a hexagonal close packing (HCP) structure called wurtzite. The structure of ZnO consists of alternating planes composed of O^{2-} and Zn^{2+} ions, which are tetrahedrally coordinated and stacked along the c-axis on an alternate basis (Fig. I.3). In addition, there are other structures such as cubic zinc blende and rock salt. Among them, wurtzite structure is the most common ZnO phase at ambient pressure and temperature [24].The zinc oxygen bond length is 0.1992 nm parallel to the c - axis and 0.1973 nm inthe other three directions of the tetrahedral arrangement of nearest neighbours [25].

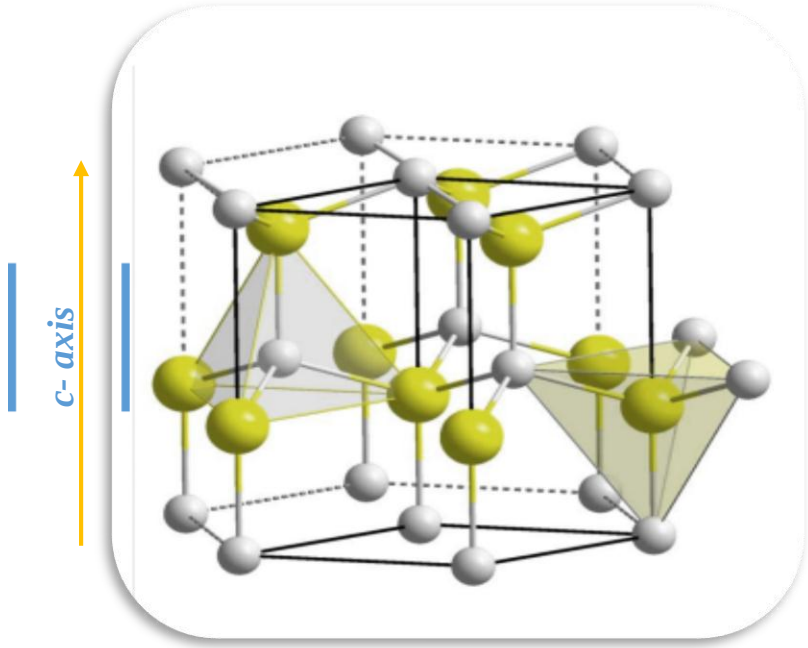

Fig.I.3 ZnO unit cell (hexagonal close packing (HCP) structure type wurtzite.

The unit cell parameters consist **a** and **c** which a = 0.325 nm and c = 0.5206 nm.

In order to describe zinc oxide, hexagonal indices can be used based on a four coordinate system with indices (hkil) . This is more suitable for zinc oxide than the three coordinate system because of the source of possible confusion in assigning planes when equivalent planes do not have the same indices. Possible confusion is avoided' using the four coordinate system as equivalent planes are indicated by permutations of the first three indices.

For example the three main reflections from the XRD spectrum of a polycrystalline powder sample of zinc oxide using the three coordinate system (hkl) are the (100), (101), and the (002) planes. Under the four coordinate system the labels are the (1010), the$(10\bar{1}1)$ and the (0002). Note that (110) is not equivalent to (101) in the hexagonal structure and this is explicit in the 4 coordinate system where these planes become $(11\bar{2}0)$ and $(10\bar{1}1)$ respectively. The following formula is used to convert from three to four indices [25].

$$i = -(h + k) \qquad \text{(I. 1)}$$

Another important characteristic of ZnO is polar surfaces. The most common polar surface is the basal plane. The oppositely charged ions produce positively charged Zn-(0001) and negatively charged $O_{(000\bar{1})}$ surfaces, resulting in a normal dipole moment and spontaneous polarization along the c-axis as well as a divergence in surface energy. To maintain a stable structure, The polar surfaces generally have facets or exhibit massive surfac reconstructions, but ZnO±(0001) are exceptions :they are atomically flat, stable and without reconstruction[26.27].

The internal stress in ZnO thin films is given by the following relationship:

$$\sigma = \left[\frac{2c_{13}^2-(c_{11}+c_{12})c_{33}}{c_{13}}\right]\left(\frac{c_{film}-c_{bulk}}{c_{bulk}}\right) \qquad (I.2)$$

Where, c_{bulk} is the unstrained lattice parameter of ZnO equals to 0.5206 nm, c_{film} is the lattice parameter of the strained films calculated from X- ray diffraction data and C_{11} = 209.7 GPa, C_{12} = 121.1 GPa, C_{13} = 105.1 GPa and C_{33} = 210.9 GPa are the stiffness constants of bulk ZnO[28].

I.4.2 native defects in ZnO

Zinc oxide (ZnO) is usually as a rather n- type conducting material. An excess of zinc, which acts to yield an electron gives the type of ZnO conductivity. The excess zinc results in a non - stoichiometric material $Zn_{1+\delta}O$ and a degree ofstructural disorder. The latter is caused by the elaboration technique and deposition parameters. Large octahedral interstitial positions exist in zinc oxide into which zinc ions can diffuse. The diffusion rate of zinc in zinc oxide has been found to be higher than that of oxygen. If an absolutely pure stoichiometric single crystal were considered, i.e. with no point defects, no impurities, no dislocations, and no grain boundaries, zinc oxide would be an insulator rather than a semiconductor at room temperature [25].

The control of defects and associated charge carriers is of paramount importance in applications that exploit the wide range of properties of ZnO materials since the defects have great effects on doping, minority carrier life time and luminescence efficiency, and may be directly involved in the diffusion mechanisms connected to growth process There are a number of intrinsic defects in ZnO with different ionization energies :O vacancy(V_O), Zn vacancy (V_{Zn}), Zn interstitial (Zni), O interstitial (O_i) and anti-site Zn(O_{Zn}). Zn interstitials

and oxygen vacancies are known to be the predominant ionic defects types [29, 30, 31].The energy levels of the native defects in ZnO film were calculated, as shown in Fig.I.4 [32].

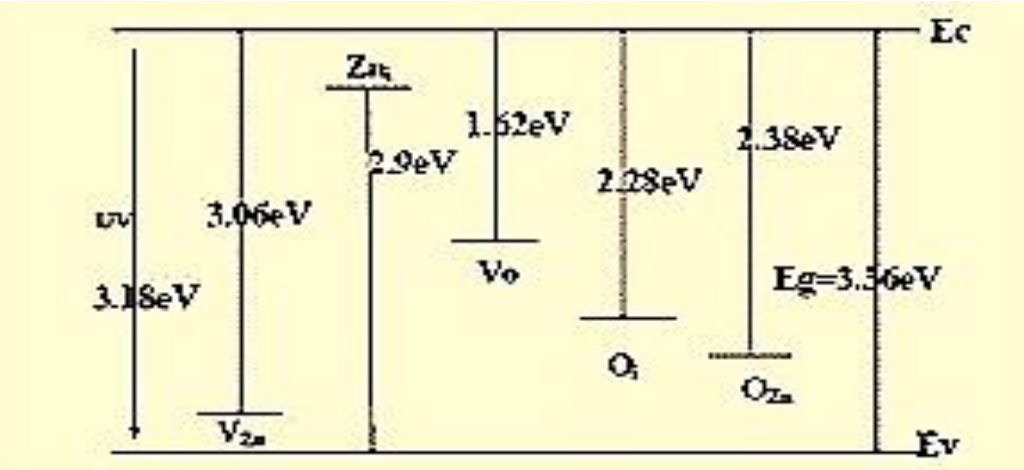

Fig.I.4. The draft of the calculated defect's levels in ZnO thin films [32].

I.4.3 Optical properties

Zinc oxide, a member in the II-VI family with a wide optical band gap (~3.3eV) and a large excitonic binding energy (60meV) [33].

The fundamental electron excitation spectrum of the film is described by means of a frequency dependence of the complex electronic dielectric constant.

Mujdat Caglar and al were found that there a real and imaginary parts of the dielectric constant decrease with increasing wavelength in the visible rang while they increase in the ultraviolet region [33]. T. Prasada Rao and al are found that optical band gap increases with increasing the compressive stress due to increase of repulsion between the oxygen 2p and the zinc 4s bands [33, 34].

I.4.4 Electronic properties

A number of groups have calculated the electronic band of ZnO [35, 36, 37]. The standard local density approximation (LDA) tends to underestimate the band gap by ~3 eV due to its failure in accurately modelling the Zn 3d electrons. However, by incorporating atomic self-interaction corrected pseudo potentials, the Zn 3d electrons can be accurately accounted. The calculation is shown in Figure 2-3 [36]. The band structure is shown along high symmetry lines in the hexagonal Brillouin zone. Both the valence band maxima and the

lowest conduction band minima occur at the Γ point k = 0 indicating that ZnO is a direct band gap semiconductor. The band gap as determined from this calculation is 3.77 eV [36], which correlates reasonably well with the experimental value of 3.4 eV, and is much closer than the value obtained from the standard LDA calculation. Advantages associated with its large band gap include high breakdown voltages, ability to sustain large electric fields, low noise enervation, and high-temperature and high-power operation [38].

The electronic structure of the surface of wurtzite ZnO was also extensivelystudied. Ivanov and Pollmann used the empirical tight-binding method (ETBM) to determine a Hamiltonian of the bulk states: the scattering theoretical method was applied to determine the nature of the surface states [40]. The calculated data was found to be in very good agreement with experimental results obtained from electron-energy-loss spectroscopy (EELS) and ultra-violet photoelectron spectroscopy (UPS). It suggests that the Zn face possesses more covalent character, arising from the Zn 4s-O 2p states, whilst the O face is more ionic. Experimentally, the ZnO valence band is split into three band states, A, B and C by spin-orbit and crystal-field splitting. Figure I.5 schematically illustrates this splitting. The A and C sub-bands are known to possess Γ7 symmetry, and the middle band B, has the Γ9 symmetry [39]

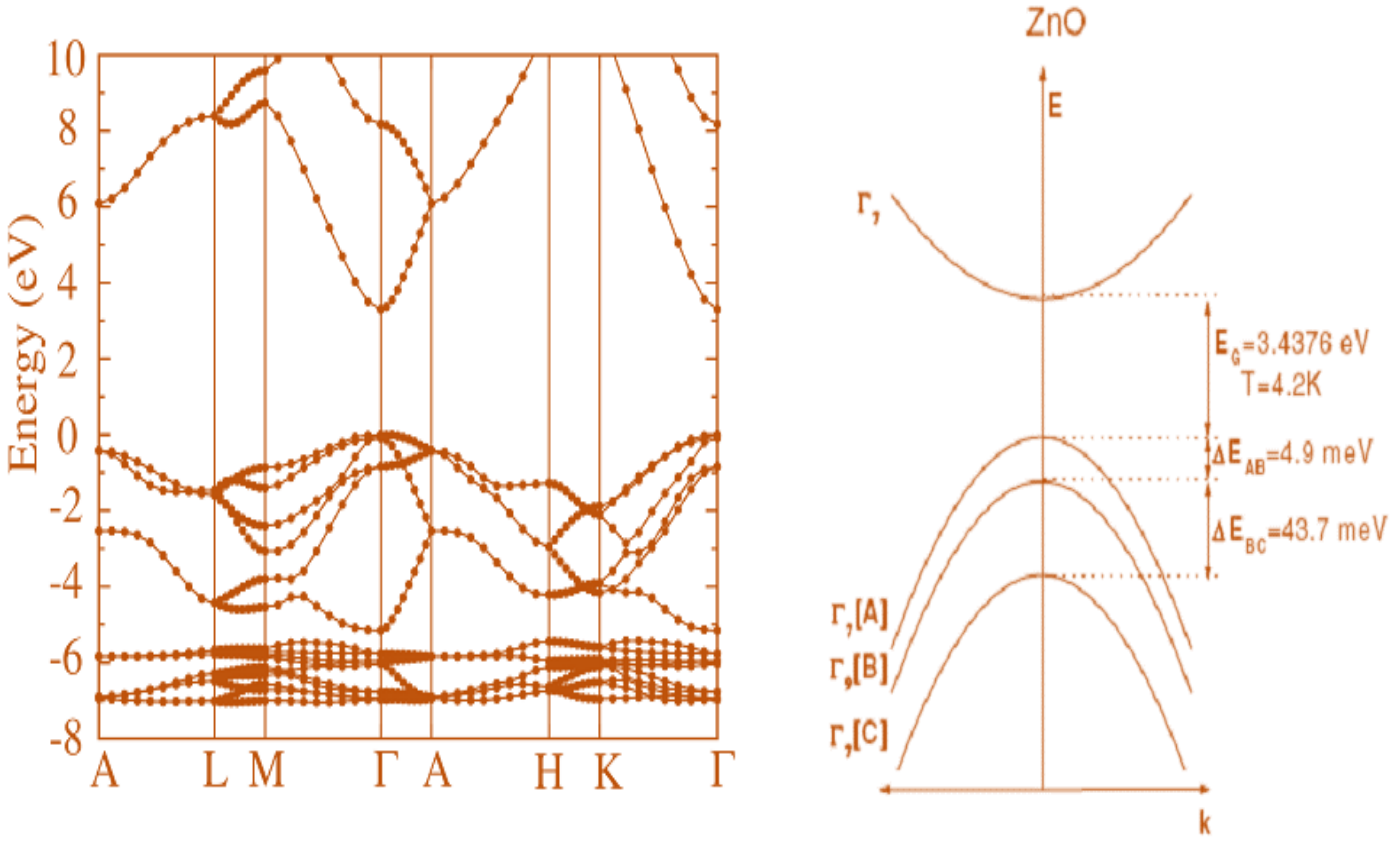

Fig.I.5. theoretical diagram of ZnO band structure a left [41]. Schematic representing the spin-orbit splitting of the valence band of ZnO into 3 sub-band states A, B and C at 4.2K a right [39]

I.4.5 Electrical properties

As-grown ZnO has always been found to be n-type. It was always assumed that the dominant donor was either oxygen vacancy V_O, or the zinc interstitial Zn_i, since most sample are grown under Zn-rich conditions. However, Kohan et al [42] and Van de Walle [43] challenged this conclusion in 2000 from different aspects. Kohan showed that both V_O and Zn_i theoretically had high formation energies in n-type ZnO, and therefore neither V_O nor Zn_i would exist in measurable quantities. Furthermore, it was also indicated that V_O and Zni were deep donors, so even if one or other were present, its ionization energy would be too high to produce free electrons. Although other theoretical analysis suggested that Zn_i was actually a shallow donor [44, 45], and had been proven by electron-irradiation experiments [46], the

high formation energy of Zn_i mentioned earlier still limited its ability to contribute to n-type conductivity.

H.L. Ma and al said that: there are two reasons to explain the change of carrier mobility with T_s. On the one hand, the concentration of donor (V_o) increases with the rise of the T_s at a certain range. Hence, the scattering of carriers (V_o) is enhanced, which reduces the carrier mobility. On the other hand, the orientation of C-axis becomes stronger with increasing T_s. The probability of grain boundary scattering for the carriers moving parallel to the surface increases, and therefore, the mobility paralleled to the surface direction reduces[47].

I.4.6 Applications of Zinc Oxide

Because of its diverse properties, both chemical and physical, zinc oxide is widely used in many areas. It plays an important role in a very wide range of applications, ranging from tyres to ceramics, from pharmaceuticals to agriculture, and from paints to chemicals.

- **. Rubber Industry**

Global production of zinc oxide amounts to about 105 tons per year, and a major portion is consumed by the rubber industry to manufacture various different cross-linked rubber products [48]. Zinc oxide is a very effective and commonly used cross linking agent for carboxylated elastomers [49,50].

- **The Pharmaceutical and Cosmetic Industries**

Due to its antibacterial, disinfecting and drying properties [51,52], zinc oxide is widely used in the production of various kinds of medicines. It was formerly used as an orally administered medicine for epilepsy. At the present time it is applied locally, usually in the form of ointments and creams, and more rarely in the form of dusting powders and liquid powders. ZnO has properties which accelerate wound healing, and so it is used in dermatological substances against inflammation and itching. In higher concentrations it has a peeling effect. It is also used in suppositories. In addition it is used in dentistry, chiefly as a component of dental pastes [53].

- **Electronics applications:**

Zinc oxide is a new and important semiconductor which has a range of applications in electronics and electro technology [54–55]. Its wide energy band (3.37 eV) and high bond energy (60 meV) [56,57] at room temperature mean that zinc oxide can be used in photo-electronic [58] and electronic equipment [59], in devices emitting a surface acoustic wave [60], in field emitters [61], in sensors [62, 63], in UV lasers [64], and in solar cells [65].

Zinc oxide is also used in gas sensors. It is a stable material whose weak selectivity with respect to particular gases can be improved by adding other elements. The sensitivity of such devices depends on the porosity and grain size of the material; sensitivity increases as the size of zinc oxide particles decreases. It is most commonly used to detect CO and CO_2 (in mines and in alarm equipment), but can also be used for the detection of other gases (H_2, SF_6, C_4H_{10}, C_2H_5OH) [66].

One of the most important applications of zinc oxide in electronics is in the production of varistors. These are resistors with a non-linear current-voltage characteristic, where current density increases rapidly when the electrical field reaches a particular defined value.

They are used, among other things, as lightning protectors, to protect high-voltage lines, and in electrical equipment providing protection against atmospheric and network voltage surges. These applications require a material of high compactness, since only such a material can guarantee the stability and repeatability of the characteristics of elements made from it [67, 68].

- **Photo-catalysis applications**

Intensive scientific work has taken place in recent years on photo-catalysis. In this process, an electron-hole pair is produced below the intensity of light by means of oxidation or reduction reactions taking place on the surface of the catalyst. In the presence of a photo-catalyst, an organic pollutant can be oxidized directly by means of a photo-generated hole or indirectly via a reaction with characteristic reactive groups (ROS), for example the hydroxyl radical $OH^{\cdot}$, produced in solution [69, 70].

The most commonly used catalysts are TiO_2 and ZnO. TiO_2 exhibits photo-catalytic activity below the intensity of UV light [71, 72]. ZnO provides similar or superior activity to that of TiO_2, but is less stable and less sensitive to photo-corrosion [73]. Better stability, however, is provided by zinc oxide of nanometric dimensions, which offers better crystallinity and smaller defects [74].

The photocatalytic activity of ZnO can be further improved, and the range of the visible spectrum for zinc oxide can be extended, by adding other components [75].

Chapter II

Spray pyrolysis and characterization methods

II.1. Introduction

In this chapter, we display a fragment around to different elaboration techniques for thin films. Then, we part the history and development of spray pyrolysis and the used equipment to elaborate our ZnO thin films. The second part of this chapter includes the different techniques and different relationships, which is used to characterize our thin films.

II.2. Thin films depositions techniques

The properties of thin films are extremely sensitive to the method of preparation, several techniques have been developed (Depending on the desired film properties) for the deposition of the thin films of the metals,alloys,ceramic,polymer and superconductors on a variety of the substrate materials.Each methods has it's own merits & demerits and of course no one technique can deposit the thin films covering all the desired aspects such as cost ofequipments, deposition conditions & nature of the substrate material etc.Thin film deposition techniques are classified in Table.II.1

In our work, we choose spray pyrolysis because this thin film deposition method is simple, cost-effective, and a wide choice of precursors can be used. The composition of the film can be easily controlled by the precursor solution. Both, dense and porous structures can be deposited by spray pyrolysis, even on large substrates when scaling up the equipment.

II.3. Spray pyrolysis technique (SP)

II.3.1 spray pyrolysis equipment

Spray pyrolysis is a processing technique being considered in research to prepare thin and thick films, ceramic coatings, and powders. Unlike many other film deposition techniques, spray pyrolysis represents a very simple and relatively cost-effective processing method It offers an extremely easy technique for preparing films of any composition. Spray pyrolysis does not require high-quality substrates or chemicals. The method has been employed for the deposition of dense films, porous films, and for powder production. Even multi layered films can be easily prepared using this versatile technique. Spray pyrolysis is has been used for several decades in the glass industry [76]and in solar cell production [77].Typical spray pyrolysis equipment consists of an atomizer, precursor solution, substrate heater, and temperature controller. The following atomizers are usually used in spray pyrolysis technique: air blast (the liquid is exposed to a stream of air) [78], ultrasonic

(ultrasonic frequencies produce the short wave length necessary for fine atomization) [79] and electrostatic (the liquid is exposed to a high electric field) [80].

Table.II.1. Classification of Thin-Film Depositon techniques [81].

EVAPORATIVE METHODS	
•Vacuum Evaporation	
Conventional vacuum evaporation	**Molecular-beam epitaxy (MBE)**
Electron-beam evaporation	**Reactive evaporation**
GLOW-DISCHARGE PROCESSES	
•Sputtering	**Plasma Processes**
Diode sputtering	**Plasma-enhanced CVD**
Reactive sputtering	**Plasma oxidation**
Bias sputtering (ion plating)	**Plasma anodization**
Magnetron sputtering	**Plasma polymerization**
Ion beam deposition	**Plasma nitridation**
Ion beam sputter deposition	**Plasma reduction**
Reactive ion plating	**Microwave ECR plasma CVD**
Cluster beam deposition (CBD)	**Cathodic arc deposition**
GAS-PHASE CHEMICAL PROCESSES	
•Chemical Vapor Deposition (CVD)	Thermal Forming Processes
CVD epitaxy	Thermal oxidation
Atmospheric-pressure CVD (APCVD)	Thermal nitridation
Low-pressure CVD (LPCVD)	Thermal polymerization
Metalorgainc CVD (MOCVD)	Ion implantation
Photo-enhanced CVD (PHCVD)	
Laser-induced CVD (PCVD)	
Electron-enhanced CVD	
LIQUID-PHASE CHEMICAL TECHNIQUES	
•Electro Processes	•Mechanical Techniques
Electroplating	**Spary pyrolysis**
Electroless plating	**Spray-on techniques**
Electrolytic anodization	**Spin-on techniques**
Chemical reduction plating	**Liquid phase epitaxy**
Chemical displacement plating	
Electrophoretic deposition	

.

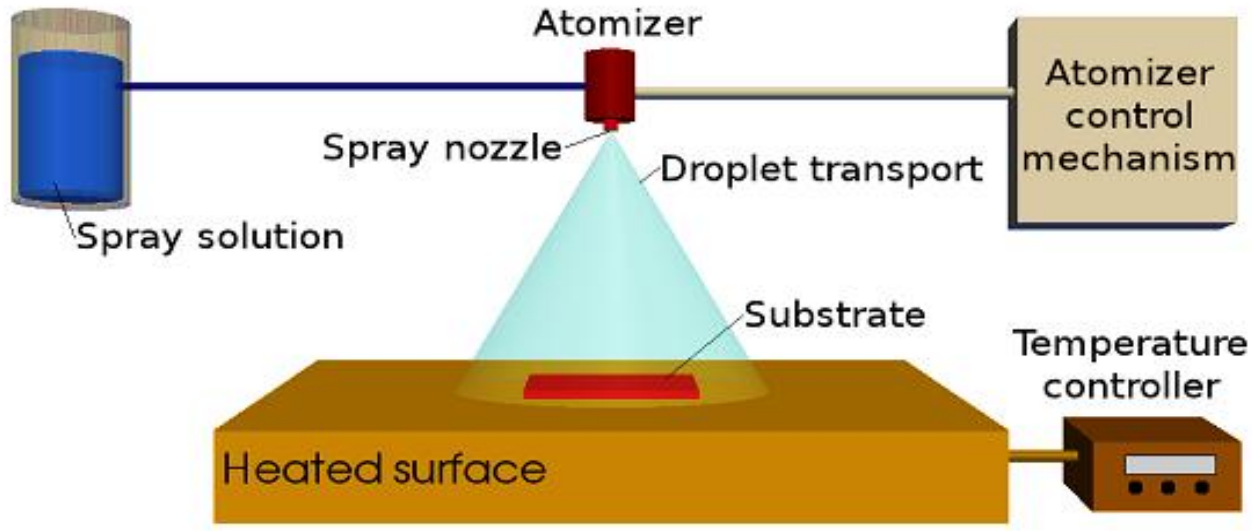

Fig.II.2. Schematic diagram of spray pyrolysis equipment.

II.3.2 spray pyrolysis process

In general case of spray pyrolysis deposition is shown in Fig.II.2, where there processing steps can be seen and considered:

- ✓ Atomization of the precursor solution.
- ✓ Aerosol transport of the droplet.
- ✓ Decomposition of the precursor to initiate film growth.

1. Precursor atomization

The atomization procedure is the first step in the spray pyrolysis deposition. The idea is to generate droplets from a spray solution and send them, with some initial velocity, towards to the hot substrate surface. Spray pyrolysis normally uses air blast, ultrasonic, or electrostatic techniques [82].

2. Aerosol Transport of Droplets

After the droplet leaves the atomizer, it travels through the ambient with an initial velocity determined by the atomizer. In the aerosol form, the droplets are transported with the aim of as many droplets as possible reaching the surface. As the droplets move through the ambient, they experience physical and chemical changes represented in Fig.II.3.

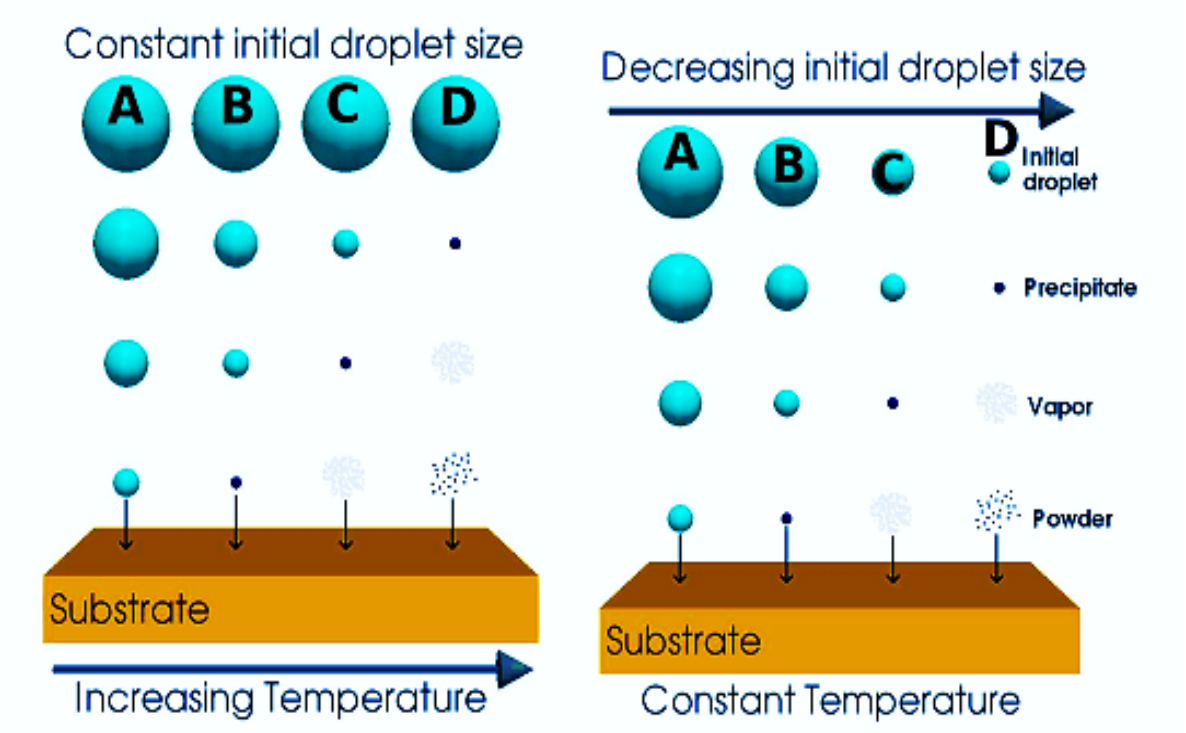

Fig.II.3 Spray pyrolysis droplets modifying whether the temperature or the initial droplet size are varied [83, 84].

As the droplet traverses the ambient, there are forces simultaneously acting on it, describing its path. Those forces are the following:

The gravitational force is the force which attracted the droplets to substrtate surface ward .The value of the force depends on the mass of the droplet. For small size of droplets, the gravitational force is too small to allow it to arrive at the substrate surface .For large size of droplets; the force of gravity is the driving force behind the droplet transport.

The stokes force is the drag experienced by the droplet due to the air resistance. The force is caused by the friction between the droplet and air molecules.

Other forces is causing droplets to significantly decrease their velocity as they approach the heated substrate. It is evident that the air temperature increases steeply due to the forced convection cooling effect of the air flow when close to the heated substrate. It depends on the thermal gradient in the transport environment, it can be concluded that it will have effect on the droplet movement.

3. Decomposition of precursor

Many processes follow simultaneously when a droplet hits the surface of the substrate: evaporation of residual solvent, spreading of the droplet, and salt decomposition. Many

models exist for the decomposition of a precursor. Most of the authors suggest that only a kind of CVD process gives high quality films by spray pyrolysis.

Viguie and Spitz were given the following processes that occur with increasing substrate temperature [83]. At low substrate temperature (processA), the droplets plashes onto the substrate surface and decomposes (see figure.II.4).At higher temperatures (processB) the solvent evaporates completely during the flight of the droplet and dry precipitate hits the substrate, where decomposition occurs. At even higher temperatures (more than the latter case), the solvent also evaporates before the droplet reaches the substrate. Then the solid precipitate melts and vaporizes without decomposition and the vapor diffuses to the substrate to undergo a CVD process (process C).At the highest temperatures (processD), the precursor vaporizes before it reaches the substrate, and consequently the solid particles are formed after the chemical reaction in the vapor phase.

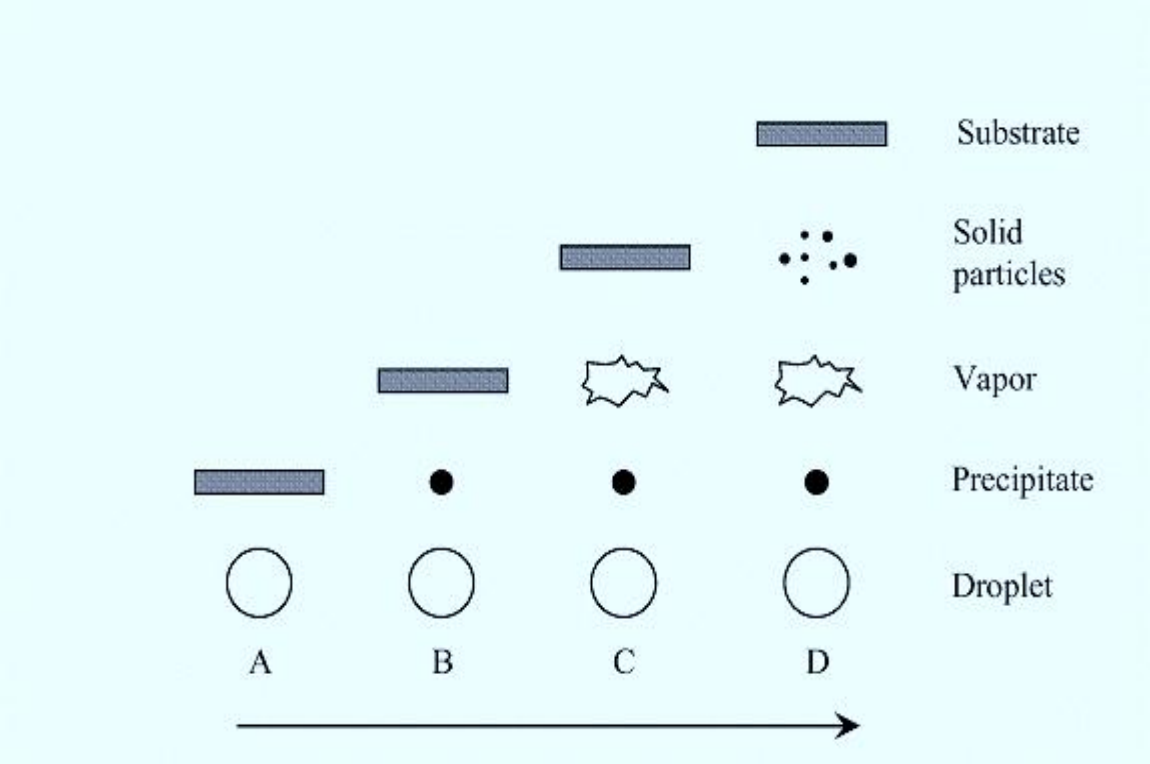

Fig.II.4. Description of the deposition processes.

II.3.3 Spray pyrolysis parameters

To elaborate thin films by spray pyrolysis technique. You should choose the precursor; the latter may be salts or organometallic material. The type of precursor directly influences three spray parameters: temperature (should be sufficiently high to decompose the precursor), precursor concentration (limits the maximal concentration in the solution) and type of solvent (restricts the choice of salts due to their insolubility in some solvents). Therefore, the optimal spray parameters usually differ considerably for each type of precursor.

The spray parameters are the following:

- Substrate temperature.
- Solution flow rate.
- Type of salt.
- Solvent.
- Deposition time.
- Nozzle - substrate distance.

II.4.Charactirization methods

A measurement of thin-film properties is indispensable for the study of thin-film materials and devices. The chemical composition, crystalline structure, and optical, electrical, and morphological properties must be considered in evaluating thin films.

The X rays diffraction is carried out to study the crystalline quality of the ZnO thin films. It is a simple and non-destructive analysis technique, which provides means to identify different phases and their distribution in the sample, texture, evaluate average grain size, internal stress, etc.

X-rays are electromagnetic waves with wavelength (0.5-50 Å) comparable to atomic separation distances. When propagating through a crystal, the X-rays interact with the lattice and are diffracted according to the Bragg's law:

$$2d_{hkl}\sin\theta = \lambda \qquad \text{(II. 1)}$$

d_{hkl}:The atomic spacing.

θ: The scattering angle..

λ: The wavelength.

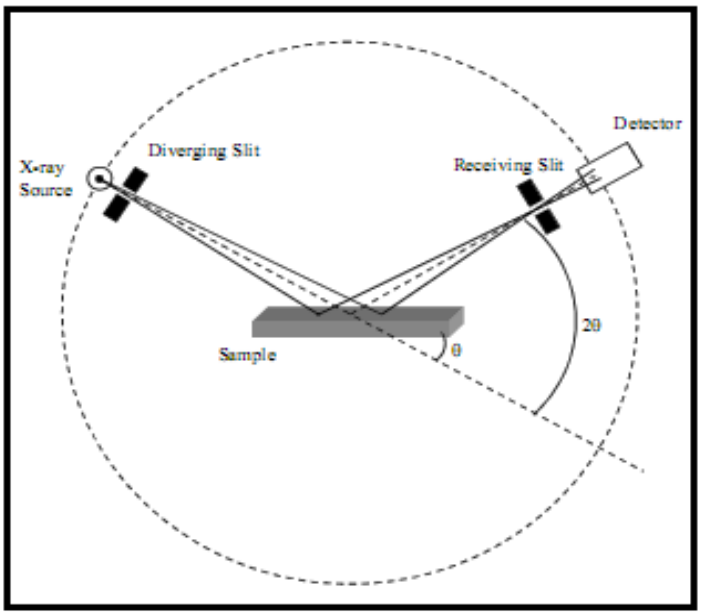

Fig. II.5: Schematics of X-ray diffractometer.

In this technique, the diffracted radiation is detected by the counter tube, which moves along the angular range of reflections. The intensities are recorded on a computer system. The X-ray diffraction data thus obtained is printed in tabular form on paper and is compared with Joint Committee Power Diffraction Standards (JCPDS) data to identify the unknown material. The sample used may be powder, single crystal or thin film. The crystallite size of the elaborated sample is estimated from the full width at half maximum (FWHM) of the most intense diffraction line by Scherrer's formula as follows [85]:

$$D = \frac{0.9\,\lambda}{\beta\,cos\theta} \qquad (II.2)$$

D: The crystallite size (nm or A°).

λ : The wavelength of X-ray (nm or A°).

β:The full width at half maxima of the peak (FWHM) in radians,

θ:TheBragg's angle (rd.).

It can be calculate the dislocations density using the grains size values according to the following relationship [85]:

$$\delta = \frac{1}{D^2} \qquad (II.3)$$

The X-ray diffraction data can also be used to determine the dimension of the unit cell using this relation [86]:

$$d_{hkl} = \left(\frac{4}{3}\,\frac{h^2+hk+k^2}{a^2} + \frac{l^2}{c^2}\right)^{-1/2} \qquad (II.4)$$

The scanning electron microscope (SEM) is a type of electron microscope that images the sample surface by scanning it with a high-energy beam of electrons in a raster scan pattern. The electrons interact with the atoms to make the sample producing signals that contain information about the surface of the sample, composition and other properties of the ZnO thin films.

The SEM uses electrons instead of light to form an image. A beam of electrons is produced at the top of the microscope by heating of a metallic filament. The electron beam follows a vertical path through the column of the microscope. It makes its way through electromagnetic lenses which focus and direct the beam down towards the sample. Once it hits the sample, other electrons such as backscattered or secondary are ejected from the sample (see Figure II.6).

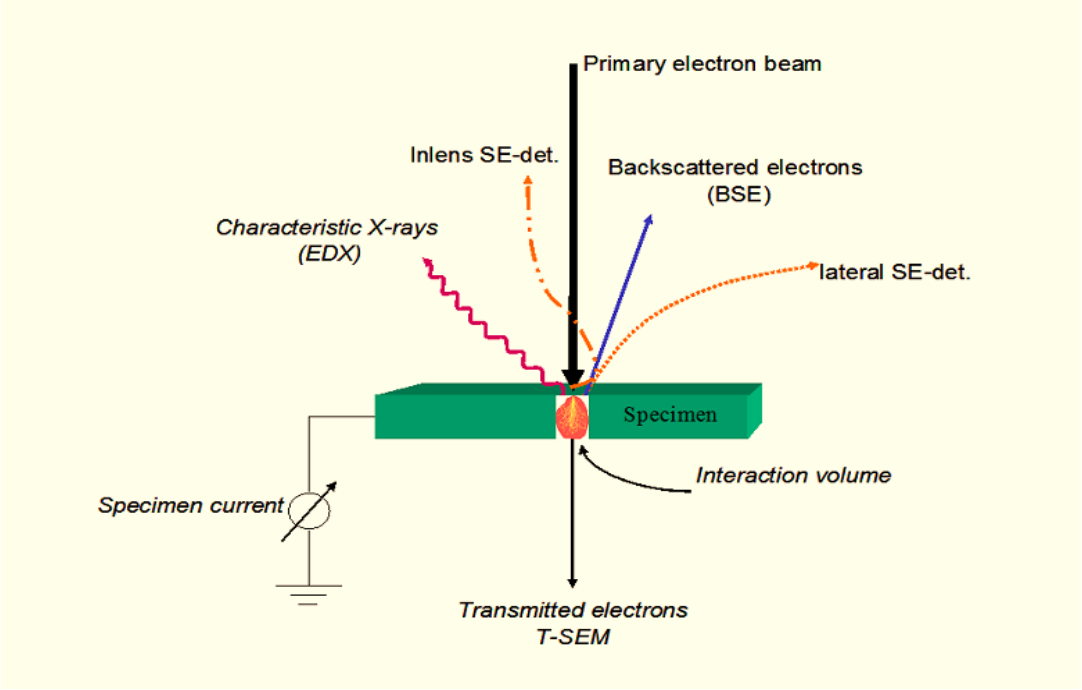

Fig.II.6. Illustration of electron-specimen interactions in SEM [87].

The SEM gives information on the surface morphology of the sample, which can help us check whether the growth has taken place or not. The SEM produces 2D images and reveals topographic features of the sample, which allows us to examine the diameter, length, shape and density of the ZnO nanostructures. However, the images from the SEM cannot definitively prove that the obtained nanostructures actually consist of ZnO.

It can be obtained from energy Energy-dispersive X-ray spectroscopy (EDS), which is most commonly attached on the SEM system. To characterize the morphologies of ZnO nanostructures deposited by spray pyrolysis , a JEOL JSM-6301F scanning electron microscope was used in our experiments. The chamber pressure is about 10^{-6} mbar. The gun voltage is 15kV.

PL measurement is a standard technique to observe defects and impurities in semiconductors. Study of luminescence processes can, not only show the content as well as the behavior of the defects and impurities in semiconductors, but also can give information on different paths for the radiative recombination. The PL spectrum and its dependence on the irradiation intensity and device temperature can deliver important information for the device characterization. Through PL measurement, we can obtain a variety of material parameters, which will be introduced respectively as follows:

- Band gap energy.
- Impurity levels and defect detection.
- Recombination mechanisms.
- Material quality.

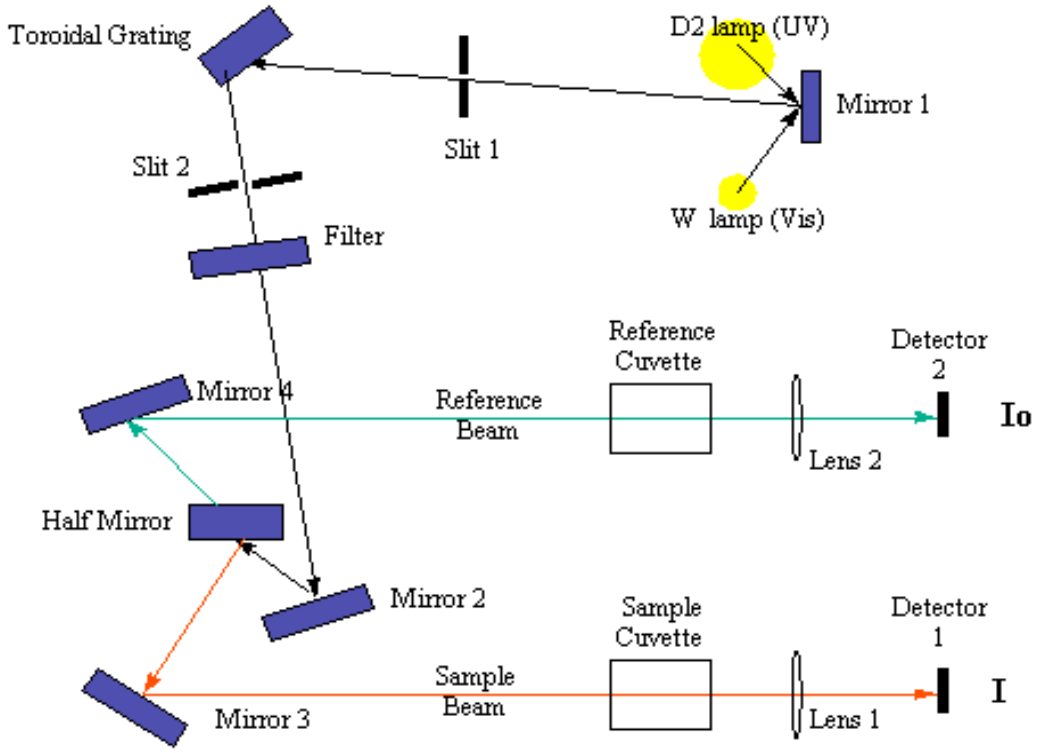

Fig.II.7. the principal operation of UV–Visible spectrophotometer.

The optical transmittance spectra in UV–Visible rang were achieved using Perkin Elmer spectrophotometer. The wavelength range between 200 nm and 1100 nm.Figure.II.7 represents the principal operation of UV–Visible spectrophotometer. The transmittance values were obtained using the following relationship [87]:

$$T = (1 - R)e^{-\alpha d} \qquad (II.3)$$

$$(\alpha h\upsilon)^2 = A(h\upsilon - E_g) \qquad (II.4)$$

Where α is the absorption coefficient which is related to wavelength, R is the reflectance and'd' is the film thickness. The optical band gap of ZnO thin films is calculated by the following expression [88, 89] (eq II.4).

Which A is a constant independent of photon energy (hv), *h* the Planck constant and E_g the energy band gap of the semi- conductor. The value of optical band gap can be found by extrapolation of the linear region to $(\alpha hv)^2 = 0$ [90] (see figure.II.8).

Ravindra and al. [91, 92] have proposed a linear relation governing the variation of refractive index with energy gap in semiconductors expressed as follows:

$$n = 4.08 - 0.62E_g \qquad (II.5)$$

Also there is a relationship between the refractive index, the transmittance, the film thickness and the reflectance of the thin films expressed as follows[93]:

$$n = \frac{(R+1)^2}{(R-1)^2} - \sqrt{\frac{4R}{(R-1)^2} - k^2} \qquad \text{(II.6)}$$

Where k is called the extinction coefficient that is equal to $\alpha\lambda/4\pi$

The dielectric constant is defined by real and imaginary parts of the dielectric constant which are related to the n and k values. The ε_1 and $\varepsilon_2$values were calculated using the formulas [94]:

$$\varepsilon_1 = n^2 - k^2 \qquad \text{(II. 7)}$$

$$\varepsilon_2 = 2nk \qquad \text{(II. 8)}$$

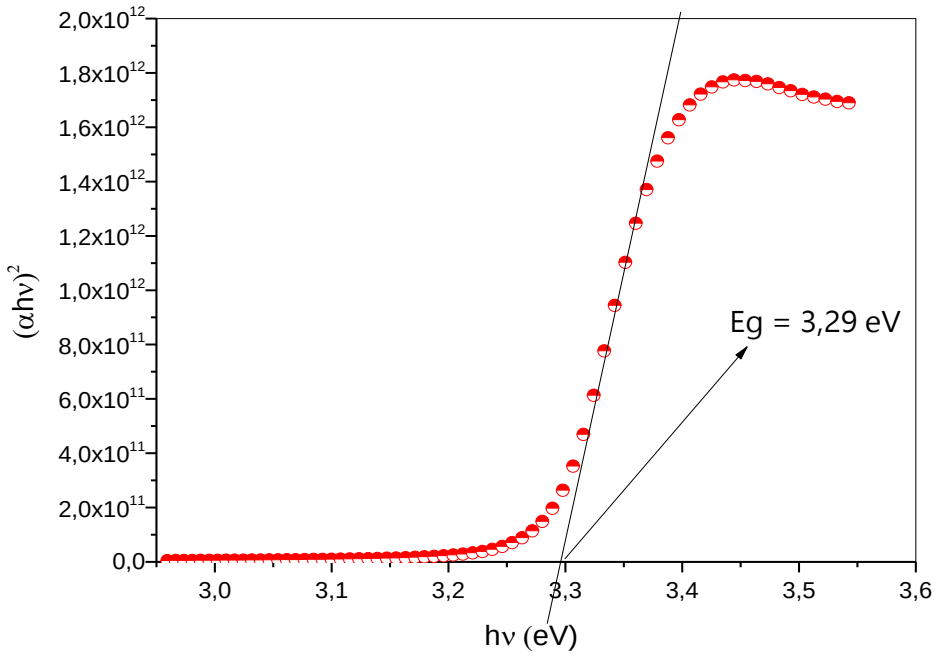

Fig.II.8. Curve represent the function$(\alpha h\upsilon)^2 = f(h\upsilon)$.

The electrical resistivity ρ of ZnO thin films is found by four points probe using the following relationship [93]:

$$\rho = \frac{4\pi}{Ln\,2} d \frac{V_{Mesured}}{I_{applied}} \qquad \text{(II.9)}$$

ρ : The electrical resistivity (Ω.cm). $V_{Mesured}$: The mesured voltage (volt).

d : the film thickness (cm). $I_{applied}$: the applied current (ampeer).

II.5. Cleaning substrate

The quality of zinc oxide thin films deposited on glass substrate using ultrasonic spray process (USP) depends on purity and surface state of the used substrate.

The process of cleaning surface for the glass and Si single crystal substrates is as follows:

- Firstly using a pen with diamond point to cut the substrates.
- Rinsing with the water distilled and then with acetone during 5 min.
- Rinsing with distilled water.
- Washing in methanol at ambient temperature in a bath with the Ultrasound for to eliminate the traces from greases and impurities stuck to surface of substrate then they are to clean in a water bath distilled with the Ultrasound.

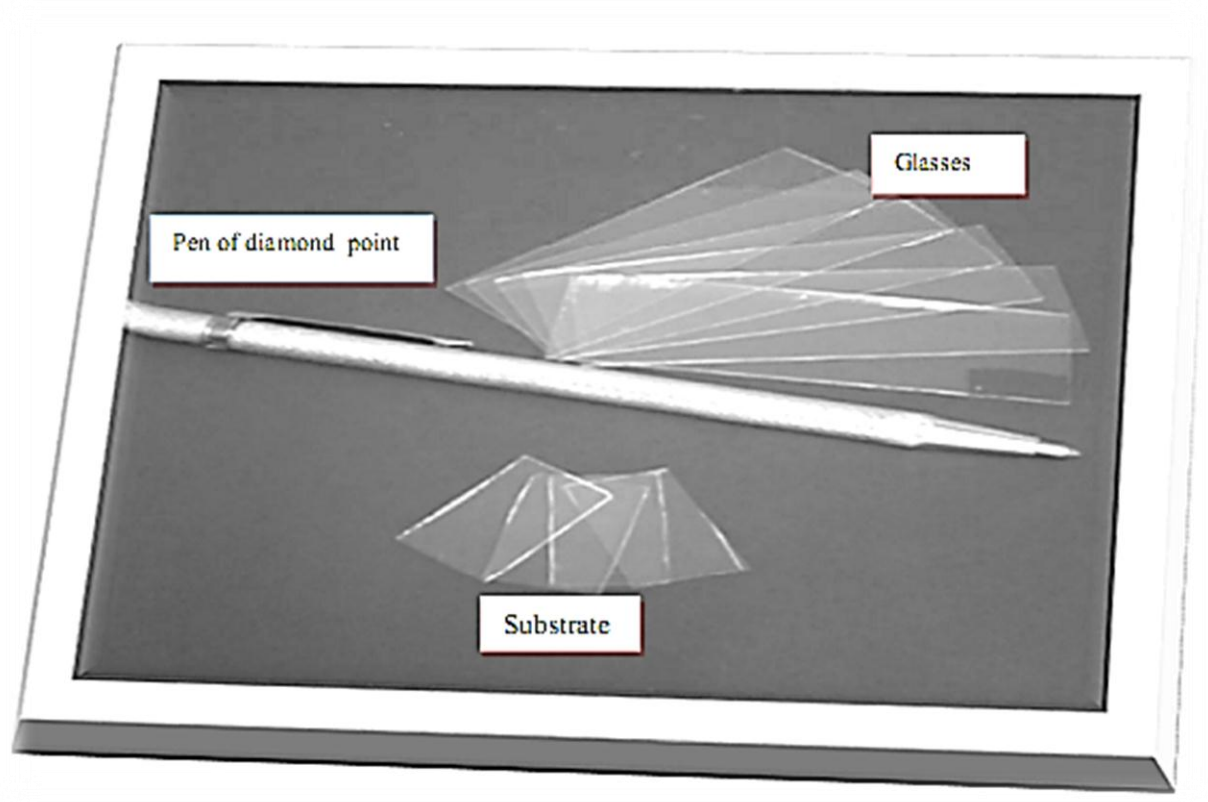

Fig.II.9. Glasses substrates and diamond pen used.

Chapter III

The solution flow rate and concentration influence on ZnO thin films properties.

III.1 Introduction

In this chapter, ZnO thin films were deposited on hot glass substrates by spray pyrolysis technique. Solution flow rate and solution concentration effect on structural, morphological, optical and electrical properties of ZnO films have been investigated.

III.2 Solution flow rate effect

III.2.1 Experimental details

The conditions of elaboration are represented in table.III.1.

Table.III.1 : the elaboration conditions.

	The influence of the solution flow rate.
Solution	**(C_{sol} = 0.1 Mol/l)**
Substrate temperature	350 °C
Deposition time	7 min
spray nozzle – substrate distance	5 cm
Solution flow rate	50 ml/h, 75 ml/h, 125 ml/h and 150 ml/h

III.2.2 The used technique

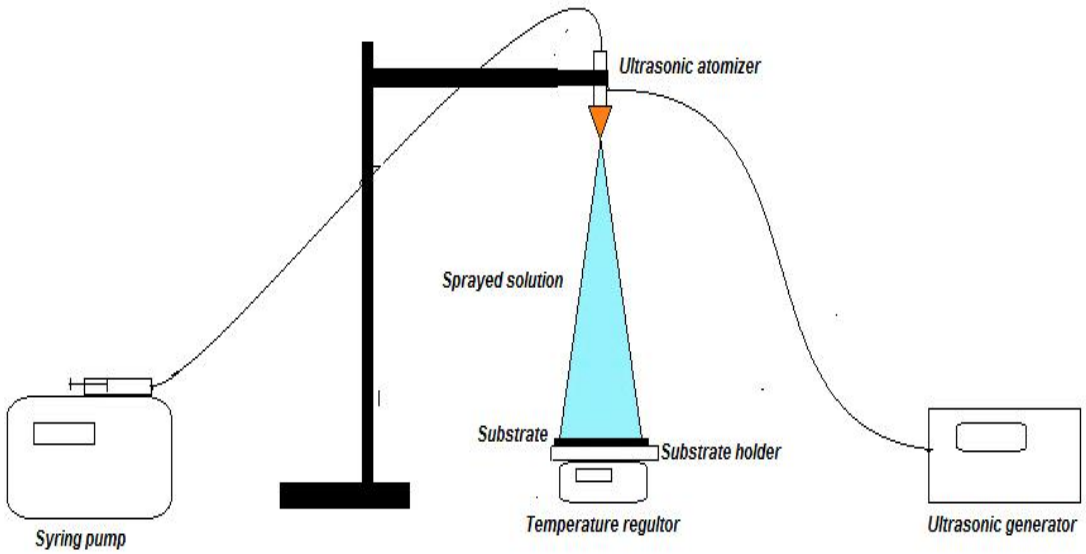

Fig.III.1 Schematics of experimental technique.

III.2.3 Structural properties

To investigate the crystalline quality of the ZnO thin films with various values of solution flow rate, XRD analysis is carried out and the results are shown in Fig.III.1.The XRD patterns of the films indicate that the ZnO thin films have a hexagonal structure type wurtzite corresponding to the JCPDS data card (36-1451) [95] with cell parameters a = 0.324 nm and c = 0.518 nm. It can be seen at 125 ml/h flow rate the preferential orientation of the crystallites changed from the conventional c-axis (002) orientation to the (100) orientation. The reason as to why the change of the preferred orientation took place could be explained by the oxygen content in the film [96]. When the solution flow rate equal to 150 ml/h, the intensity of (002) peak is lower than other samples. It can be explained by presence an amorphous phase in film network due to the increasing of droplets number with high velocity. In this case, the the films have low cristallinity.

The crystallite size (D) of the ZnO films was calculated using the classical Scherrer formula (mentioned in chapter II) [85].

It is well known that the crystallite size measured by this method is usually less than the actual value. This is the consequence of internal stress and defects in deposited thin films [97]. The variation of average grain size and lattice stress in the ZnO thin films with solution flow rate is illustrated in fig.III.3. The estimated values of stress σ in the films grown at different solution flow rate are shown in fig.III.3. The positive values of estimated stress for the films indicate that the lattice constant c is lower than the unstressed bulk sample. The positive sign indicates that the films are in a state of tensile stress. It's well known that the tensile stress is likely responsible of resulting from the oxygen vacancies which exist in ZnO thin films. However, the compressive stress may be due to zinc interstitials [98].

The obtained films have a polycrystalline nanostructure; the obtained crystallite size is ranged from 36.79 to 20.11 nm. As seen that the average grain size is reduced with increasing of solution flow rate. It could be explained by increasing of stress due to the rise of internal strain in the formed crystallites. The increase of the stress can be accounted by increasing of solution particles number, which creates defects in the film network. Above 125ml/h flow rate, we noticed a decrease of stress and an increase in the crystallite size; this can be due to the change in growth direction at this flow rate.

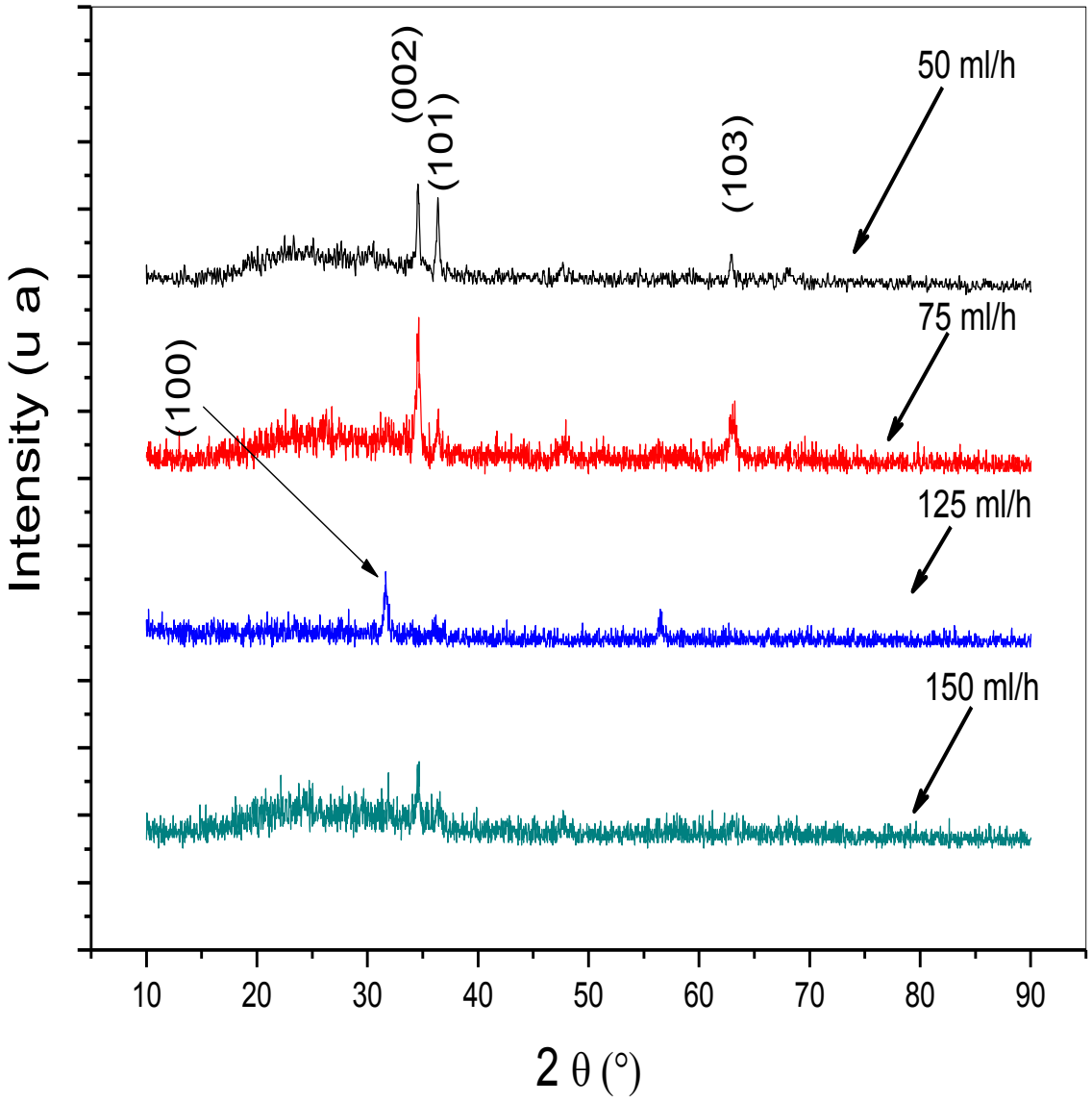

Fig.III.2 the XRD pattern of ZnO thin films.

TableIII.2: crystallites size and internal stress vs the solution flow rate.

Solution flow rate (ml/h)	*Crystallites size (nm)*	*Internal stress(GPa)*
50	*36.79*	*2.02*
75	*29.44*	*2.08*
125	*19.97*	*2.53*
150	*20.11*	*1.93*

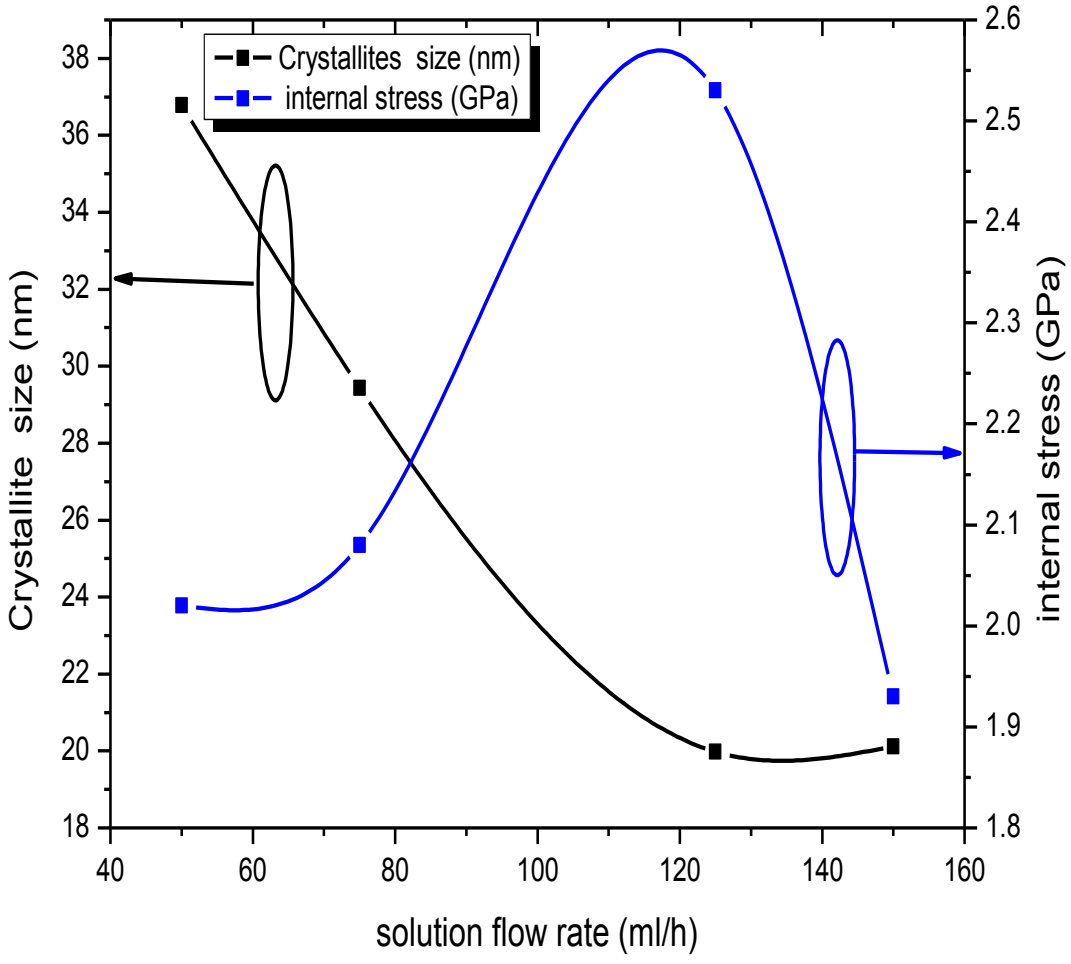

Fig.III.3. Crystallite size and internal stress as function of solution flow rate.

III.2.4 Morphological properties

The SEM analysis of the ZnO thin films was done to study surface morphology. The SEM images of ZnO thin film synthesized at substrate temperature equal to 350 ° C with solution flow rate of 50 ml/h, 75 ml/h, 125 ml/h and 150 ml/h (Fig. III.4). The SEM images show that ZnO thin films synthesized for a solution flow rate equals 50 ml/h exhibit a smooth and uniform surface (Fig.III.4 (a)). From the crystallite size curve, this sample has a larger grains than other samples because a few numbers of droplets with low velocity fall onto substrate surface which permit to growth the film with better way .

When, we increase the solution flow rate more than 50 ml/h the film surface changed to the granular surface and the grain size decreases due to the increasing of the velocity and numbers of droplets (Fig.III.4 (b, c and d)). In this case, the nucleation step was fast in the film which done a film with low crystallinity.

The cross sectional images show that the film with a solution flow rate equals 50 ml/h grow parallel to the substrate surface. When, we increase the solution flow rate more than 50 ml/h, the growth has been changed from parallel to perpendicular shape due by the increasing of droplets velocity. Furthermore, the thickness of ZnO thin films increases with increasing the solution flow rate.

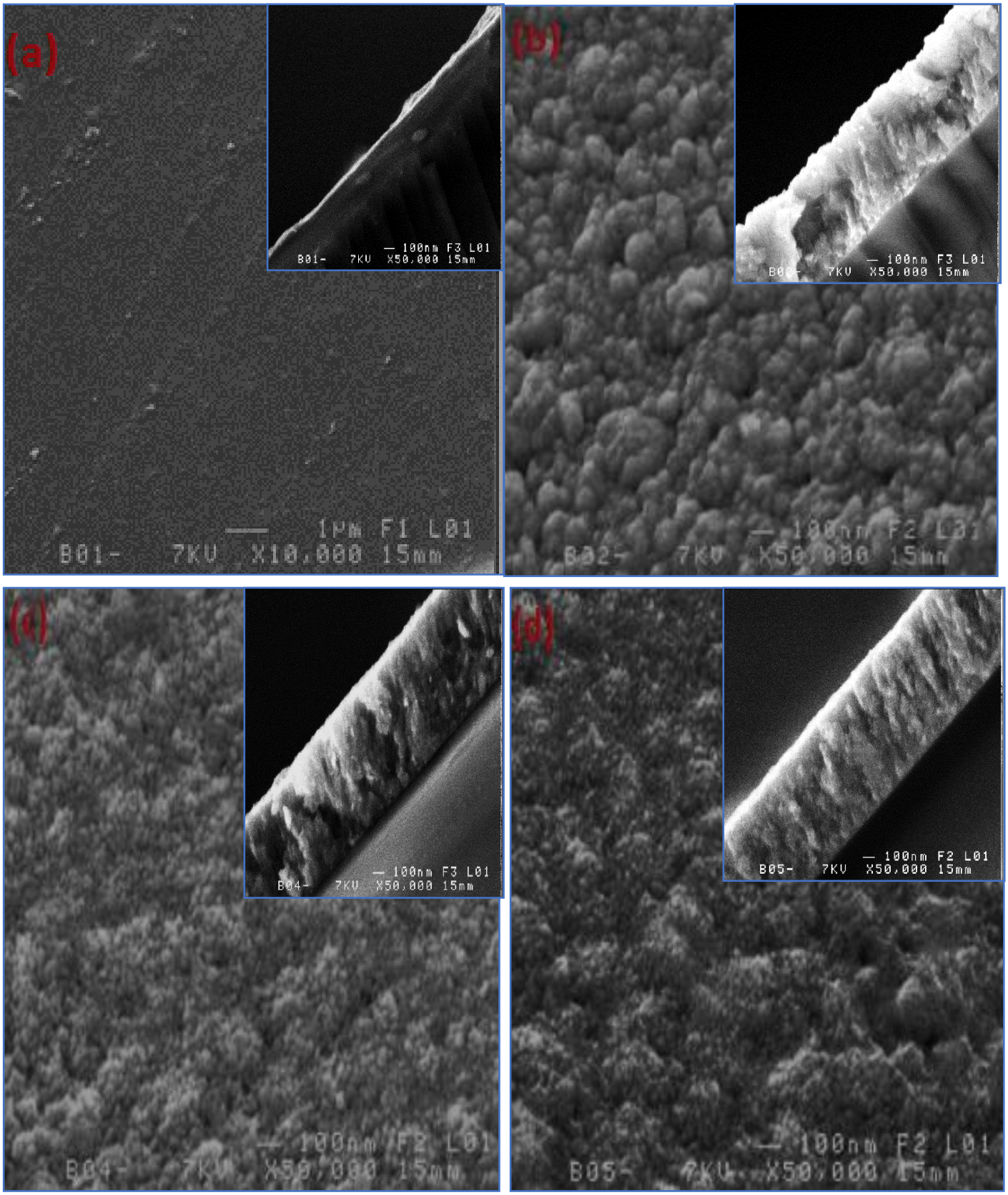

Fig.III.4. the SEM images for our samples of ZnO thin films prepared at different values of solution flow rate: (a) 50 ml/h, (b) 75ml/h, (c) 125 ml/h and (d) 150 ml/h.

III.2.5 Deposition rate

The deposition rate of our samples was calculated by division the film thickness on the time of deposition. The experimental results show that deposition rate increases with increasing the solution flow rate . This increase of deposition rate could be accounted by increasing of the solution volume sprayed onto substrate surface due to rise in the solution flow rate [99].

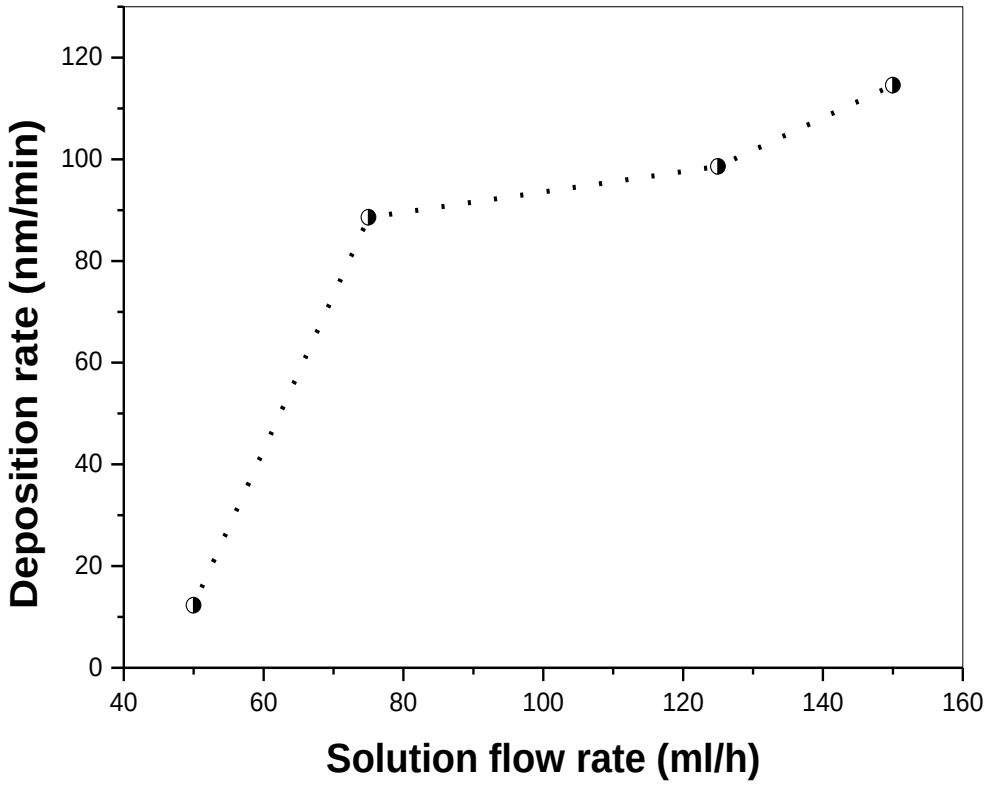

Fig.III.5. deposition rate of ZnO thin films as a function of solution flow rate.

III.2.6 Optical properties

The transmittance spectra of ZnO thin films elaborated at 350 °C have shown in Fig.III.6. The optical transparency equal to 80% in visible rang. The optical band gap of ZnO thin films was calculated by the expression (mentioned in chapter II).

The optical band gap energy increases with increasing the solution flow rate (Fig.III.6). It can be explain by decreases of the crystallite size [100, 101] and increases of

film thickness [102]. The refractive index of ZnO thin films elaborated at different solution flow rate is calculated using Ravindra relation (see the equation II.4) [103, 104].

The values of refractive index of our samples decrease when the solution flow rate increases (Fig.III.7). This decrease is attributed to increase of grains boundaries due to the decrease of the crystallite size [105].

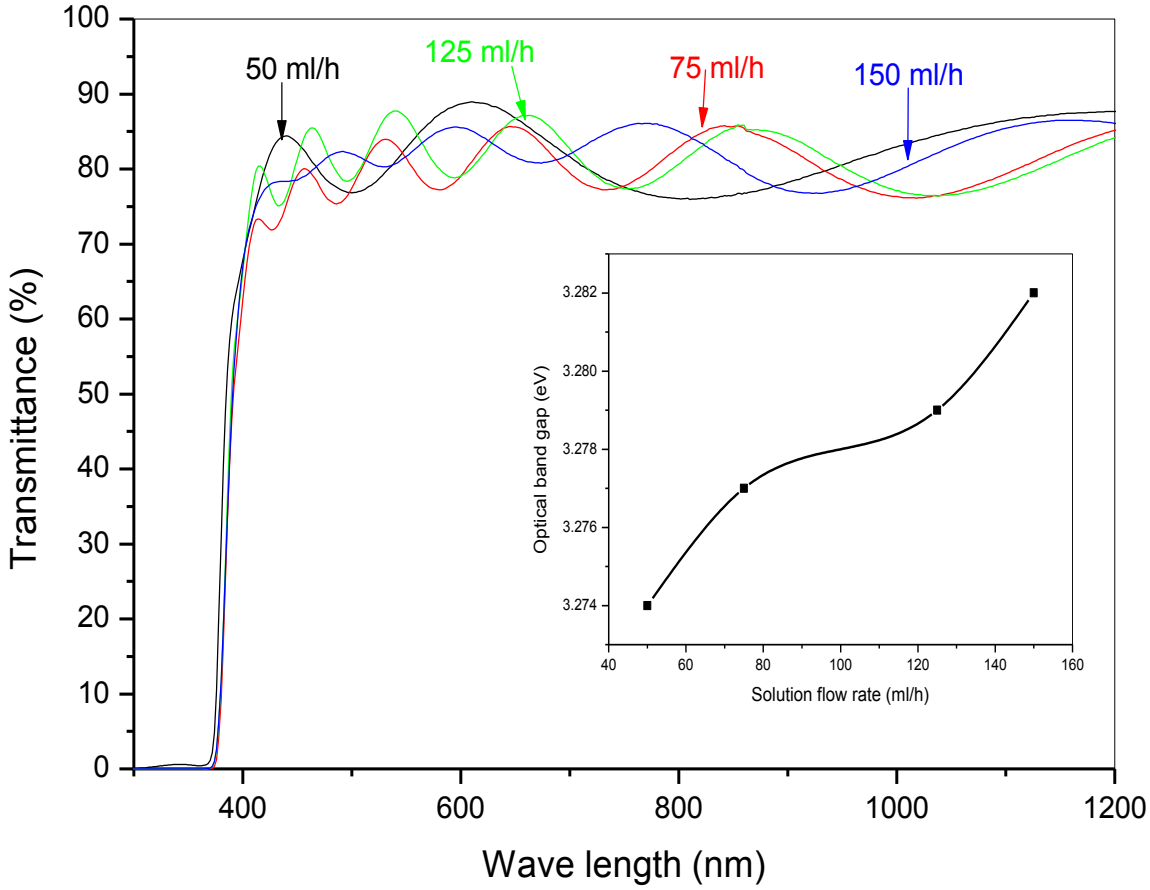

Fig.III.6 Transmittance spectra and optical band gap as function of solution flow rate

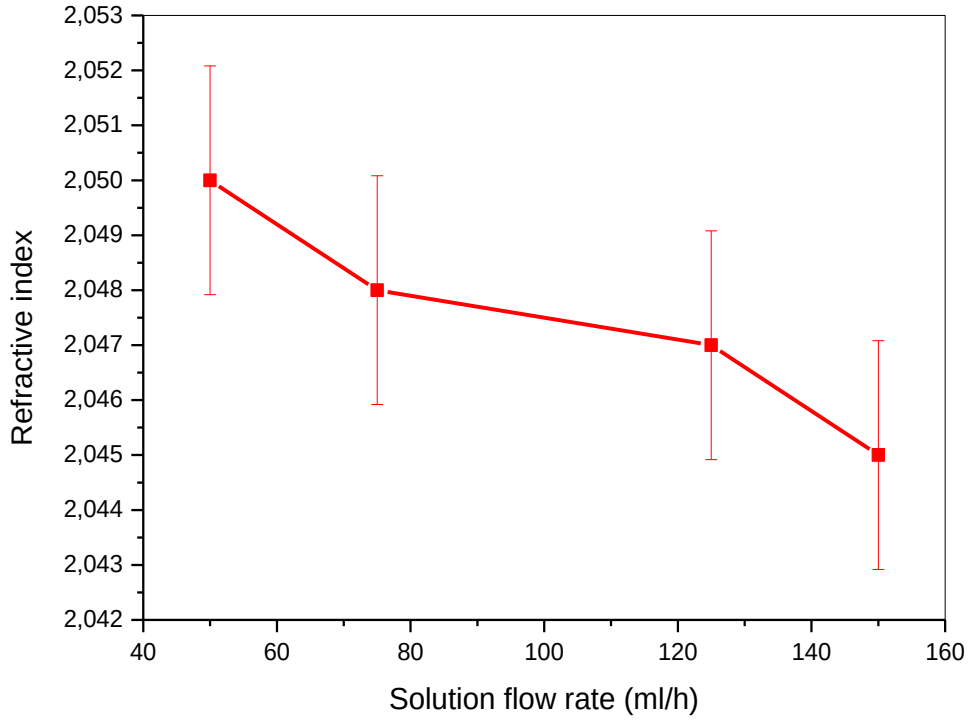

Fig.III.7 refractive index of ZnO as function of solution flow rate.

III.2.7 Electrical properties

The electrical resistivity of ZnO thin films elaborated at different values of solution flow rate is illustrated in Table. III.3. As seen the resistivity increases with increasing the solution flow rate. This increase in electrical resistivity could be explained by reduction of crystallite size which increases the probability of grain boundary scattering [106].

Table.III.3 The resistivity of ZnO thin films at different solution flow rate.

Solution flow rate (ml/h)	Crystallite size D (nm)	Resistivity ρ (Ω. cm)
50	**36.79**	**1.59×10^{-2}**
75	**29.44**	**2.6×10^{1}**
125	**19.97**	**2.7×10^{1}**
150	**20.11**	**4.3×10^{1}**

III.3.Solution concentration effect

III.3.1 Experimental details

ZnO thin films were prepared using a solution contains a zinc acetate dihydrate $ZnC_4H_6O_4.2H_2O$ and methanol CH_3OH as a solvent. The solution was sprayed on heated glass substrates by ultrasonic spray technique. The solution concentration was varied from 0.1 mol/l to 0.2 mol/l. At the beginning of the deposition procedure, the substrates were chemically cleaned. In all samples, the solution flow rate was fixed at 50 ml/l. The deposition temperature equals 350°C, The spray nozzle- substrate distance equal to 5 cm and the deposition time equals 7 min. The elaborated films were characterized in order to study their properties. The films structure was analyzed by X-ray diffraction using XPERT-PRO diffractometer with a Cu $_{K\alpha}$ radiation (λ=0.15405 nm). The optical transmittance spectra in UV–Visible rang were achieved using Perkin Elmer lambda 25 spectrophotometer. The electrical resistivity was measured by two points method.

III.3.2 Structural properties

To identify the crystalline quality of the ZnO thin films elaborated at various solution concentrations. The x rays diffraction is carried out to this study. Figure.III.9 shows the XRD diffraction peaks of the samples. All diffraction peaks such as (100), (002), (101), (110) and (103) indicate that the ZnO films are polycrystalline and crystalized at hexagonal wurtzite structure (JCPDS NO. 36-1451) [94]. It can be seen in the sample elaborated at 0.1 mol/l, all the crystallites have oriented preferentially along to the (002) plane. The appearance of (002) plane in XRD spectrum of this sample refer to this direction of growth in ZnO thin films has a lower surface energy [107, 108] and high atomic density [109]. When, the solution concentration equal to 0.125 mol/l, a competition is created between the (100) plane and (002) plane. In addition, the emergence of other diffraction peaks with significant intensity.

The latter attributed to increase of nucleation sites due to increase of matter quantity deposited on substrate surface. In the case of 0.15 mol/l and 0.2 mol/l, the intensity of (100) plane increases and became predominant, this indicate to the improvement of crystallinty of the films attributed to the increase of electrostatic interactions between the spices due to increase of solution concentration. It can be explained the change of the preferred orientation by the higher deposition rate which leads to change the stoichiometry of the films: the

decrease of incorporation of oxygen atoms with increasing of deposition rate in the elaborated film [110, 111]. The relationship between the intensity of the plane (002) and the deposition rate is shown in figure.III.10. T.V. Vimalkumar and al are found that the intensity of (002) peak decreases with increasing the deposition rate [112].

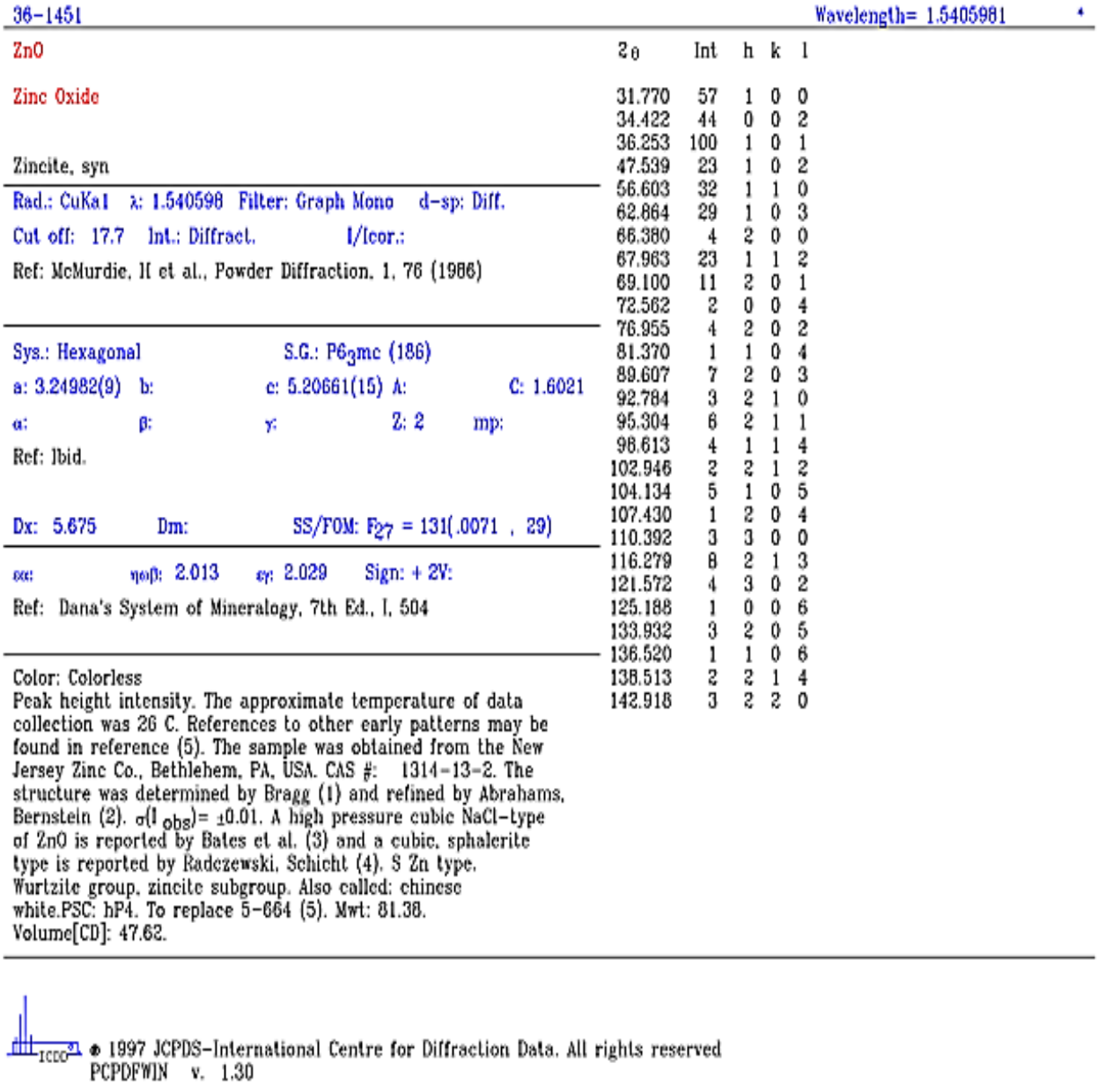

36-1451 Wavelength= 1.5405981

ZnO

Zinc Oxide

Zincite, syn

Rad.: CuKa1 λ: 1.540598 Filter: Graph Mono d-sp: Diff.

Cut off: 17.7 Int.: Diffract. I/Icor.:

Ref: McMurdie, H et al., Powder Diffraction, 1, 76 (1986)

Sys.: Hexagonal S.G.: $P6_3mc$ (186)

a: 3.24982(9) b: c: 5.20661(15) A: C: 1.6021

α: β: γ: Z: 2 mp:

Ref: Ibid.

Dx: 5.675 Dm: SS/FOM: F_{27} = 131(.0071 , 29)

ωα: ηωβ: 2.013 εγ: 2.029 Sign: + 2V:

Ref: Dana's System of Mineralogy, 7th Ed., I, 504

Color: Colorless
Peak height intensity. The approximate temperature of data collection was 26 C. References to other early patterns may be found in reference (5). The sample was obtained from the New Jersey Zinc Co., Bethlehem, PA, USA. CAS #: 1314-13-2. The structure was determined by Bragg (1) and refined by Abrahams, Bernstein (2). $\sigma(I_{obs})$= ±0.01. A high pressure cubic NaCl-type of ZnO is reported by Bates et al. (3) and a cubic, sphalerite type is reported by Radczewski, Schicht (4). S Zn type. Wurtzite group, zincite subgroup. Also called: chinese white.PSC: hP4. To replace 5-664 (5). Mwt: 81.38. Volume[CD]: 47.62.

2θ	Int	h	k	l
31.770	57	1	0	0
34.422	44	0	0	2
36.253	100	1	0	1
47.539	23	1	0	2
56.603	32	1	1	0
62.864	29	1	0	3
66.380	4	2	0	0
67.963	23	1	1	2
69.100	11	2	0	1
72.562	2	0	0	4
76.955	4	2	0	2
81.370	1	1	0	4
89.607	7	2	0	3
92.784	3	2	1	0
95.304	6	2	1	1
98.613	4	1	1	4
102.946	2	2	1	2
104.134	5	1	0	5
107.430	1	2	0	4
110.392	3	3	0	0
116.279	8	2	1	3
121.572	4	3	0	2
125.188	1	0	0	6
133.932	3	2	0	5
136.520	1	1	0	6
138.513	2	2	1	4
142.918	3	2	2	0

Fig.IV.1: JCPDS NO. 36-1451 folder.

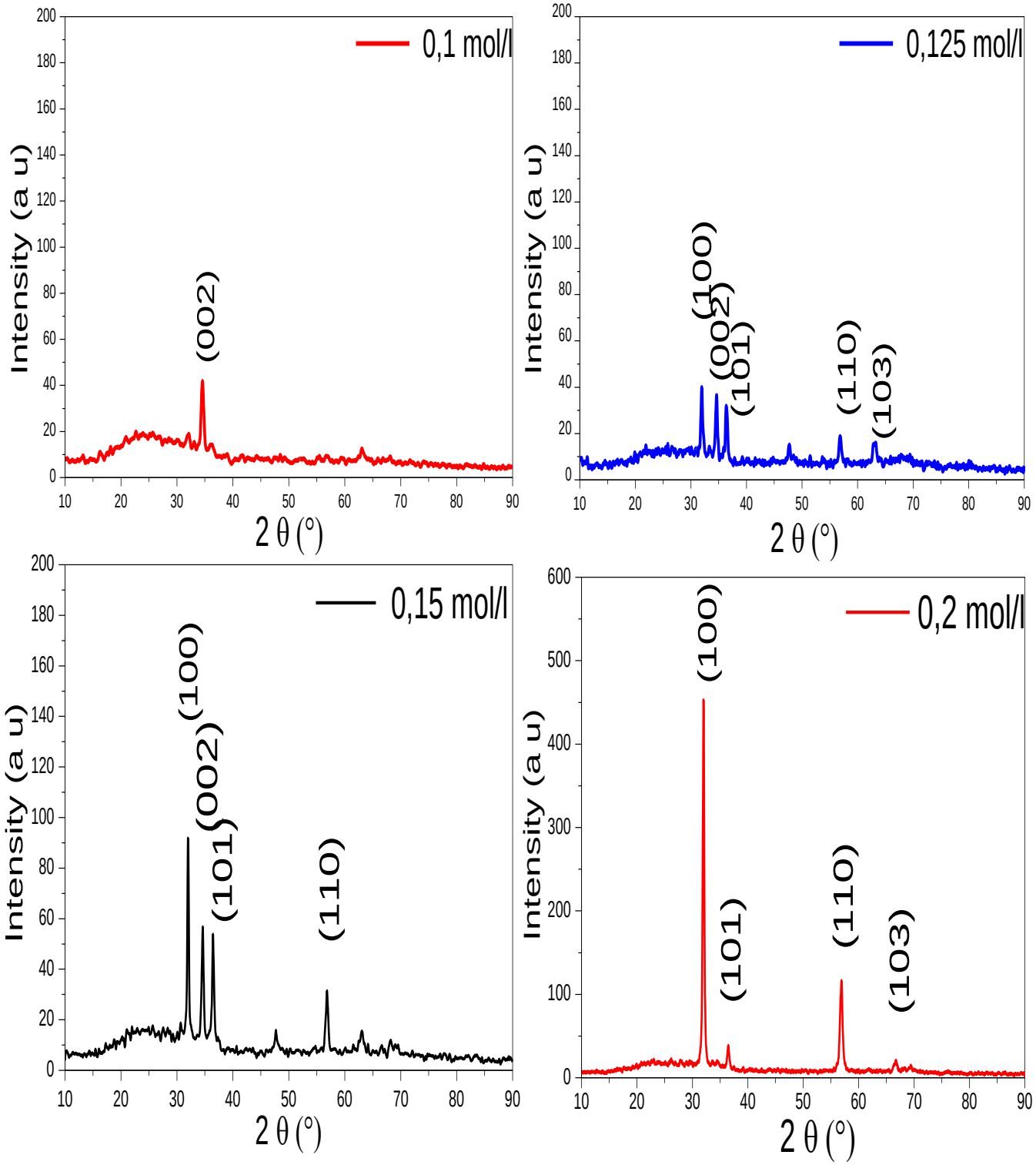

Fig.III.9. the XRD pattern of ZnO thin films as function of solution concentration.

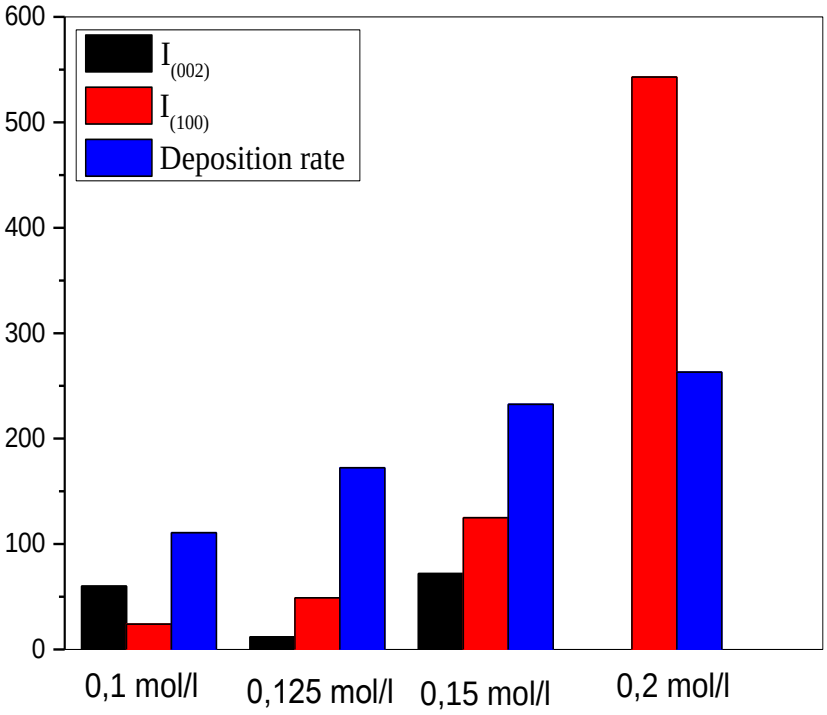

Fig.III.10. (100) and (002) planes intensity and deposition rate as function of solution concentration.

Figure.III.11 represent the variation of crystallite size as function of solution concentration. The grain size increase with increasing the solution concentration. This indicates that the crystalline state of ZnO thin films is improved with increasing the solution concentration confirmed by the decrease of dislocations density (see figure.III.11). It can interpreted the grain size behavior as follow: the increase of grain size is attributed to increase of nucleation sites; the latter confirmed by the appearance of weak peaks in XRD patterns. The rise of solution concentration leads to large grains absorb small grains in order to increase the grain size [113, 114].

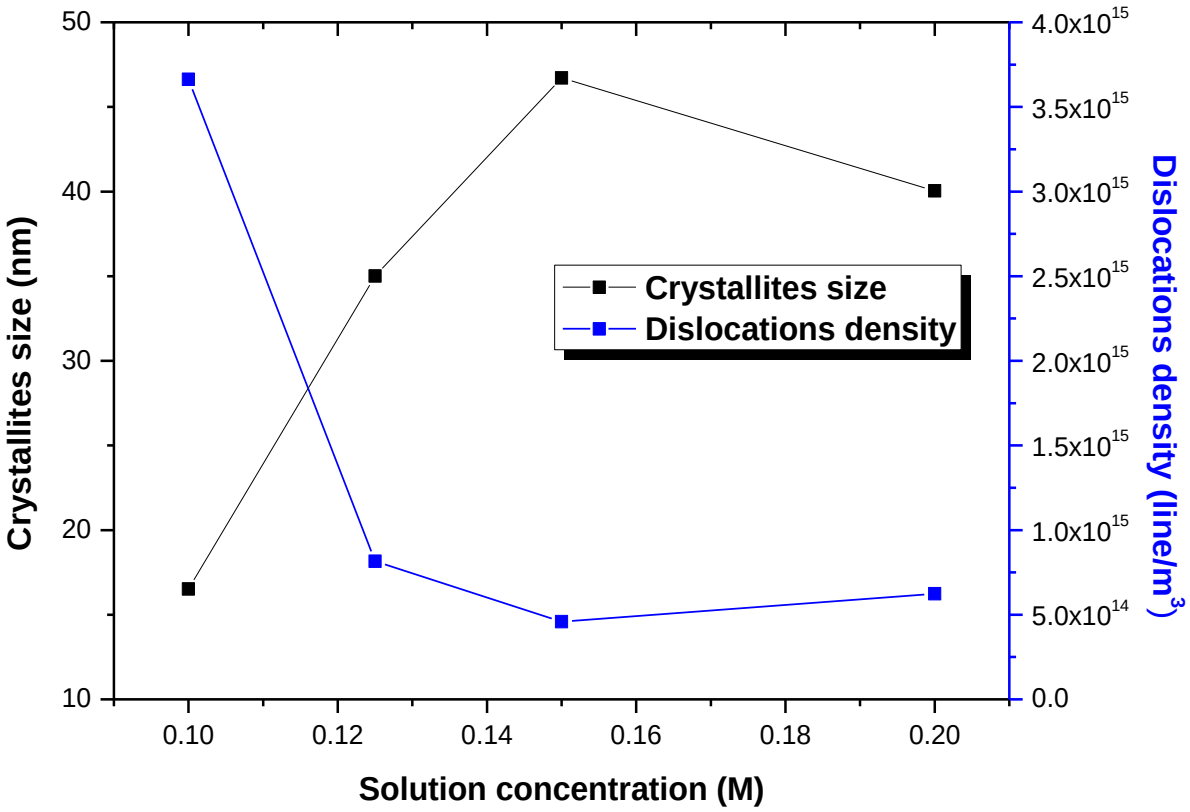

Fig.III.11 variation of grain size as function of solution concentration**.**

III.3.3 Optical properties

The deposition rate of the elaborated films increases with raising of the solution concentration. The raise of the film thickness is attributed to increase of matter quantity deposited on substrate surface due to rise of solution concentration (see figure.III.10) [111].

The optical transmittance of ZnO thin films prepared at various values of solution concentration is shown in figure.III.12. The solution concentration demonstrates a significant impact on the transmittance of ZnO thin films in visible rang, a maximum value of visible transmittance equal to 88 % is observed in the sample prepared when the solution concentration equal to 0.1 mol/l (the film thickness equal to 580 nm). It can be remarked that the optical transmittance of ZnO thin films decreases with increasing the solution concentration. The transmittance behavior causes by the increase of film thickness. The roughness of surface increase with increasing the solution concentration, this is confirmed by disappearance of interference fringe in transmittance curve of sample deposited at higher

solution concentration. This is correlated with XRD analysis which exhibit a highly textured along to (100) plane. The optical band gap is found using the Tauc relationship [115, 101].

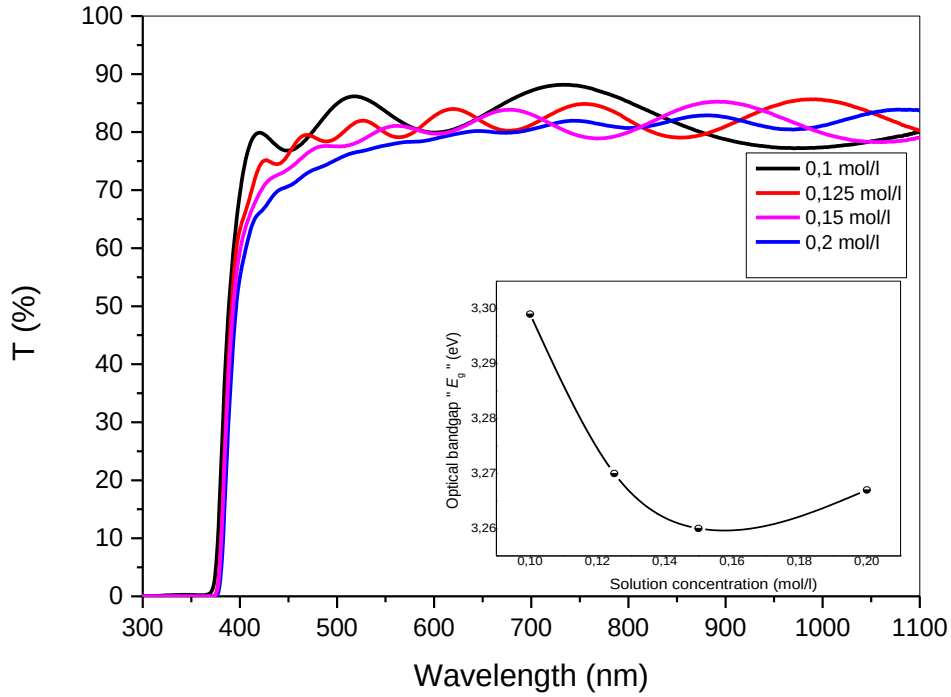

F

ig.III.12 the transmittance spectra and optical band gap as function of solution concentration.

The optical band gap of ZnO thin films is found to decrease with increasing the solution concentration. It may be explain in one hand, the decrease of optical band gap by the increase of the grain size. In other hand, the increase of film thickness leads to increase the presence of adsorbed oxygen. The latter leads to decrease the number of free carriers which is the result of the decrease of optical band gap according to effect of Burstein-Moss.

III.3.4 Electrical properties

Figure.III.13 shows the variation of electrical resistivity as function of solution concentration. As seen that the resistivity of samples increases with increasing the solution concentration. According to XRD spectra, the crystallinty of the samples improves with increasing the solution concentration. The improvement of crystalline state of the samples

leads to decrease the number of electrons scattering centers and trapping centers, which is the result of the decrease of electrical resistivity [116]. However, the electrical resistivity of ZnO thin films increases with solution concentration. Therefore, the roughness of the film surface is responsible factor, which leads to increase the resistivity of the samples. The roughness of the surface is indicated by the disappearance of interference fringe in transmittance spectrum of the film deposited at higher solution concentration. The roughness film leads to appear the adsorbed oxygen situated on the surface. The adsorbed oxygen captures the conduction electrons and fixes them to the surface, which leads to increase the electrical resistivity.

Fig.III.13 Electrical resistivity of ZnO thin films as function of solution concentration.

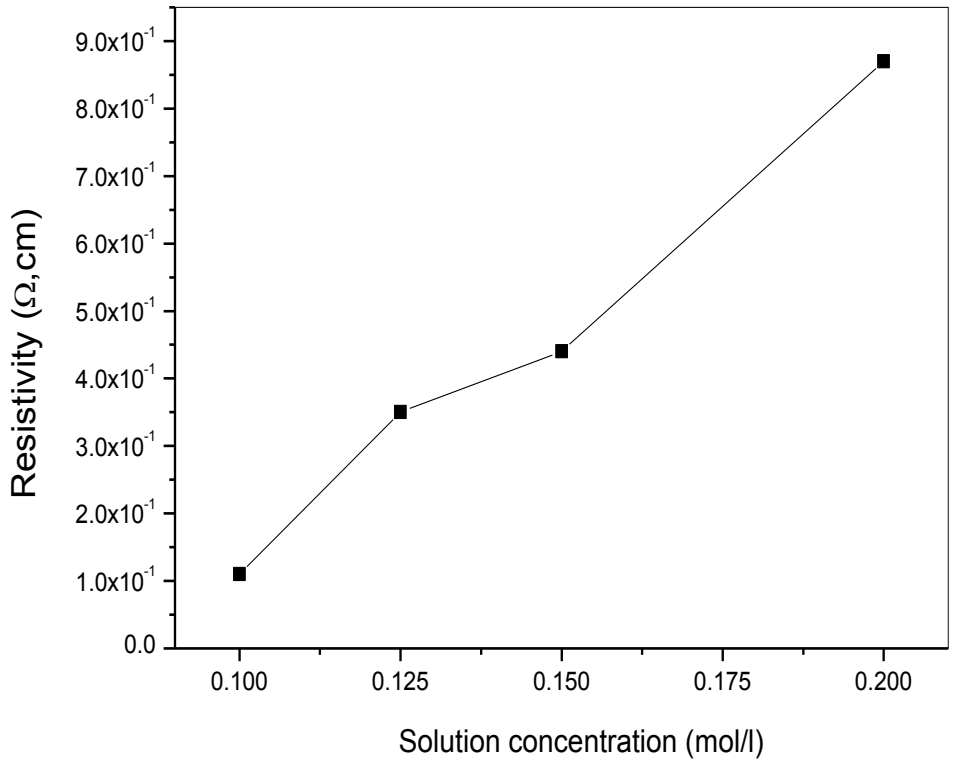

III.4 Conclusion

ZnO thin films were prepared using ultrasonic spray pyrolysis method (USP). Solution flow rate and solution molarity effect on ZnO thin films properties such as crystalline state, crystallites orientation, optical transparency, optical band gap and electrical conductivity was investigated. In the case of solution flow rate parameter, we found that the films are polycrystalline. The crystallite size decreases with increasing the solution flow rate. The optical transparency of our films invisible rang depending on solution flow rate. The optical band gap increases with the solution flow rate. And the case of solution concentration, we observed that the crystalline state is modified by varying of the solution concentration. When the solution concentration raised from 0.1 mol/l to 0.2 mol/l. The preferred orientation of crystallites change with changing the solution concentration. The resistivity increases from $1.1 \times 10^{-1}\Omega.cm$ to $8.1 \times 10^{-1}\Omega.cm$. The optical transmittance of the elaborated samples reach to 88%. Finally, it can be conclude that the solution flow rate and solution concentration have a significant impact on ZnO thin properties. The obtained results shows that the optimal values of two recently studied parameters for photovoltaic applications are 50 ml/h and 0.1 mol/l respectively. This study demonstrated that the ZnO thin characteristics depend of oxygen content in elaborated films.

Chapter IV

Influence of substrate temperature

IV.1 Introduction

As commonly known, that the ZnO thin films properties are significant effected by technique of elaboration and deposition parameters. In the case of spray pyrolysis, the main parameter which is widely influenced on ZnO thin films properties is substrate temperature which controls the spices energy and motion onto substrate surface. In this chapter, ZnO thin films have been deposited by ultrasonic spray pyrolysis. Substrate temperature effect on structural, optical and electrical properties of ZnO films have been investigated.

IV.2 Experimental details

ZnO thin films were prepared by spraying a solution contains a 0.1 mol/l of zinc acetate (***$ZnC_4H_6O_4.2H_2O$***) in a volume of methanol CH_3OH as a solvent on heated glass substrates using ultrasonic spray process. Before the deposition, the substrates were chemically cleaned. In all samples, the solution flow rate was kept at 50 ml/l. The deposition temperature equals 250 °C, 300 °, 350°C, 450°C and 500°C. The spray nozzle- substrate distance equal to 5 cm. The films were prepared in atmospheric pressure for 5 min as a time of deposition. The elaborated films were characterized in order to study their properties. The films structure was analyzed by X-ray diffraction using XPERT-PRO diffract meter with a Cook radiation (λ=0.15405 nm). The optical transmittance spectra in UV–Visible rang was achieved using Perkin Elmer spectrophotometer.

IV.3 Sprayed solution droplets

Figure.IV.1 represents the relationship between substrate temperature and droplets projections surface, which it indicates that the latter was decreased with increasing the substrate temperature. It can be explained this relationship by the decrease of sprayed solution droplets volume due to the evaporation of solvent farther the substrate surface results of the increase of substrate temperature.

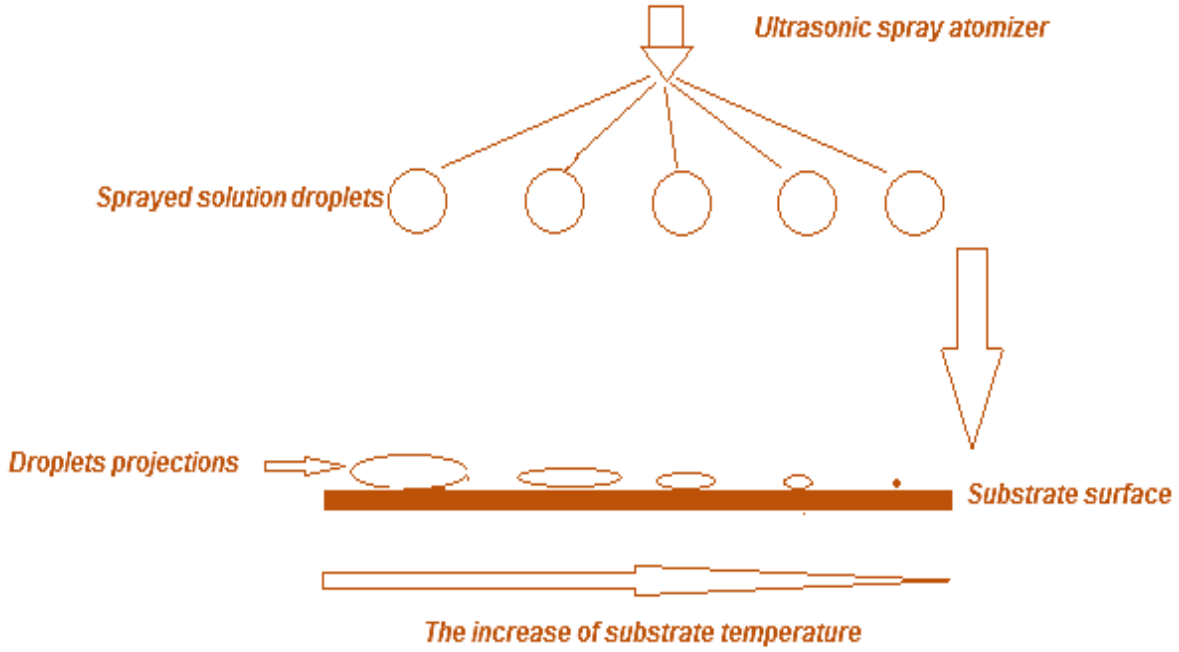

Fig.IV.1 schematics represent the influence of substrate temperature on solution droplets.

[Thin Film Deposition Using Spray Pyrolysis, DAINIUSPEREDNIS and LUDWIGJ.GAUCKLER, Journal of Electro-ceramics, 14,103–111, 2005.] Modified

IV.4. Structural properties

IV.4.1 XRD analysis

The X rays diffraction is carried out to study the crystalline quality of the ZnO thin films elaborated at various substrate temperatures. Figure.IV.2 shows the XRD pattern of the samples.

It can be seen that the formation of ZnO crystallites in the films elaborated at low deposition temperature (less than 350°C). Those crystallites have oriented along to the (100) orientation which c-axis is parallel to substrate surface. The appearance of this orientation attributed to thermal energy which is lower than kinetic energy of sprayed particles. This leads to presence of organic materials residual on substrate surface [117]. After T_s= 350 °C, a ZnO crystallites were formed which were oriented preferentially along to the (002) orientation perpendicular to substrate surface according to (JCPDS NO. 36-1451) [94]. It well known, that the preferred orientation of ZnO thin films is (002) orientation, because the surface energy and lattice strain at this orientation will be minimized [118]. The appearance of ZnO compound attributed to increase of deposition temperature leads to improve of zinc oxidation.

IV.4.2 Crystallite size

The crystallite size (*D*) represent the crystalline quality of the ZnO films was calculated using the classical Scherrer formula. [96]. Figure. IV.3 represents the variation of crystallite size with the substrate temperature. The crystallite size is calculated from the (002) diffraction peak.

It can be remarked that crystallite size increases with increasing the substrate temperature (see figure.IV.3). It can explain this variation as follow: At the beginning $Ts < 350\ °C$, the majority of grains have small size was formed due to the amount of ZnO results of weak oxidation of zinc atoms due to substrate temperature. This provoke the formation of small islands and the growth mode is layer by layer such as the lower layer consist ZnO solid films and the upper layer of zinc acetate [119].

At Ts$\geq 350\ °C$ the increase of grain size is attributed to increase of nucleation sites due to increase of zinc oxidation with increasing the substrate temperature. This engender the

decrease the total surface energy and the growth mode changed to islands growth, which explain the appearance of 002 orientation perpendicular of substrate surface.

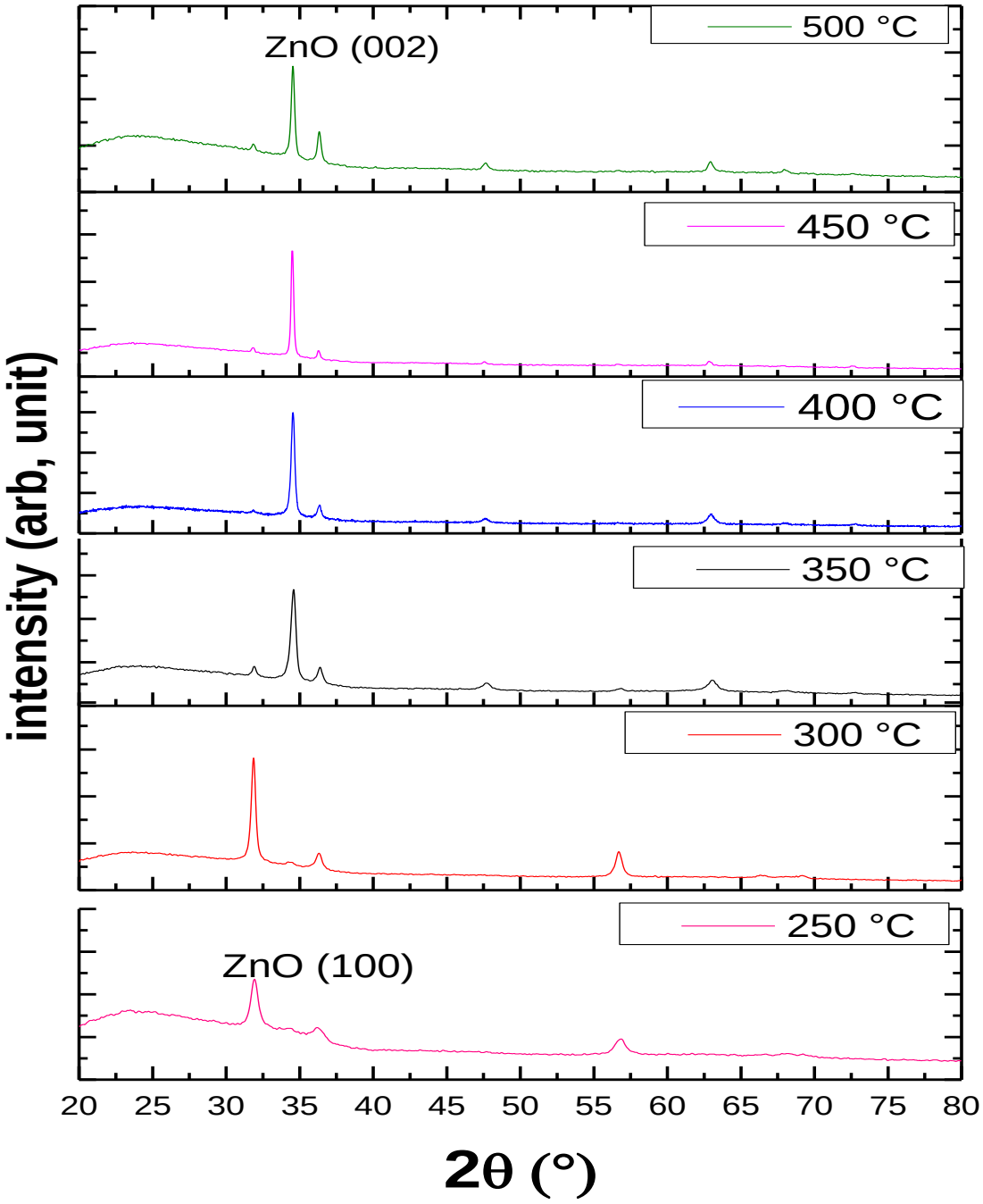

Fig.IV.2 *XRD patterns of zinc oxide as function of substrate temperature.*

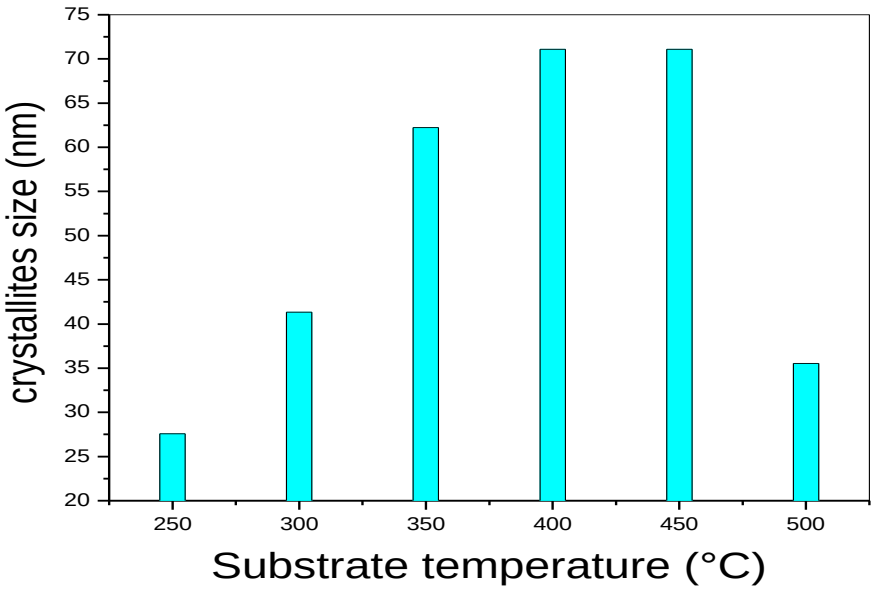

Fig.IV.3 crystallite size of ZnO thin films as a function of substrate temperature.

IV.4.3 Strain and lattice parameter

It can be seen that the lattice parameter c decreases for the films deposited at substrate temperature increase from 250 °C to 300 °C. The decrease of lattice parameter is attributed to increase of compressive strain which permit to create a small grains oriented parallel to the substrate surface.The increase of substrate temperature more than 300 °C engender the increase of lattice parameter. The rise of lattice parameter ***r***esults of the decrease of lattice strain ε due to reduction in defect density inside the films, which involves a network relaxation [120, 121]. In this case, the crystalline state of the films has been improved and the growth mode changed to island growth with increasing the substrate temperature due to decrease total surface energy which impose the sprayed material species to create a small island perpendicular on substrate surface. The decrease of lattice parameter c in the films elaborated at 500 °C may be due to the deterioration of crystallinity of these films.

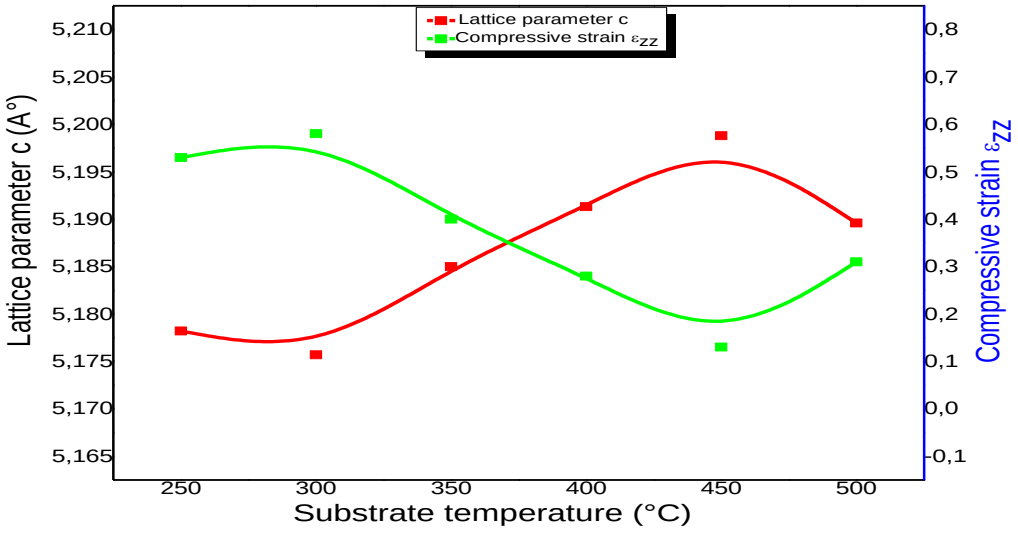

Fig.IV.4 lattice parameter and compressive strain as a function of substrate temperature.

Table.1 the structural parameters of ZnO thin films as function of substrate temperature.

Substrate temperature (°C)	Film thickness (nm)	Cell parameters (nm)		Crystallite size D (nm)	Micro-strain (***ε***) x100
		c	a		
250	695	0.51782	0.32363	10,36	-0,53
300	565	0.51757	0.32348	20,72	-0,58
350	450	0.51850	0.32406	62,23	-0,40
400	200	0.51913	0.32445	71,1	-0,28
450	140	0.51988	0.32492	71,09	-0,13
500	110	0.51896	0.32435	30.99	-0.31

IV.5 deposition rate

The deposition rate of zinc oxide (ZnO) thin films elaborated at various substrate temperature is displayed in Figure.IV.5. It can be observed that deposition rate decreases with increasing the substrate temperature.it can be explained the decrease of deposition rate as follow; at low substrate temperatures $(Ts < 350\ °C)$ the chemical reaction to forming ZnO solid films did not complete due to kinetic energy of solution droplets which is more than thermal energy . In this case, the growth mode is layer by layer such as the lower layer consist ZnO thin films and the upper layer of zinc acetate [119]. It can be observed, the increase of substrate temperatures,$(Ts \geq 350\ °C)$provoke the decrease of deposition rate. It can be explain by the evaporation of solution farther the substrate surface.

Fig.IV.5 Deposition rate of ZnO thin films as function of substrate temperature.

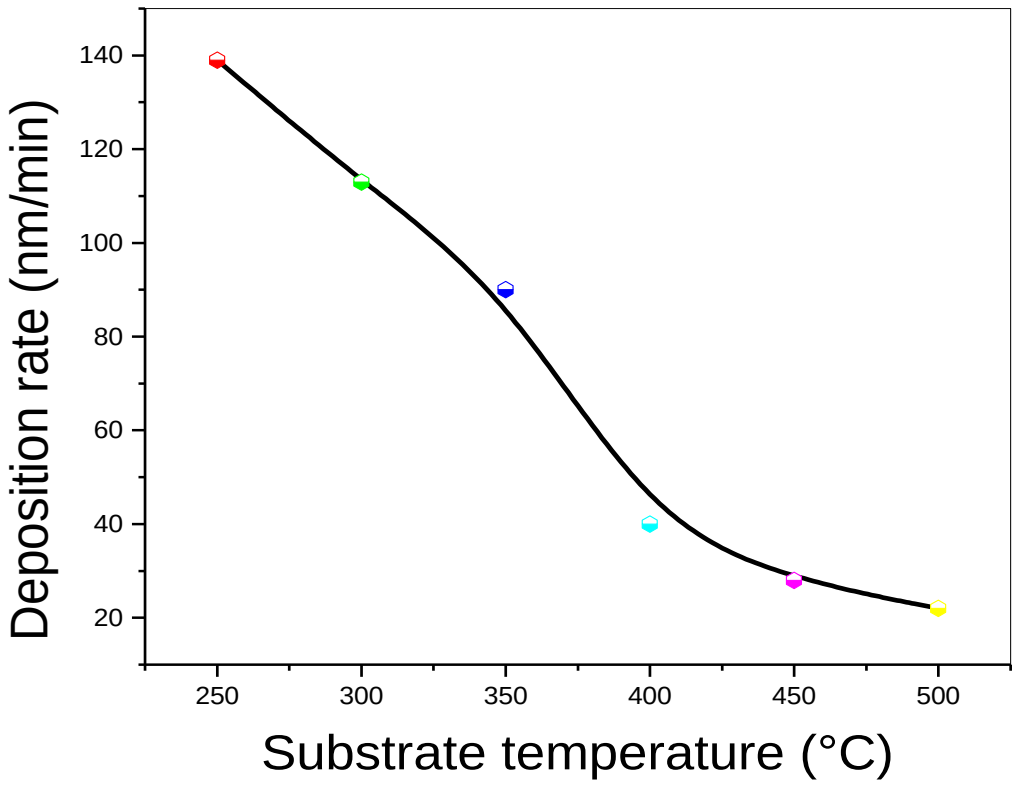

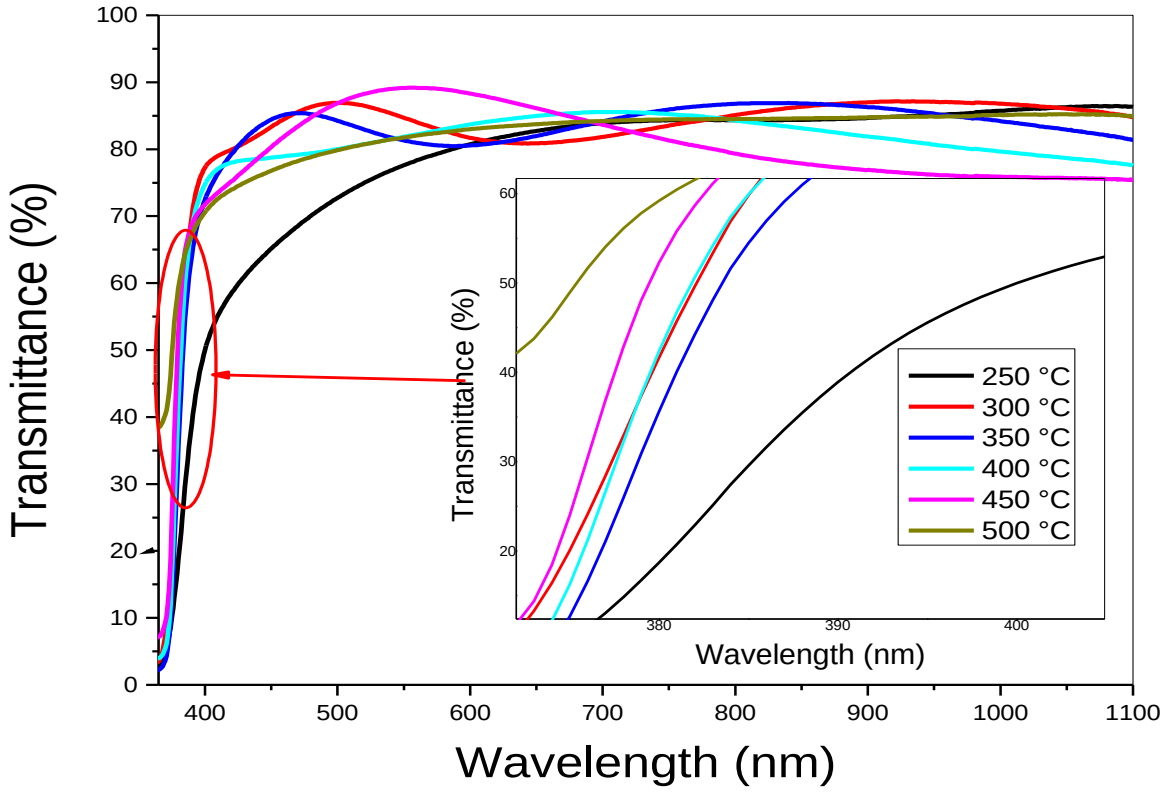

Fig.IV.6 Transmittance spectra of ZnO thin films as a function of wavelength.

IV.6 Optical properties

IV.6.1 Optical transmittance

The optical transmittance of ZnO thin films elaborated at different substrate temperature is displayed in figure. IV.6. The substrate temperature exhibit an important influence on the transmittance of ZnO thin films in visible rang, a maximum value of visible transmittance reaches 90% in the film which deposited at 450 °C. The result indicates that the sample have relatively high quality with very few internal defects or impurities and the crystallization of this sample is completed, which reduces the photon scattering.

IV.6.2 Optical band gap Eg

It can observed that optical band gap increases with the increase the substrate temperature (see figure.IV.7 and IV.8). The raise of optical band gap might be accounted by

the decrease of disorder associated with the stress state of the samples[122] and the improvement the crystalline state of films due to rise the substrate temperature [123].

Figure.7 represent another attitude repose onto the first diversion of transmittance data $dT/d\lambda$ as a function of photon energy $h\nu$ [124]. The optical band gap values were obtained from photon energy which corresponding the summit of peak in the curve $dT/d\lambda = f(h\nu)$. It can be seen that optical band gap increases with increasing the substrate temperature. The increase of band gap could be explained by the improvement of films crystallinity due to rise of substrate temperature. It can be remarked that full width and half maximum (FWHM) of peak which corresponding the band gap decreases with substrate temperature, which confirm that the crystalline state was improved with increasing the substrate temperature.

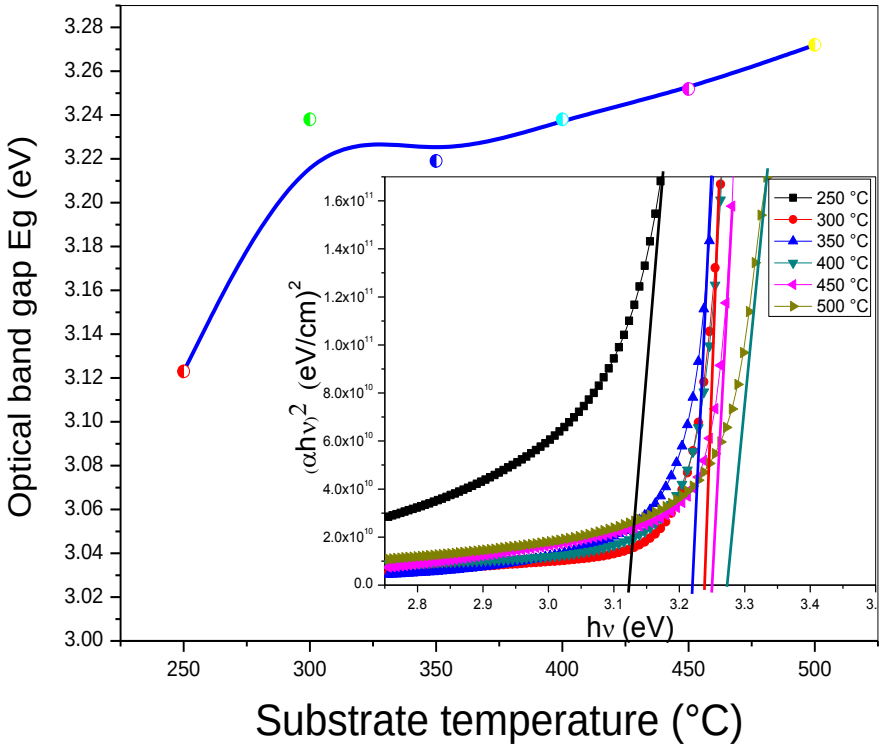

Fig.IV.7 Optical band gap of ZnO thin films synthesized at different Ts. The inset is plot of $(\alpha hv)2$vs hv.

Table.2 optical band gap values of ZnO thin films deposited at various substrate temperatures.

Substrate temperature Ts (°C)	*Optical band gap Eg (eV)*	
	$dT/d\lambda$	$(\alpha h\upsilon)^2$
250	3.235	3.123
300	3.28	3.238
350	3.279	3.219
400	3.288	3.240
450	3.298	3.252

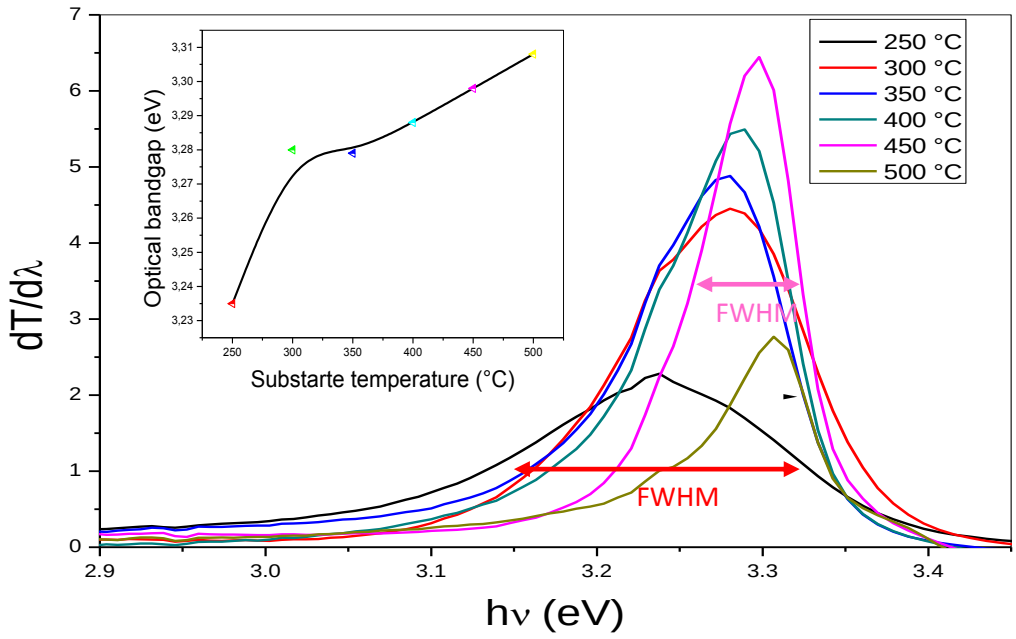

Fig.IV.8 *first derivate of transmittance versus photon energy. The inset is plot of Eg vs Ts*

IV.7 Electrical conductivity

Figure.IV.9 represents the variation of electrical conductivity of ZnO thin films as a function of substrate temperature. It well known, that the Inequality in atomic percent of state of ZnO thin films. metal and oxygen atoms creates a free carriers in thin film which gives the

electrical conductivity of TCO thin films. It can be seen the electrical conductivity increases with increasing the substrate temperature until 450 °C. The increase of electrical conductivity can be explained by increasing of zinc oxidation due to the increase of substrate temperature. It can be explained as follow; for Ts=250 °C and Ts=300 °C a partial decomposition of zinc acetate. In this case, a few free carriers have been created results of the non-stoichiometry of ZnO solid film which was obtained. The increase of substrate temperature (Ts≥350 °C) provokes the improvement of zinc atoms oxidation. In this case, the growth direction is changed and the obtained ZnO thin films become more and more compact [106]. The decrease of conductivity at 500 °C attributed to the deterioration of crystalline state of elaborated films.

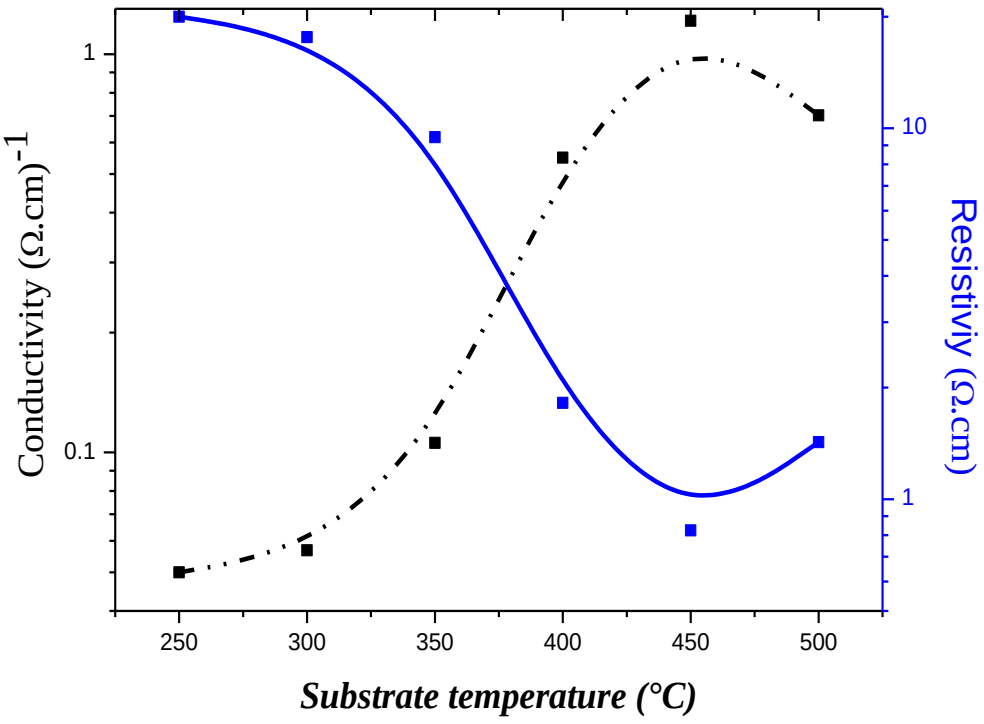

Fig.IV.9 *electrical conductivity of ZnO thin films as a function of substrate temperature.*

IV.8 Photoluminescence spectra

Figure.IV.10 displays the room temperature photoluminescence spectra in wavelengths ranging from the ultraviolet (UV) to the visible light for all the elaborated thin films. There are three peaks, the first is stronger located at 386 nm (3.21 eV) near band edge (NBE) corresponding of UV emission originates from the exciton recombination for the films prepared at substrate temperature equal to 250°C, 300°C, 350°C, 400°C and 500°C [125]. However, it is situated at 375 nm (3.3 eV) for the film elaborated at 450°C. It can be observed, the intensity of this peak increases with substrate temperature. This indicates the film cristallinity improves with the increase of substrate temperature [126]. The other peaks are weak as compared with the first peak. The second peak is positioned at 483 nm equivalent the bleu-green emission which may be result from the electron transition from the level of the ionized oxygen vacancies to the valence band [127]. The third situated at 531nm (green emission). This emission consequence to the formation of oxygen anti-sites (Ozn) in the beginning stage of building up of the (002) plane, which the substrate temperature may not be able to supply enough Zn ions to fill the plane fully [112].

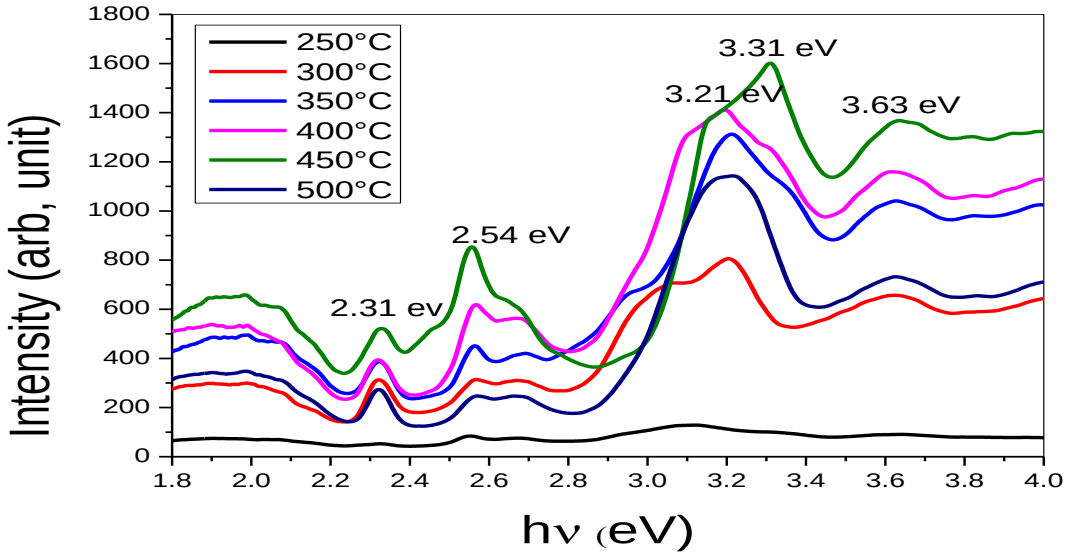

Fig.IV.10 PL spectra of ZnO thin films as a function of substrate temperature.

IV.9 Conclusion

ZnO thin films were prepared by ultrasonic spray pyrolysis method using $Zn(CH_3COO)_2 \cdot 2H_2O$ as the precursor. The orientation of crystallites depend of substrate temperature. Weak oxidation of zinc atoms gives a ZnO thin films oriented preferentially along to 100 plane. The obtained results shows that the elaborated films have good optical transmittance in visible rang.

The elaborated films have UV emission increases with increasing the substrate temperature. The electrical conductivity is varied between 0.05 $(\Omega\ cm)^{-1}$ and 1.2 $(\Omega\ cm)^{-1}$. Finally, it can be conclude that the optimal value of substrate temperature is 450 °C for thin films used in photovoltaic applications.

Chapter V:

Tin doping concentration and Annealing temperature effect on ZnO thin films properties.

V.1 Introduction

This chapter contains two parts, the first part talk about of the effect of tin concentration in ZnO thin films properties of elaborated film.the second part focused to study the influence of annealing temperature on structural, optical and electrical properties.

V.2 the effect of tin doping concentration

V.2.1 experimental details

TableVI.1. the experimental details

	Tin doped Zinc oxide (Sn/ZnO)
Solution concentration Solution flow rate	**0.1 mol/l** **50 ml/h**
Substrate temperature	**450 °C**
Deposition time	**5 min**
spray nozzle – substrate distance	**5 cm**
Tin doping concentration (x 10^{-3} mol/l)	**0, 1, 2, 3, 4, 5**
USED TECHNIQUE	**Ultrasonic spray process (USP)**

V.2.2 Structural properties

V.2.2.1 XRD analysis

Fig.V.1 displays the X-ray diffraction patterns of undoped and Sn-doped ZnO thin films deposited on a glass substrate. The diffraction patterns fit correctly with the ZnO structure, according to the JCPDS Card File No.:36-1451[94]. It was apparent that ZnO thin films deposited on glass substrate composed of a ZnO phase oriented along to the c axis with a significant (002) peak, indicating that the layers are highly textured along the c axis. These observations are in agreement with those reported in [128].

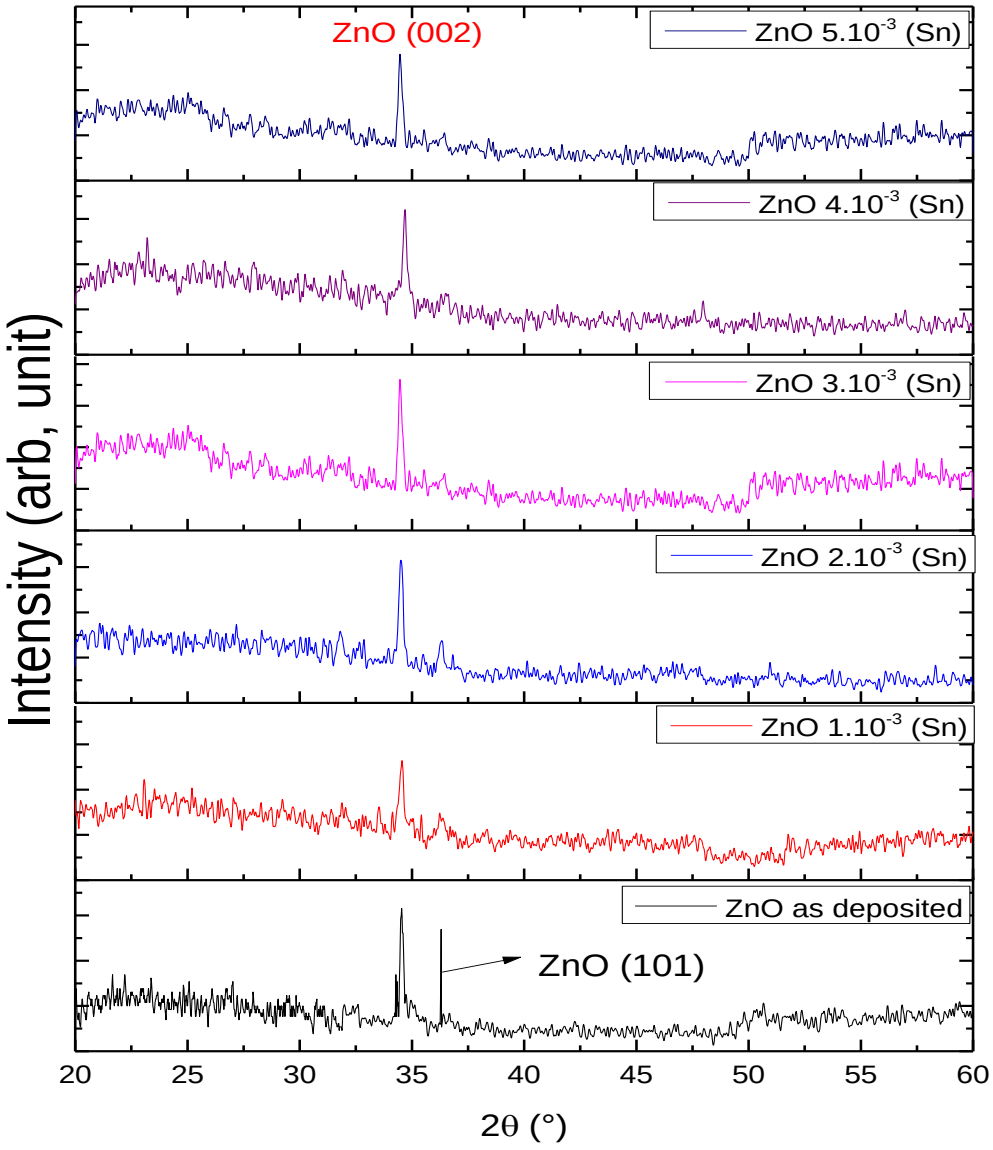

FigV.1 XRD spectra of Sn/ZnO thin films elaborated by ultrasonic spray process (USP)

V.2.2.2 Crystallite size and stress

The variation of crystallite size and compressive stress of undoped ZnO thin films and tin doped ZnO is displayed in figure.V.2. It can be seen that the crystallite size increase with increasing the Sn doping concentration. This can be attributed to micro-strains produced by residual stress [129, 130]

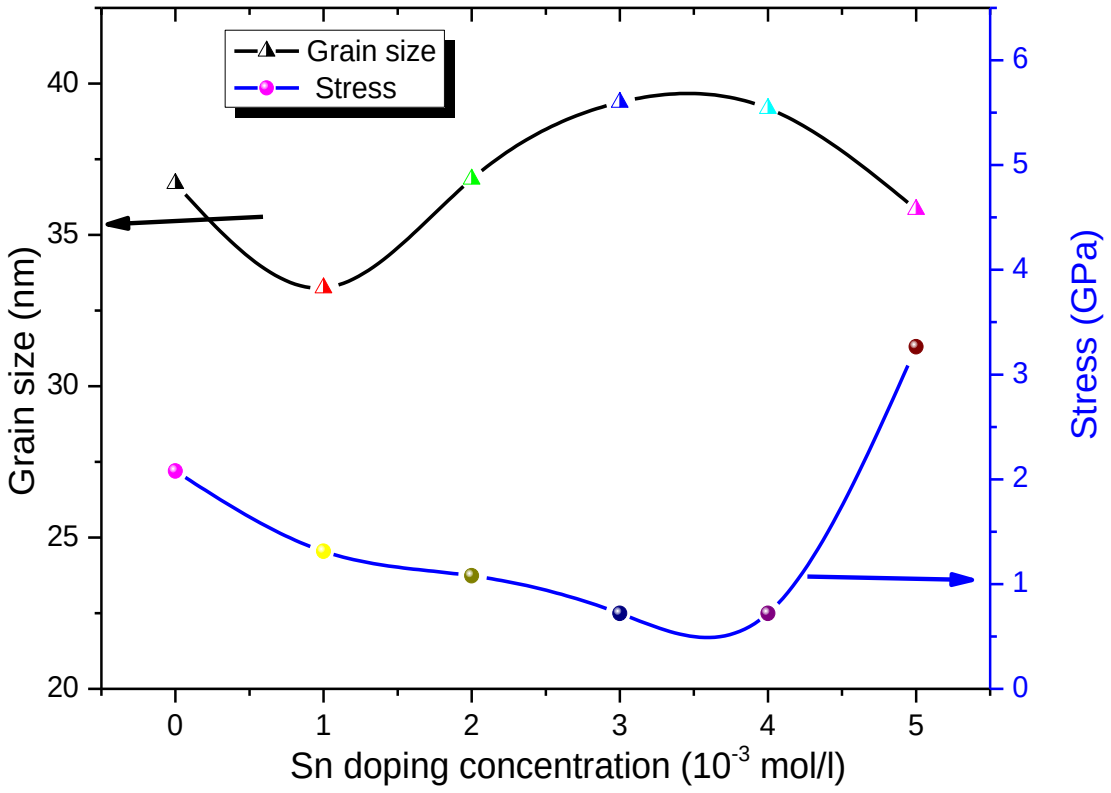

FigV.2 Crystallite size and compressive stress of Sn/ZnO thin film

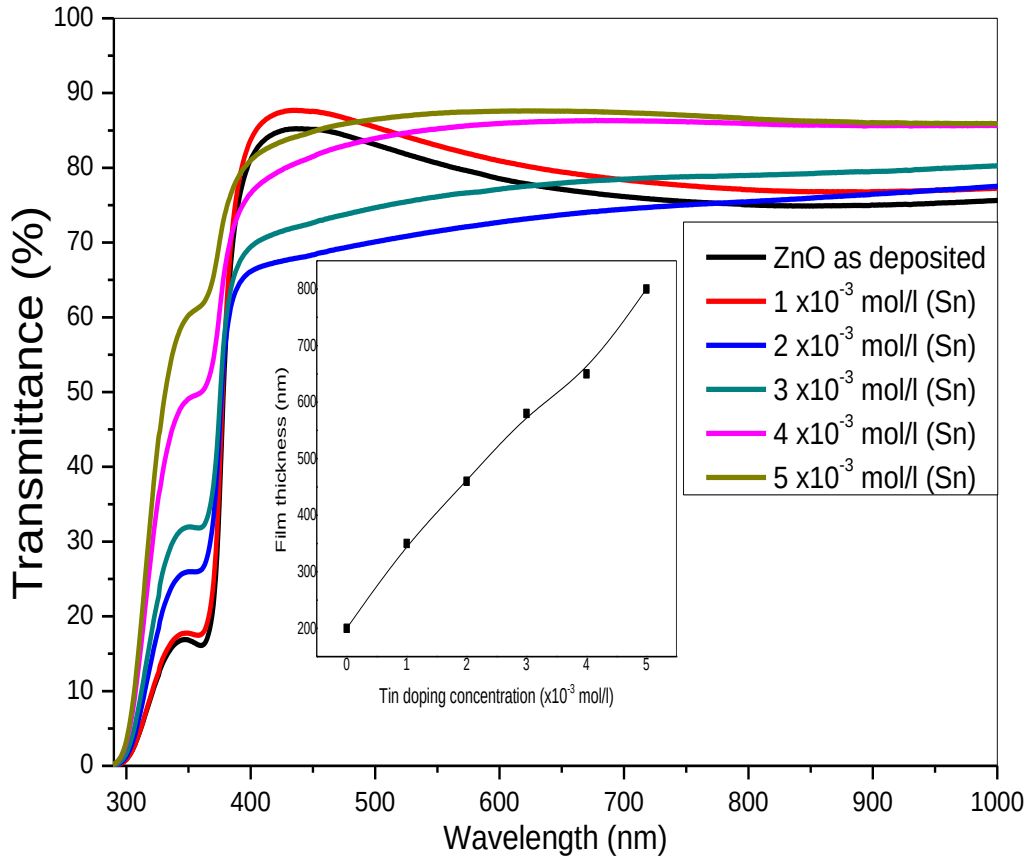

FigV.3 transmittance spectra and film thickness of undoped ZnO and Sn doped ZnO thin films.

V.2.3 Optical properties

The optical transmittance of ZnO thin films elaborated at different tin doping concentration is displayed in figure.V.3. As seen that the transmittance of ZnO thin films in visible rang around to 80%. The increase of tin concentration leads to decrease the optical band gap due to increase the films thickness.

Figure.V.4 represents the variation of optical band gap as a function of tin doping concentration. It can be seen that the optical band gap decreases with increasing the tin concentration. It can be interpreted the decrease of optical band gap by the increase of grain size. Many researchers have reported that the optical band gap decreases with increasing doping level [131]. Hamberg and Granvist [132] showed that the band gap shift is the result of

two competing mechanisms: a widening due to the Burstein Moss effect and a narrowing due to electron–ion and electron–electron scattering. Burstein–Moss effects are enhanced as the electron concentration increases.

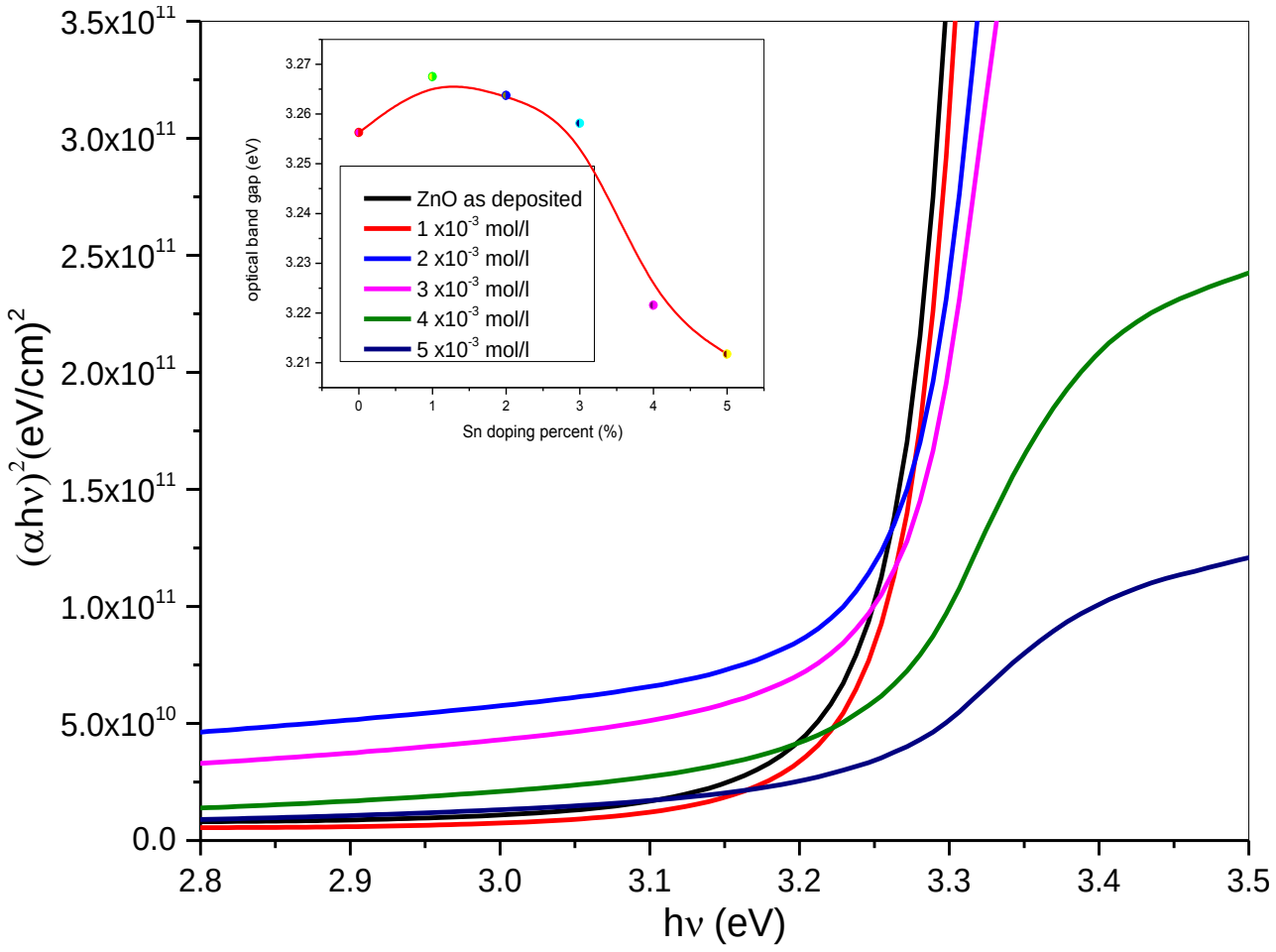

FigV.4. plot of $(\alpha hv)2$ vshv. The inset is optical band gap of ZnO thin films

V.2.2.4 Electrical resistivity

Figure.V.5 represent the resistivity as a function of tin concentration. As seen that the resistivity of the films decreases with increasing the tin concentration. It can be explain the decrease of resistivity by increasing of crystallite size and reduced of scattering grain boundaries. Other side, the increase of film conductivity due to the increase in carrier concentration of TZO thin films was due to the substitutional incorporation of Sn^{4+} ions at Zn^{2+} cation sites.

The increase of electrical resistivity after 3.10^{-3} mol/l of Sn doping concentration might be due to deterioration of crystalline state of elaborated films results of increase of tin doping quantity incorporated in ZnO thin films network in few time of deposition. In this case, a rapidly deposition of Sn/ZnO thin films leads to deteriorate the crystalline state of the films.

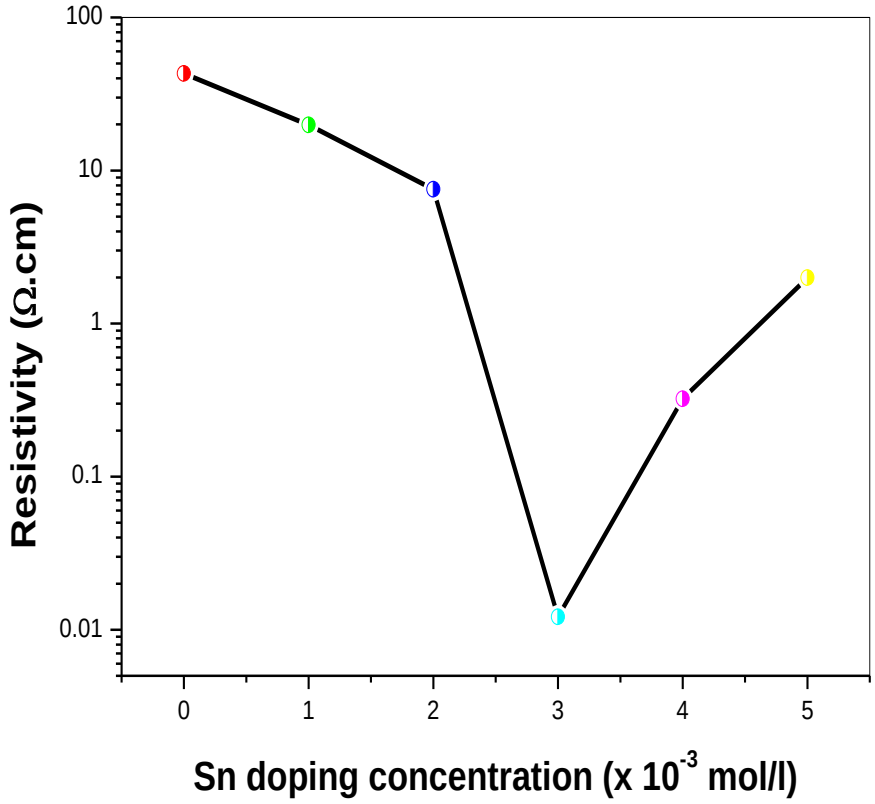

FigV.5. electrical resistivity of ZnO thin films synthesized at different tin concentration.

V.3 the effect of annealing temperature

V.3.1 experimental details

Table.V.4 experimental details.

	effect of annealing temperature
Solution concentration	**0.1 mol/l**
Solution flow rate	50 ml/h
Deposition temperature	450 °C
Deposition time	5 min
spray nozzle – substrate distance	5 cm
Annealing temperature (°C)	500, 550 and 600
USED TECHNIQUE	Ultrasonic spray process (USP)

V.3.2 Structural properties

V.3.2.1 XRD analysis

Figure V.6 represent the XRD pattern of ZnO thin films treated at different values of annealing temperature. As seen that ZnO thin films crystallized at hexagonal close packing (hcp) and all crystallites was oriented along to (002) orientation. It can be observed that crystalline state of elaborated films improved with increasing the annealing temperature [133].

Table.V.5 film thickness of ZnO thin films as a function of annealing temperature..

samples	*Film thickness (nm)*
As deposited	*630*
Annealed at 500 °C	*457*
Annealed at 550 °C	*400*
Annealed at 600 °C	*280*

V.3.2.2 Crystallites size

The variation of crystallites size as a function of annealing temperature is displayed in figure.V.7. It is quite clear that the crystallites size increases after annealing treatment, which might be due to recrystallization of the film [134].

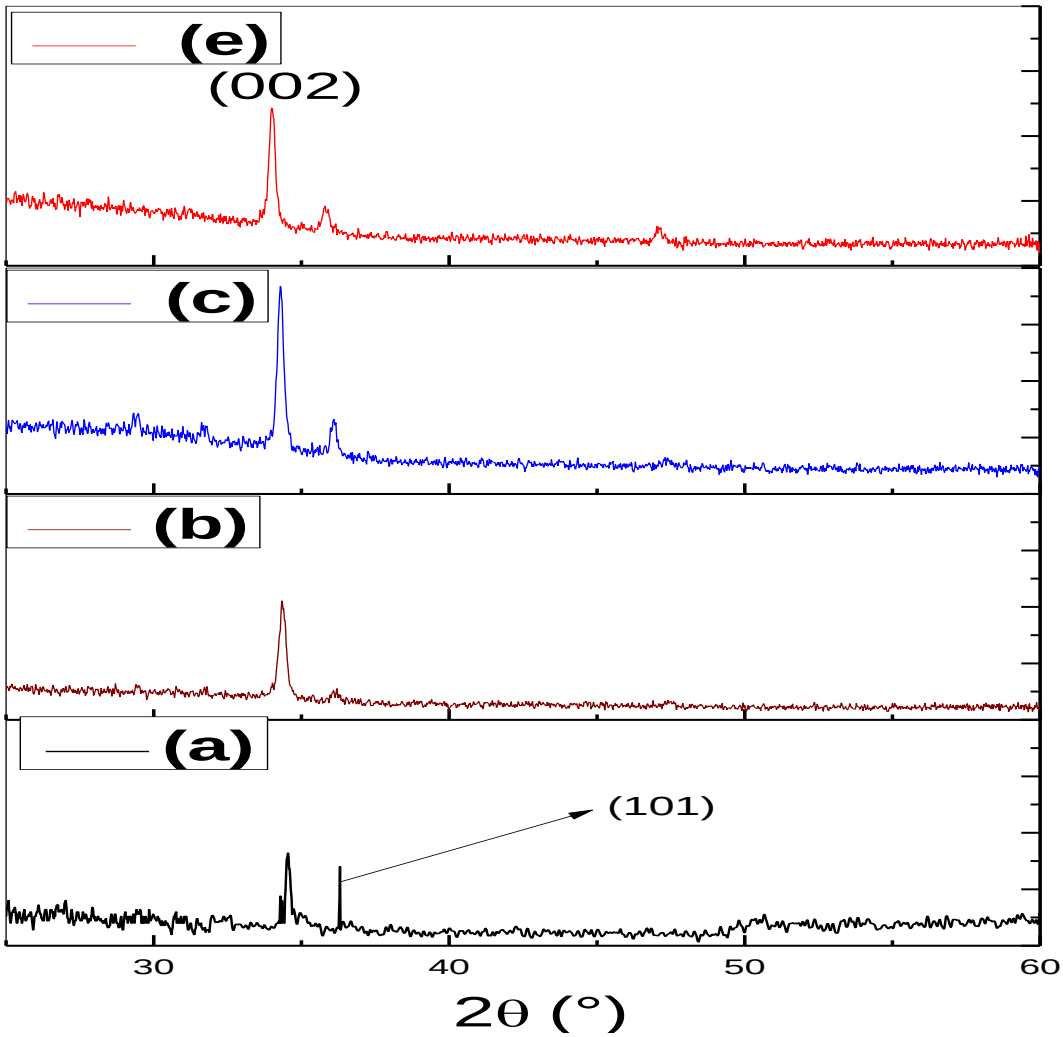

FigV.6 XRD pattern of ZnO thin films (a) as deposited, (b) annealed at 500 °C, (c) annealed at 550 °C and (d) annealed at 600 °C.

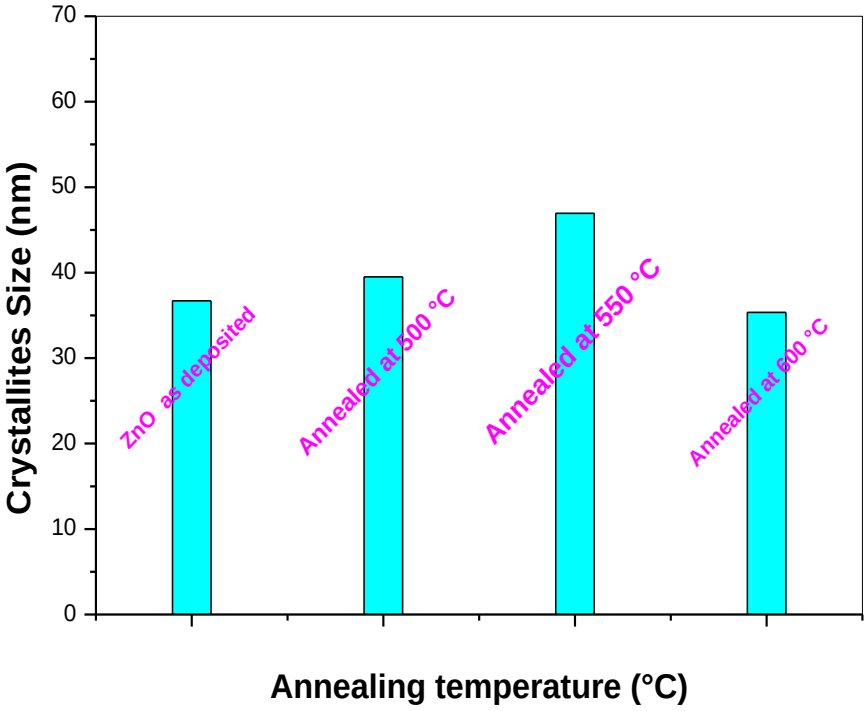

Fig.V.7 Crystallite size of undoped ZnO thin films as a function of annealing temperature.

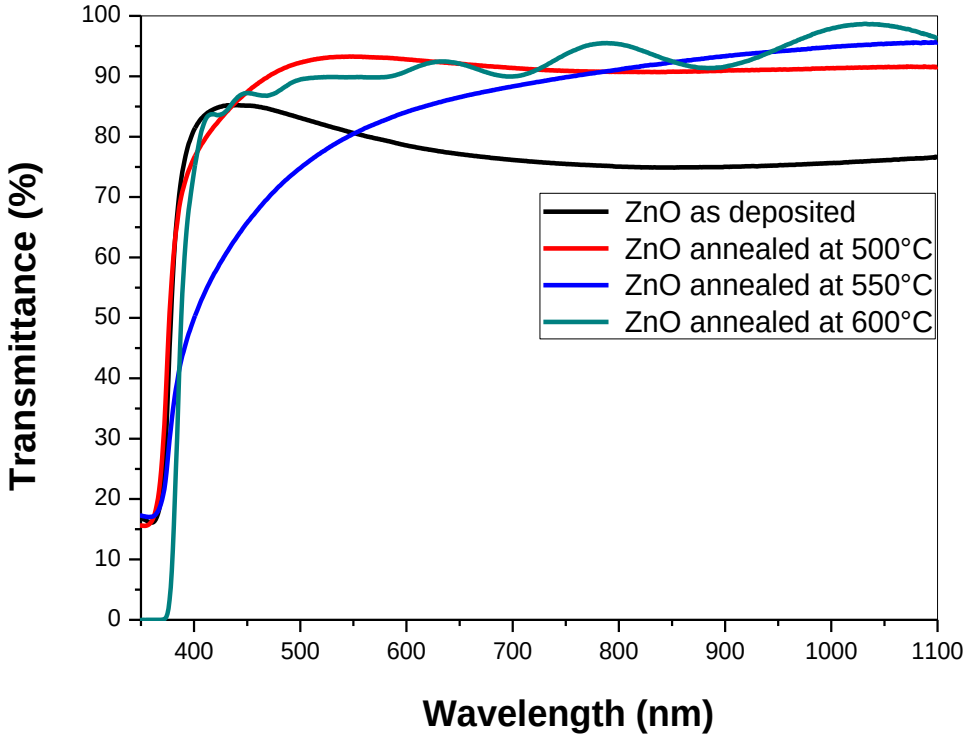

Fig.V.8 transmittance spectra of ZnO thin films

V.3.3. Optical properties

The effect of annealing temperature on undoped ZnO thin films transparency is shown in figure.V.8. It can be observed that the transmittance of elaborated films increases with increasing the annealing temperature. The transmittance behavior of films as a function of annealing temperature might be due to the improvement of crystalline state of films which provoke the reduction of structural defects [134]. Figure.V.9 represent the variation of optical band gap as a function of annealing temperature. It can be explain the optical band gap behavior by the increase of crystallites size a due to increase the annealing temperature.

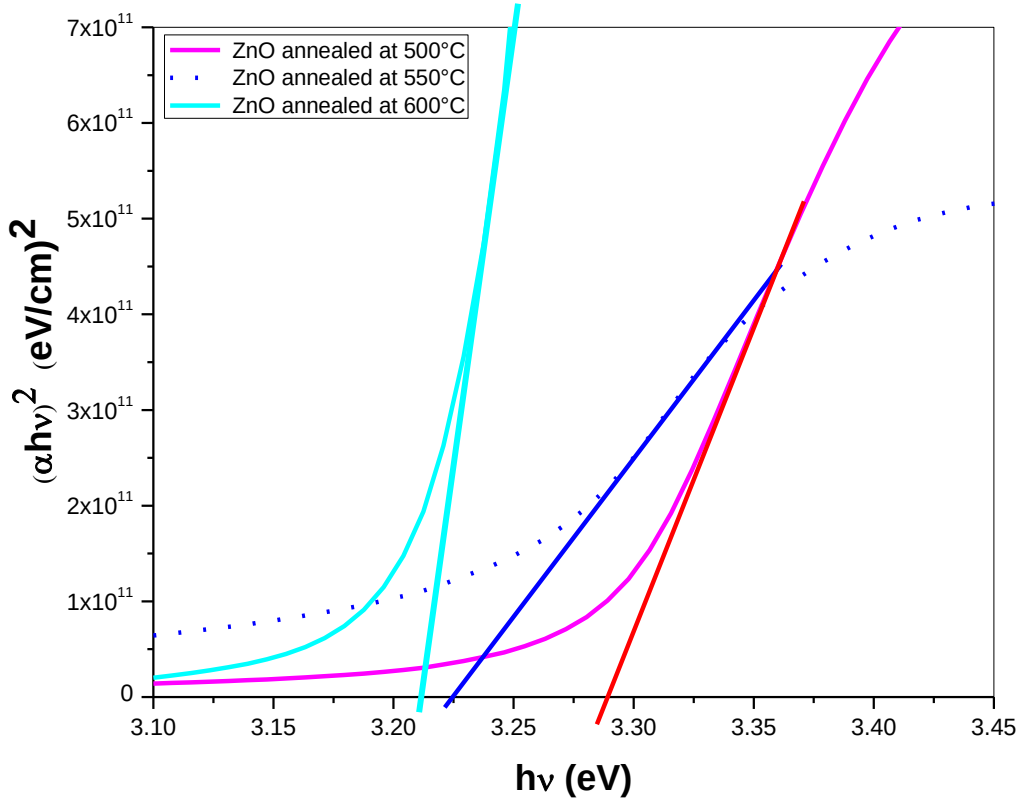

Fig.V.9 transmittance spectra of ZnO thin films.

V.3.4. Electrical resistivity

Figure.V.10 represents the variation of electrical resistivity of ZnO thin films as a function of annealing temperature. It can be seen the electrical resistivity decreases with increasing the annealing temperature. The decrease of electrical resistivity can be explained by increasing of zinc oxidation due to improve of films crystallinity attributed to the increase of annealing temperature until 550 °C. the films annealed at 600 °C have a columnar grains, the electron transferring becomes difficult, and therefore the resistivity of the sample increases again[106].

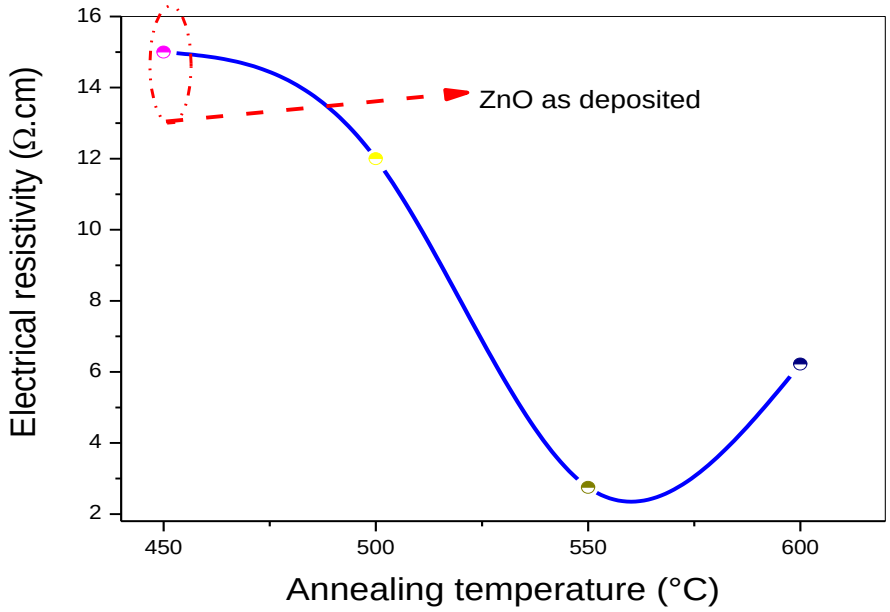

Fig.V.10 electrical resistivity of ZnO thin films as a function of annealing temperature.

Table.V.5 the important obtained results of studied parameters on ZnO thin films properties

Studied parameters	Resistivity ($\Omega.cm$)	Optical band gap (eV)	Maximum visible transmittance (%)	Maximum grain size (nm)	Film thickness (nm)	Structure and preferred orientation
solution flow rate	$1.59.10^{-2}$ - 43	3.27 - 3.28	~ 89	~36.7	86-800	**Hexagonal type wurtzite**
						Along to (002) plane at 50 ml/h
Solution concentration	$1.1.10^{-2}$ - $8.1.10^{-2}$	3.26 - 3.29	~ 89	~46.7 at 0.15 mol/l	770 - 1850	**Hexagonal type wurtzite**
						Along to (100) plane at 0.2 ml/h
Substrate temperature	0.82-20	3.1-3.2	~ 89.5	~71	110-695	**Hexagonal type wurtzite**
						Along to (002) plane at 450 °C
Tin doping concentration	10^{-2} - 43	3.21-3.25	~ 88	~39	200-800	**Hexagonal type wurtzite**
						Along to (002) plane at 3.10^{-3} mol/l
Annealing temperature	2.75 -15	3.2 - 3.28	~ 95 at 600 °C	~ 46	280-630	**Hexagonal type wurtzite**
						Along to (002) plane at 550 °C

General conclusion and future work.

The original objective of this project was to produce transparent conducting films of ZnO by ultrasonic spray pyrolysis process (USP). our work in this project had concentrated on the use of· zinc acetate as a precursor. For this, we are modified some parameters such as solution flow rate, solution concentration, substrate temperature (Ts), tin doping and annealing temperature. The elaborated thin films were prepared in thin films laboratory in the material science Department, University of biskra. The obtained results shows that the films of ZnO were elaborated have been structured at hexagonal shape. For the undoped films were deposited at deferent values of solution flow rate varying from 50 ml/h to 150 ml/h. the crystallite size decreases from 36.79 nm to 19.97 nm due to the increase of compressive stress. The films have a good transmittance in visible rang around to 80%. The optical band gap increase from 3.27 eV to 3.28 eV. The electrical resistivity varied between $1.59 \times 10^{-2} \Omega.cm$ to $43\ \Omega.cm$. for the films deposited at 50 ml/h with varying the solution concentration, the preferred orientation of crystallites changed from (002) plane to (100) plane. The latter leads to increase the crystallite size reach to 46.7 nm. A maximum value of visible transmittance equal to 88 % is observed in the sample prepared when the solution concentration equal to 0.1 mol/l (the film thickness equal to 580 nm). The resistivity increases from 1.1 x $10^{-1}\Omega$.cm to 8.1 x $10^{-1}\Omega$.cm. For the films deposited with varying the substrate temperature from 250 °C to 500 °C. We are founded that the grain size increase from 27.56 nm to 71.09 nm. The optical transparency reach to 89% in the film deposited at 450 °C. The resistivity decreases from 20 Ω.cm to 8.2 x $10^{-1}\Omega$.cm. The elaboration of ZnO thin films with changing tin concentration (tin doping) displays that the crystalline state is improved with increasing the tin concentration in elaborated film.

The grain size increase from 12.85 nm to 39.18 nm. The optical transmittance and optical band gap of the films are decreased with increasing the tin concentration. The electrical resistivity decreases from 43 Ω.cm to 1.2 x 10^{-2}Ω.cm. the studied of annealing temperature shows that the crystalline state of elaborated films improved with increasing the annealing temperature until 550°C. The crystallite size varied between 12.85 nm to 46.94 nm. The elaborated films have a good optical transparency in visible rang. The optical band gap varied between 3.20 eV and 3.28 eV. The electrical resistivity varied between 2.75 Ω.cm and 15 Ω.cm.

Depending on the results of the current study we found that ZnO thin films elaborated at low value of solution flow rate (50 ml/h) are more appropriate for use as transparent oxide front layer in solar cells application. However, the films deposited at deposition temperature equal to 450 °C treated at 550 °C are more suitable for applications as electrodes in solar cells.

According to the above results, the poor properties for the ZnO thin films are mostly due to the amount of oxygen atoms in the elaborated films. So the amount of oxygen plays a mainly role onto sprayed zinc oxide thin films properties. Our future work is trying to find a way to improve the properties of the ZnO thin films, i.e. to control the amount of oxygen including into the films.

[1] C. Klingshirn, ZnO : Material, Physics and Applications. Chem Phys Chem, 8(6) (2007) 782-803.

[2] D.R. Lide, CRC Handbook of Chemistry and Physics. 82 ed. 2001/2, LLC: CRC Press. 4-134.

[3] C.W. Bunn, The lattice-dimensions of zinc oxide. Proceedings of the Physical Society, 47(5) (1935) 835-842.

[4] D.R. Clarke, Varistor Ceramics. J. Am. Ceram. Soc., 82(3) (1999) 485-502.

[5]K.Wasa, M. Kitabatake, H. Adachi, Thin Film Materials Technology: sputtering of compound materials (2004).

[6] W.A. Bryant, The fundamentals of chemical vapour deposition, Journal ofMaterials Science, 12 (7) (1977) 1285-1306.

[7] R.N. Ghoshtagore, Mechanism of CVD Thin Film $Sn0_2$ Formation, Journal of the Electrochemical Society, 125 (l) (1978) 110-117.

[8] T. Suntola, Atomic layer epitaxy, Thin Solid Films, 216 (1) (1992) 84-89.

[9] R.R. Chamberlin, J.S. Skarman, Chemical Spray Deposition Process for Inorganic Films, Journal of Electrochemical Society, 113(1) (1966) 86-89.

[10] C.J. Brinker, A.J. Hurd, G.C. Frye, K.J. Ward , CS. Ashley, Sol-Gel Thin Film Formation, Journal of Non-Crystalline Solids, 121 (1-3) (1990) 294-302.

[11] C.C. Chen, M.M. Nasrallah, H.U. Anderson, Synthesis and Characterization of (Ce02) o.8 (SmOi.5) o.2 thin Films from polymeric precursors, Journal of the Electrochemical Society, 140 (12) (1993) 3555-3560.

[12] C.J. Brinker, G.C. Frye, AJ. Hurd, CS. Ashley, Fundamentals of Sol-Gel Dip Coating, Thin Solid Films, 201 (1) (1991) 97-108.

[13] J.M. Mochel, US Patent 2,564,707, electrically conducting coating on glass and other ceramic bodies (1951).

[14] J.E. Hill, R.R. Chamberlin, Process for Making Conductive Film, US Patent 3,148,084, (1964).

[15]. S. Sun, C. Murray, D. Weller, L. Folks, A. Moser, Monodisperse FePt nanoparticles and ferromagnetic FePt nanocrystal superlattices. Science, 287 (2000) 1989–1992.

[16] C. T. Black, C. B. Murray, R. L. Sandstrom, S. Sun, Spin-dependent tunneling in self-assembled cobalt-nanocrystal superlattices. Science, 290 (2000) 1131–1134.

[17] E. V. Shevchenko, D. V. Talapin, N. A.Kotov, S. O'Brien, C. B. Murray, structural diversity in binary nanoparticle superlattices, Nature, 439, (2006)55–59.

[18] Venables, J. A. Introduction to Surface and Thin Film Processes; Cambridge University Press, 2000.

[19] Pimpinelli, A.; Villain, J. Physics of Crystal Growth; Cambridge University Press, 1999.

[20] Freund, L. B.; Suresh, S. Thin Film Materials: Stress, Defect Formation and Surface Evolution; Cambridge University Press, 2003.

[21] Bishop, K. J. M.; Wilmer, C. E.; Soh, S.; Grzybowski, B. A. Nanoscale Forces and Their Uses in Self-assembly. Small 2009, 5, 1600–30.

[22] S. Brochen, electrical properties of ZnO single crystale, doctoral thesis, Grenoble University (2006).

[23]T. V. VIMALKUMAR, Highly conductive and transparent ZnO thin film using Chemical Spray Pyrolysis technique: Effect of doping and deposition parameters, doctoral thesis, Cochin University of Science and Technology, Kerala, India (2011).

[24] C. Ruiqun, Synthesis of zinc oxide nanostructures by wet oxidation process, doctoral thesis, Auckland University, (2011).

[25]A. J. C. Fiddes, Deposition of zinc oxide by spray pyrolysis, doctoral thesis, Durham University, (1993).

[26] O. Dulub, LA. Boatner, U. Diebold, STM study of the geometric and electronic structure of ZnO(0001)-Zn, (000-1)-O, (10-10), and (11-20) surfaces, Surf. Sci. 519 201(2002).

[27] B. Meyer, D. Marx, Density-functional study of the structure and stability of ZnO surfaces, Phys. Rev. B 67 035403(2003).

[28] A. Hafdallah, Etude du dopage des couches minces de ZnO élaborées par spray Ultrasonique, Magister thesis, Université of Constantine, (2005).

[29] A. Janotti, CG. Vande Walle, Native point defects in ZnO. Phys Rev B 76 (2007) 165202.

[30] M.D. Mc Cluskey, SJ. Jokela Defects in ZnO. J Appl Phys 2009;106:071101.

[31]R.Vidya, P. Ravindran, H. Fjellvåg, B.G. Svensson, E. Monakhov, M.Ganchenkova, Energetics of intrinsic defects and their complexes in ZnO investigated by density functional calculations. Phys Rev B 83 (2011) 045206.

[32] B.X. Lin, Z.X. Fu, Y.B. Jia, Green luminescent centerinun doped zinc oxide films deposited on silicon substrates, Appl Phys Lett 79 (2001) 943.

[33] T. Prasada Rao ,M.C. Santhosh Kumar ,A. Safarulla, V. Ganesan, S.R. Barman, C. Sanjeeviraja Physica B 405 (2010) 2226–2231

[34]R.Ghosh, D.Bask, S.Fujihara, Effect of substrate-induced strain on the structural, electrical, and optical properties of polycrystalline ZnO thin films, J.Appl.Phys.96 (2004) 2689.

[35]J.E. Jaffe, J.A. Snyder, Z. Lin, A.C. Hess, LDA and GGA calculations for high-pressure phase transitions in ZnO and MgO. Physical Review B, 62(3) (2000) 1660.

[36] D. Vogel, P. Krüger, J. Pollmann, Ab initio electronic-structure calculations for II-VI semiconductors using self-interaction-corrected pseudo-potentials. Physical Review B, 52(20) (1995) R14316.

[37] M. Usuda, N. Hamada, T. Kotani, M. van Schilfgaarde, All-electron GW calculation based on the LAPW method: Application to wurtzite ZnO, Physical Review B, 66(12) (2002) 125101.

[38]U. Ozgur, , Y.I. Alivov, C. Liu, A. Teke, A comprehensive review of ZnO materials and devices. Journal of Applied Physics, 98(4) (2005).

[39] B.K. Meyer, H. Alves, D.M. Hofmann, W. Kriegseis, Bound exciton and donor-acceptor pair recombinations in ZnO. physica status solidi (b), 241(2) (2004) 231-260.

[40] I. Ivanov, J. Pollmann, Electronic structure of ideal and relaxed surfaces of ZnO: A prototype ionic wurtzite semiconductor and its surface properties. Physical Review B, 24(12) (1981) 7275.

[41]A. Janotti, C.G.Vande Walle. «Fundamentals of zinc oxide as a semiconductor». Reports on Progress in Physics 72.12 (2009) 126501.

[42] A.F. Kohan, G. Ceder, D. Morgan, C.G. Van de Walle, First-principles study of native point defects in ZnO. Physical Review B, 61(22) (2000) 15019.

[43] C.G. Van de Walle, Hydrogen as a Cause of Doping in Zinc Oxide. Physical Review Letters, 85(5) (2000) 1012.

[44] F. Oba, S.R. Nishitani, S. Isotani, H. Adachi, Energetics of native defects in ZnO. Journal of Applied Physics, 90(2) (2001) 824-828.

[45] S.B. Zhang, S.H. Wei, A. Zunger, Intrinsic n-type versus p-type doping asymmetry and the defect physics of ZnO. Physical Review B, 63(7) (2001) 075205.

[46] D.C.Look, J.W. Hemsky, J.R. Sizelove, Residual Native Shallow Donor in ZnO. Physical Review Letters, 82(12) (1999) 2552.

[47] H.L. Ma, Z.W. Liu, D.C. Zeng, M.L. Zhong, H.Y. Yu, E. Mikmekova, Nanostructured ZnO films with various morphologies prepared by ultrasonic spray pyrolysis and its growing process Applied Surface Science 283 (2013) 1006–1011.

[48] A. Das, D.Y. Wang, A. Leuteritz, K. Subramaniam, H.C. Greenwell, U. Wagenknecht, G. Heinrich, Preparation of zinc oxide free, transparent rubber nano-composites using a layered double hydroxide filler. J. Mater. Chem. 21 (2011) 7194–7200.

[49] U.K. Mandal, D.K. Tripathy, S.K. De, Dynamic mechanical spectroscopic studies on plasticization of an ionic elastomer based on carboxylated nitrile rubber by ammonia. Polymer 37 (1996) 5739–5742.

[50] L. Ibarra, A.M. Fernandez, M. Alzorriz, Mechanistic approach to the curing of carboxylated nitrile rubber (XNBR) by zinc peroxide/zinc oxide. Polymer 43 (2002) 1649–1655.

[51]H. Liu, D. Yang, H. Yang, H. Zhang, W. Zhang, Y. Fang, Z. Liu, L. Tian, B. Lin, J. Yan, Comparative study of respiratory tract immune toxicity induced by three sterilization nanoparticles: Silver, zinc oxide and titanium oxide. J. Hazard. Mater, 248 (2013) 478–486.

[52]M. Mirhosseini, F. Firouzabadi, Antibacterial activity of zinc oxide nanoparticle suspensions on food-borne pathogens. Int. J. Dairy Technol, 65 (2012) 1–5.

[53] P. Mason, Journal of Physiological and medicinal zinc. Pharm. 276 (2006) 271–274.

[54] Y. Liu, J. Zhou, A. Larbot, M. Persin, Preparation and characterization of nano-zinc oxide. Mater. Process. Technol. 189 (2007) 379–383.

[55] K.D Gunaratne, C. Berkdemir, C.L. Harmon, A.W. Castelman, Investigating the relative stabilities and electronic properties of small zinc oxide clusters. J. Phys. Chem. A 116 (2012) 12429–12437.

[56] Y.C. Kong, D.P. Yu, B. Zhang, W. Fang, S.Q. Feng, Ultraviolet-emitting ZnO nanowires synthesized by a physical vapor deposition approach. Appl. Phys. Lett. 78 (2001) 407–409.

[57]S. Venkatesh, K. Jeganthan, Investigations on the growth and characterization of vertically aligned zinc oxide nanowires by radio frequency magnetron sputtering. J. Solid State Chem, 200 (2013) 84–89.

[58] M.Purica, E. Budianu, E. Rusu, ZnO thin films on semiconductors substrate for large area photo-detector applications. Thin Solid Films 383 (2001) 284–286.

[59] T.Aoki, Y. Hatannaka, D.C. Look, ZnO diode fabricated by excimer-laser doping. Appl. Phys. Lett. 76 (2000) 3257–3258.

[60] C.R. Gorla, N.W. Emanetoglu, S. Liang, W.E. Mayo,; Y. Lu, M. Wraback, H. Shen, Structural, optical and surface acoustic wave properties of epitaxial ZnO films grown on (011 over-bar 2) sapphire by metalorganic chemical vapor deposition. J. Appl. Phys. 85 (1999) 2595–2602.

[61] S.H. Jo, J.Y.Lao, Z.F. Ren, R.A. Farrer, T. Baldacchini, J.T. Fourkas, Field-emission studies on thin films of zinc oxides nanowires. Appl. Phys. Lett. 83 (2003) 4821–4823.

[62]M.S. Arnold, P. Avouris, Z.W. Pan,; Z.L. Wang, Field-effect transistors based on single semiconducting oxide nanobelts. J. Phys. Chem. 107 (2003) 659–663.

[63] W.Water, S.E. Chen, T.H. Meen, L.W. Ji, ZnO thin film with nanorod arrays applied to fluid sensor. Ultrasonics 52 (2012) 747–752.

[64] H.Q. Yan, R.R. He, J. Johnson, M. Law, R.J. Saykally, P.Yang, Dendritic nanowire ultraviolet laser array. J. Am. Chem. Soc. 125 (2003) 4728–4729.

[65] N. Senoussaoui, M. Krause, J. Müller, E. Bunte, T. Brammer, H. Stiebig, Thin-film solar cells with periodic grating coupler. Thin Solid Films 397 (2004) 451–452.

[66] S. Roy, S. Basu, Improved zinc oxide films for gas sensor applications. Bull. Mater. Sci. 25 (2002) 513–515.

[67] C. Tsonos, A. Kanapitsas, D. Triantis, C. Anastasiadis, I. Stavrakas, P. Pissis, E. Neagu, Interface states and MWS polarization contributions to the dielectric response of low voltage ZnO varistor. Ceram. Int. 37 (2011) 207–214.

[68]Y. Tu, J. He, Q. Wang, M. Liu, G. L. Xu, Ding, Measurement of thermally stimulated current in ZnO varistor. Proc. CSEE 30 (2010) 116–121.

[69] N. Jain, A. Bhargava, J. Panwar, Enhanced photocatalytic degradation of methylene blue using biologically synthesized "protein-capped" ZnO nanoparticles. Chem. Eng. J. 243 (2014) 549–555.

[70] S.M. Lam, J.C. Sin, A.Z. Abdullah, A.R. Mohamed, Degradation of wastewaters containing organic dyes photocatalyzed by zinc oxide: A review. Desalin. Water Treat. 41 (2012) 131–169.

[71] T.J. Kuo, C.N. Lin, C.L. Kuo, M.H. Huang, Growth of ultralong ZnO nanowires on silicon substrates by vapor transport and their use as recyclable photocatalysts. Chem. Mater. 19 (2007) 5143–5147.

[72] S. J. Darzi, A.R. Mahjoub, Investigation of phase transformations and photocatalytic properties of sol–gel prepared nanostructured ZnO/TiO2 composites. J. Alloy. Compd. 486 (2009) 805–808.

[73]C. Hariharan, Photocatalytic degradation of organic contaminants in water by ZnO nanoparticles: Revisited. Appl. Catal. A Gen. 304 (2006) 55–61.

[74] Q.Xiao, L.L. Ouyang, Photocatalytic photodegradation of xanthate over Zn1−xMnxO under visible light irradiation. J. Alloy. Compd. 479 (2009) L4–L7.

[75] M. Bizarro, High photocatalytic activity of ZnO and ZnO:Al nanostructured films deposited by spray pyrolysis. Appl. Catal. B Environ. 97 (2010) 198–203.

[76] J.M.Mochel, U S Patent 2 564,707(1951).

[77] J.E.Hilland R.R.Chamberlin, USPatent3, 148,084(1964).

[78] A.R.Balkenende, A.Bogaerts, J.J.Scholtz, R.R.M.Tijburg, andH.X.Willems, Philips

Journal of Research, 50 365 (1996) (3–4).

[79] S.P.S.Aryaand, H.E.Hintermann, Thin Solid Films, 193, 841(1990) (1–2).

[80]C.H.Chen, E.M.Kelder, P.J.J.M.vanderPut, J.Schoonman, J. Mater.Chem., 6 (5), 765 (1996).

[81] K. Seshan, Handbook of thin-film deposition processes and techniques, Second Edition, william andrew publishing, Norwich, New York, U.S.A. (2002).

[82]D. Perednis, Thin film deposition by spray pyrolysis and the application in solid oxide fuel cells, Dissertation, Eidgenossische Technische Hochschule (ETH) Zurich, (2003).

[83] .J.C.Viguie, J.Spitz, J. Electrochem.Soc., 122(4), 585 (1975).

[84]W.Siefert, Thin Solid Films, 120 (1984) 275–282.

[85]I.B. Kherchachi, H.Saidi, A. Attaf, N. Attaf, A. bouhdjar, H. bendjdidi Y. Benkhetta, R. Azizi M. Jlassi. Influence of solution flow rate on the properties of SnS_2 films prepared by ultrasonic spray. Optik 127 (2016) 4043–4046

[86] M. Mazhdi, J. Saydi, M. Karimi, J. Seidi, F. Mazhdi, A study on optical, photo-luminescence and thermoluminescence properties of ZnO and Mn doped-ZnO nanocrystalline particles, Optik 124 (2013) 4128–4133.

[85] T. Otto, W. Habicht, E. Dinjus, M. Zimmerman, Catalyst Characterization with FESEM/EDX by the Example of Silver-Catalyzed Epoxidation of 1, 3-Butadiene," in Scanning Electron Microscopy (2012).

[86]K.L.Chopra, Thin Film Phenomena, McGraw-Hill, New York, (1969) 734–735.

[87]S.Major, A.Banerjee, K.L.Chopra, K.C.Nagpal, Thin Solid Films 143 (1986) 19.

[88] G.Shanmuganathan ,I.B.ShameemBanu ,S.Krishnan ,B.Ranganathan, Journal of Alloys and Compounds 562 (2013) 187–193.

[89] A. Bouraiou, M.S.Aida, O.Meglali, N.Attaf, Curr. Appl. Phys. 11 (2011) 1173e–1178e.

[90]N.M.Ravindra, V.K.Srivastava, Infrared Phys.19(1979)603.

[91]V.P.Gupta, N.M.Ravindra, Phys.Stat.Sol.B100 (1980)715.

[92] J. Pankov, Optical Processes in Semiconductors, London, 1971.

[93] J.N.Hodgson, Optical Absorption and Dispersion in Solids, Chapman and Hall Ltd., 11 New fetter Lane London EC 4, 1970.

[94] Joint Committee on Powder Diffraction Standards Powder Diffraction File. 1988 International Center for Diffraction: Swarthmore, PA (card 36-1451).

[95] R. Jayakrishnan, K. Mohanachandran, R. Sreekumar, C. SudhaKartha, K.P. Vijay kumar, ZnO thin Films with blue emission grown using chemical spray pyrolysis, Mater. Sci. Semicond. Process. 16 (2013) 326–331.

[96] K. Venkateswarlu, A. Chandra Bose, N. Rameshbabu, X-ray peak broadeningstudies of nano-crystalline ydroxyapatite by Williamson–Hall analysis, Physica.B 405 (2010) 4256–4261.

[97] A. Ashour, M.A. Kaid, N.Z. El-Sayed, A.A. Ibrahim, Physical properties of ZnO thin films deposited by spray pyrolysis technique, Appl. Surf. Sci. 252 (2006) 7844–7848.

[98] M. Mekhnache, A. Drici, L. Saad, Hamideche, H. Benzarouk, A. Amar, L. Cat-tin, J.C. Bernède, F.M. Guerioune, Properties of ZnO thin films deposited on (glass, ITO and ZnO:Al) substrates, Superlatt. Microstruc. 49 (2011) 510–518.

[99] C.M. Mahajan, M.G. Takwale, Intermittent spray pyrolytic growth of nanocrystalline and highly oriented transparent conducting ZnO thin films: Effect of solution spray rate, Alloys Comp. 584 (2014) 128–135.

[100] A. Mosbah, S. Abed, N. Bouhssira, M.S. Aida, E. Tomasella, Preparation of highly textured surface ZnO thin films, Mater. Sci. Eng. B. 129 (2006) 144–149.

[101] M. Caglar, S. Ilican, Y. Caglar, F. Yakuphanoglu, Electrical conductivity and optical properties of ZnO nanostructured thin film, Appl. Surf. Sci. 255 (2009) 4491–4496.

[102] T. PrasadaRao, M.C. Santhosh kumar, Effect of thickness on structural, optical and electrical properties of nanostructured ZnO thin films by spray pyrolysis,Appl. Surf. Sci. 255 (2009) 4579–4584.

[103] N.M. Ravindra, V.K. Srivastava, Variation of refractive index with energy gap in semiconductors, Infrared Phys. 19 (1979) 603–604.

[104] V.P. Gupta, N.M. Ravindra, Comments on the Moss Formula, Phys. Stat. Sol. B 100 (1980) 715–719.

[105] M. Mazilu, N. Tigau, V. Musat, Optical properties of undoped and Al-doped ZnO nanostructures grown from aqueous solution on glass substrate, Optik. Mater. 34 (2012) 1833–1838.

[106] H.L. Maa, Z.W. Liua, D.C. Zenga, M.L. Zhonga, H.Y. Yua, E. Mikmekovaa, , Appl. Surf. Sci. 283 (2013) 1006–1011.

[107] N.Fujimura, T.Nishihara, S.Goto, J.Xu, T.Ito, J.Cryst.Growth130 (1993)269.

[108] Z.K.Tang, G.K.L.Wong,P.Yu,M.Kawasaki,A.Ohtomo,H.Koinuma, Y.Segawa, Appl Phy Lett 72 (1998) 3270–3272

[109] B.Sang,A.Yamada,M.Konagai, Japanese Journal of Applied Physics 37 (Part1)(1998)L206–L208.

[110] T.PrasadaRao, M.C.Santhoshkumar, Appl.Surf.Sci.255 (2009)4579.

[111] Y. Benkhetta, A. Attaf, H. Saidi, A. Bouhdjar, H. Bendjedidi, I.B. Kherkhachi, M. Nouadji, N.Lehraki, Optik 127 (2016) 3005–3008.

[112] T.V. Vimalkumar et al, ZnO thin films, Applied Surface Science, 256 (2010) 6025–6028.

[113] J. Yan, G. Wu, W. Dai, N. Guan, L. Li, ACS Sustainable Chem. Eng. 2, 1940 (2014).

[114] D. Georgescu,L.Baia, O. Ersen, M. Baia,S.Simon, J. Raman Spectrosc. 43 7, (2012) 876–883

[115] J.I.Pankove, Optical Processes in Semiconductors, Prentice-HallInc.,Englewoord Cliffs,NJ,1971.

[116] R. Swapna, M. Ashok, G. Muralidharan, M.C. Santhosh KumarJournal of Analytical and Applied Pyrolysis 102 (2013) 68–75.

[117] M. Krunks, E. Mellikov Thin Solid Films 270 (1995) 33-36.

[118]S.Amirhaghi, V.Craciun, D.Cracium, J.Elders, I.W.Boyd, Low temperature growth Of highly transparent c-axis oriented ZnO thin films by pulsed laser Deposition, Micro-electron.Eng.25 (1994)321–326.

[119]MurugadossG2012 J.Mater.Sci.Technol. 28 587–93

[120] MalleKrunks, EnnMellikov,Thin Solid Films 270 (1995) 33-36.

[121] P.R.Benger, K.Chang, P.Bhattacharya, J.Sing, K.K.Bajaj, Appl.Phys.Lett.53 (1988)684–686.

[122] L F Koao, F B Dejene, H C Swart, Conference Paper Proceeding SAIP 2015.

[123] S.Singh,T.Ganguli,R.Kumar,R.S.Srinivasa, S.S.Major,Thin Solid Films.517 ,661(2008)

[124] A. Bedia, F.Z. Bedia, M. Aillerie, N. Maloufi, B. Benyoucef Energy Procedia74 (2015) 529 – 538.

[125]Wang Y F, Yao J H, Jia G, Lei H, 2011, Acya Physica Polonica A, 119 (3) 451-454.

[126] S.Amirhaghi,V. Cracium, D. Creacium, J. Elders and I. W. Boyd, Microelecron. Eng. 25 (1994) 321.

[127] S. Yadav Raghavendra, M. Priya, C. Pandey Avinash, Ultrasonics Sonochemistry 15(2008) 863–870.

[128] Khaldun A.Salman,Khalid Omar,Z.Hassan,Mater.Lett.68(2012)51.

[129]P.M.RatheeshKumar, K.P.SudhaKartha, Vijayakumar, J.Appl.Phys.98 (2005)023509.

[130]C.E.Benouis,M.Benhaliliba, A.SanchezJuarez,M.S.Aida,F.Chami,F.Yakuphanoglu,J.Alloys Compd.490(2010)62.

[131]MujdatCaglar, YaseminCaglar, SalihaIlican, Phys.Stat.Sol.4 (3) (2007)1337.

[132]I.Hamberg, C.G.Granvist, J.Appl.Phys.60 (11) (1986) 123.

[133] A.Zaier, A.Meftah, A.Y.Jaber, A.A.Abdelaziz, M.S.Aida Journal of King Saud University–Science (2015) 27,356–360

[134] Jamilah Husna, M. Mannir Aliyu, M. Aminul Islam, P. Chelvanathan, N. Radhw Hamzah, M. Sharafat Hossain, M.R. Karimc, Nowshad Amin Energy Procedia 25 2012 55 – 61

ABSTRACT:

Elaboration and characterization of thin layers of zinc oxide (ZnO) deposited by ultrasonic spray for photovoltaic and optoelectronic applications.

In this work we have prepared thin layers of Zinc oxide (ZnO) by ultrasonic spray technique (USP). We have modified some parameters such as the solution flow rate, the concentration of the solution, the substrate temperature (Ts), the tin concentration and the annealing temperature. The result obtained demonstrated that our ZnO films were crystallized according to the wurtzite hexagonal structure. For undoped layers deposited in deferent flow values from 50 ml / h up to 150 ml / h. the grain size decreased from 36.79 nm to 20.11 nm. The transmittance is about 80% in the visible range.

The resistivity varies from 1.59 × 10^{-2} Ω.cm up to 43Ω.cm. for thin layers elaborated in deferent concentration value.

The maximum transmittance value is 88% (the film thickness is 580 nm). The resistivity varied from 1.1 x 10^{-1}Ω.cm up to 8.1 x 10^{-1}Ω.cm. For thin layers prepared in deferent substrate temperature varied from 250 ° C to 500 ° C. The grain size was found to increase from 27.56 nm to 71.09 nm. The optical transparency is about 85%. The resistivity was decreased from 20 Ω.cm to 8.2 x 10-1Ω.cm.

For thin layers deposited from changing the tin concentration, the grain size ranged from 12.85 nm to 39.18 nm. The transmittance is about 80%. The varied electrical resistivity from 43 Ω.cm to 1.2 x 10-2Ω.cm. The study of the annealing temperature has been indicated that the crystalline state of our thin layers will improve with increasing annealing temperature. The grain size varied between 12.9 nm and 46.94 nm. The varied electrical resistivity from 2.75 Ω.cm to 15 Ω.cm.

Keywords:

Zinc oxide (ZnO), Ultrasonic spray, Solution concentration - Substrate temperature , Tin doping concentration, Annealing temperature.

Résumé ***Elaboration et caractérisation des couches minces d'oxyde de zinc(ZnO) déposées par spray ultrasonique en vue d'applications photovoltaïques et optoélectroniques.***

Dans ce travail nous avons élaboré des couches minces d'oxyde de Zinc (ZnO) par la technique de spray ultrasonique (SPU). Nous avons modifié quelque paramètres tels que, le débit de la solution, la concentration de la solution, la température du substrat (Ts), la concentration d'étain et la température de recuit. Le résultat obtenu démontrées que nos films de ZnO ont été cristallisées selon la structure hexagonale de type wurtzite. Pour les couches non-dopées déposes dans déférent valeurs du débit de 50 ml/h jusqu'à 150 ml/h. la taille des grains diminué de 36.79 nm jusqu'à 20.11 nm. La transmittance est environ 80% dans le domaine de visible. La résistivité varié de $1.59 \times 10^{-2} \Omega.cm$ jusqu'à $43\ \Omega.cm$. pour les couches minces élaborées dans déférent valeur de concentrations. La valeur maximale de transmittance est égale à 88 % (l'épaisseur du film est égale à 580 nm). La résistivité varié de 1.1 x $10^{-1}\Omega$.cm jusqu'à 8.1 x $10^{-1}\Omega$.cm. Pour les couches minces élaborées dans déférent valeur de la température du substrat varié de 250 °C to 500 °C. On a trouvées la taille des grains augmente de 27.56 nm à 71.09 nm. La transparence optique est environ de 85%. La résistivité a été diminuée de 20 Ω.cm à 8.2 x $10^{-1}\Omega$.cm. Pour les couches minces déposées à partir de changer la concentration d'étain, la taille des grains varié de 12.85 nm à 39.18 nm. La transmittance est environ de 80 %. La résistivité électrique variée de 43 Ω.cm à 1.2 x $10^{-2}\Omega$.cm. L'étude de la température de recuit a été indiquée que l'état cristallin de nos couches minces va améliorer avec l'augmentation de température du recuit. La taille des grains variée entre 12.9 nm et 46.94 nm. La résistivité électrique variée de 2.75 Ω.cm à 15 Ω.cm.

Mots clées :

Oxyde de Zinc (ZnO) - spray ultrasonique - concentration de la solution - temperature de substrat - percentage d'étain - temperature de recuit.

ملخص

تحضير وتشخيص الشرائح الرقيقة لأكسيد الزنك الموضعة بتقنية الرش فوق الصوتى من أجل التطبيقات الضوئية الكمونية والضوئية الإلكترونية.

في هذا العمل قمنا بتحضير الشرائح الرقيقة لأكسيد الزنك بتقنية الرش فوق الصوتي. غيرنا بعض العوامل مثل تدفق المحلول، تركيز المحلول، درجة حرارة المسند، نسبة القصدير ودرجة حرارة التلدين. النتائج المتحصل عليها أثبتت أن كل الشرائح قد تبلورت وفق البنية السداسية. من أجل الشرائح المحضرة بتغيير في قيم تدفق المحلول من 50 مل / سا إلى 150مل / سا. يتناقص مقاس الحبيبات من 20.11 نانو متر إلى 36.79 نانو متر. النفاذية في المجال المرئي تقارب 80 %. المقاومية تتغير من1.59×10^{-2} أوم. سم إلى 43 أوم. سم. من أجل الشرائح المحضرة بتغيير في قيم تركيز المحلول تكون القيمة الأعظمية للنفاذية 88 %. المقاومية تتغير من1.1×10^{-1} أوم. سم إلى 8.1×10^{-1} أوم.سم. من أجل الشرائح المحضرة بتغيير في درجة حرارة المسند من 250 م° إلى 500 م ° تتزايد مقاس الحبيبات من 27.56 نانو متر إلى 71.09 نانو متر وتصل قيمة النفاذية إلى 85 %. المقاومية الكهربائية تتناقص من 20 أوم. سم إلى 8.2×10^{-1} أوم. سم. عند التغيير في نسبة القصدير نجد أن مقاس الحبيبة يتغير من 12.85 نانو متر إلى 39.18 نانو متر. أما قيمة النفاذية فتصل إلى حوالي 80%. المقاومية تتغير من43 أوم. سم إلى 1.2×1^{-2}أوم.سم. دراسة تأثير درجة حرارة التلدين بينت ان الحالة البلورية لأكسيد الزنك تتحسن مع الزيادة في درجة حرارة التلدين أما مقاس الحبيبة فيتغير من 12.9 نانو متر إلى 46.94 نانو متر. المقاومية تتغير من2.75 أوم. سم إلى 15أوم.سم.

كلمات مفتاحية

أكسيد الزنك، رش فوق صوتي، تركيز المحلول، درجة حرارة المسند، نسبة القصدير، درجة حرارة التلدين.

Optik 127 (2016) 3005–3008

Contents lists available at ScienceDirect

Optik

journal homepage: www.elsevier.de/ijleo

Influence of the solution flow rate on the properties of zinc oxide (ZnO) nano-crystalline films synthesized by ultrasonic spray process

Y. Benkhetta*, A. Attaf, H. Saidi, A. Bouhdjar, H. Bendjedidi, I.B.Kherkhachi, M. Nouadji, N. Lehraki

Physics of Thin Films and Applications Laboratory, University of Biskra, BP 145 RP, 07000 Biskra, Algeria

ARTICLE INFO

Article history:
Received 30 May 2015
Accepted 22 November 2015

Keywords:
Zinc oxide, Ultrasonic spray,
Nano-crystalline films, Solution flow rate

ABSTRACT

In this paper, ZnO nano-crystalline films were synthesized onto hot glass substrates by ultrasonic spray pyrolysis technique. The solution contains zinc acetate dihydrate ($ZnC_4H_6O_4{\cdot}2H_2O$) mixed with methanol. The influence of the solution flow rate on the properties of ZnO was investigated. All films deposited were characterized by various techniques such as X-ray diffraction to determine the films structure, the scanning electron microscopy (SEM) for the morphology of the surfaces and UV–visible spectroscopy to determine the optical proprieties. The results show that ZnO nano-crystalline films have a hexagonal structure at type wurtzite. The crystallite size was varied between 36.79 and 20.11 nm, the optical transmission around 80% in visible rang and the optical band gap is varied from 3.274 to 3.282 eV.

1. Introduction

ZnO is one of the promising II–VI semiconducting materials for optoelectronics and photovoltaic applications. It is a non-toxic, n type and direct wide band gap material (E_g = 3.3 eV at 300 K) with good electrical conductivity and high optical transparency in the visible and near infrared region. [1,2]. ZnO thin films are preferred as inexpensive and stable transparent conducting oxide materiel (TCO) in solar cells as anti-reflection coatings, liquid crystal displays, surface acoustic wave devices [1,3], gas sensors [4,5],and field effect transistors [6,7]. The spray pyrolysis method is one of the many techniques, which is widely used for the deposition of ZnO thin films, it is simple, flexible, low cost and applicable for large-scale production in short time. This technique can offer expertise solution to the surface engineering research and industrial applications. It is well known, that the growth steps of film such as nucleation, condensation and subsequent growth are strongly related and largely influenced by used technique and deposition parameters. In the case of spray pyrolysis, the two major parameters which are widely influenced on film growth steps are substrate temperature which controls the particles energy and motion onto substrate and the spray's volume flux arriving to the substrate surface which is controlled by a parameter namely solution flow rate.

In present work, ZnO nano-crystalline films have been deposited by ultrasonic spray pyrolysis. Solution flow rate effect on structural, morphological, optical and electrical properties of ZnO films have been investigated.

2. Experimental details

ZnO thin films were prepared by spraying a solution containing a 0.1 M of zinc acetate dihydrate $ZnC_4H_6O_4{\cdot}2H_2O$ in absolute volume of methanol CH_3OH as a solvent on heated glass substrates using ultrasonic spray process. The substrates were chemically cleaned before the deposition. In all depositions the substrates were heated at temperature equals to 350 °C. The distance from the spray nozzle and substrate was fixed at 5 cm. The films were prepared in atmospheric pressure for 7 min as a time of deposition. The elaborated films were characterized in order to study their structural, morphological and optical properties. The structure of the films was analyzed by X-ray diffraction using D8 ADVANCE diffractometer with a Cu K-α radiation (λ = 0.15405 nm). The surface morphology was analyzed by a scanning electron microscopy (JSM6301F). The optical transmittance spectra were obtained using UV–visible spectrophotometer by using glass as reference in a wavelength range of 200–1200 nm.

3. Results and discussion

3.1. Structural properties

To investigate the crystalline quality of the ZnO thin films with various values of solution flow rate, XRD analysis is carried out and the results are shown in Fig. 1. The XRD patterns of the films

* Corresponding author. Tel.: +213 699775342.
E-mail address: benkhetta.youcef@yahoo.fr (Y. Benkhetta).

http://dx.doi.org/10.1016/j.ijleo.2015.11.236
0030-4026/

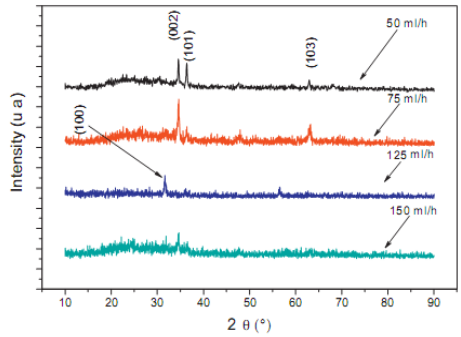

Fig. 1. The XRD pattern of ZnO thin films.

indicate that the ZnO thin films have a hexagonal structure type wurtzite corresponding to the JCPDS data card (36–1451) [8] with cell parameters $a = 0.324$ nm and $c = 0.518$ nm. It can be seen at 125 ml/h flow rate the preferential orientation of the crystallites changed from the conventional c-axis (0 0 2) orientation to the (1 0 0) orientation. The reason as to why the change of the preferred orientation took place could be explained by the oxygen content in the film [9]. When the solution flow rate equal to 150 ml/h, the intensity of (0 0 2) peak is lower than other samples. It can be explained by presence an amorphous phase in film network due to the increasing of droplets number with high velocity. In this case, the films have low cristallinity.

The crystallite size (D) of the ZnO films was calculated using the classical Scherrer formula given by [10]:

$$D = \frac{k\lambda}{\beta \cos\ \theta} \tag{1}$$

where, the constant k is the shape factor (usually equal to 0.9), λ is the wavelength of X–ray, θ is the Bragg's angle and β is the full width of the half maxima (FWHM). It is well known that the crystallite size measured by this method is usually less than the actual value. This is the consequence of internal stress and defects in deposited thin films [11]. The variation of average grain size with solution flow rate is illustrated in Fig. 2. The lattice stress in the ZnO thin films is calculated from the following relation:

$$\sigma = \left[\frac{2c_{13}^2 - (c_{11} + c_{12})c_{33}}{c_{13}}\right]\left(\frac{c_{film} - c_{bulk}}{c_{bulk}}\right) \tag{2}$$

Where, c_{bulk} is the unstrained lattice parameter of ZnO equals to 0.5206 nm, c_{film} is the lattice parameter of the strained films calculated from X-ray diffraction data and $C_{11} = 209.7$ GPa,

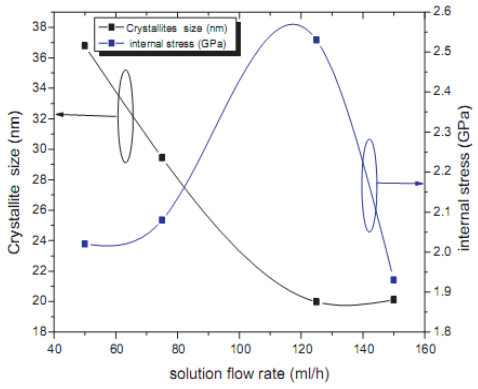

Fig. 2. Crystallite size and internal stress as function of solution flow rate.

$C_{12} = 121.1$ GPa, $C_{13} = 105.1$ GPa and $C_{33} = 210.9$ GPa are the stiffness constants of bulk ZnO. The estimated values of stress σ in the films grown at different solution flow rate are shown in Fig. 2. The positive values of estimated stress for the films indicate that the lattice constant c is lower than the unstressed bulk sample. The positive sign indicates that the films are in a state of tensile stress. It is well known that the tensile stress is likely responsible of resulting from the oxygen vacancies which exist in ZnO thin films. However, the compressive stress may be due to zinc interstitials [12]. The obtained films have a polycrystalline nanostructure; the obtained crystallite size is ranged from 36.79 to 20.11 nm. As seen that the average grain size is reduced with increasing of solution flow rate. It could be explained by increasing of stress due to the rise of internal strain in the formed crystallites. The increase of the stress can be accounted by increasing of solution particles number, which creates defects in the film network. Above 125 ml/h flow rate, we noticed a decrease of stress and an increase in the crystallite size; this can be due to the change in growth direction at this flow rate.

3.2. Morphological properties

The SEM analysis of the ZnO thin films was done to study surface morphology. The SEM images of ZnO thin film synthesized at substrate temperature equal to 350 °C with solution flow rate of 50 ml/h, 75 ml/h, 125 ml/h and 150 ml/h (Fig. 4). The SEM images show that ZnO thin films synthesized for a solution flow rate equals 50 ml/h exhibit a smooth and uniform surface (Fig. 4(a)). From the crystallite size curve, this sample has a larger grains than other samples because a few numbers of droplets with low velocity fall onto substrate surface which permit to growth the film with better way. When, we increase the solution flow rate more than 50 ml/h the film surface changed to the granular surface and the grain size decreases due to the increasing of the velocity and numbers of droplets (Fig. 4(b) – (d)). In this case, the nucleation step was fast in the film which done a film with low crystallinity.

The cross sectional images show that the film with a solution flow rate equals 50 ml/h grow parallel to the substrate surface. When, we increase the solution flow rate more than 50 ml/h, the growth has been changed from parallel to perpendicular shape due by the increasing of droplets velocity. Furthermore, the thickness of ZnO thin films increases with increasing the solution flow rate.

3.3. The deposition rate

The deposition rate of our samples was calculated by division the film thickness on the time of deposition. The experimental results show that deposition rate increases with increasing the solution flow rate (Fig. 3). This increase of deposition rate could be accounted by increasing of the solution volume sprayed onto substrate surface due to rise in the solution flow rate [13].

3.4. Optical properties

The transmittance spectra of ZnO thin films elaborated at 350 °C have shown in Fig. 5. The optical transparency equal to 80% in visible rang.

The optical band gap of ZnO thin films was calculated by the following expression:

$$(\alpha h\upsilon) = A\left(h\upsilon - E_g\right)^{\frac{1}{2}} \tag{3}$$

where, α is absorption coefficient, A is the constant independent of photon energy ($h\upsilon$), h is the Planck constant and E_g is the energy band gap of the semi- conductor equals the energy which provide an electron; in order to do a direct transition between valence and

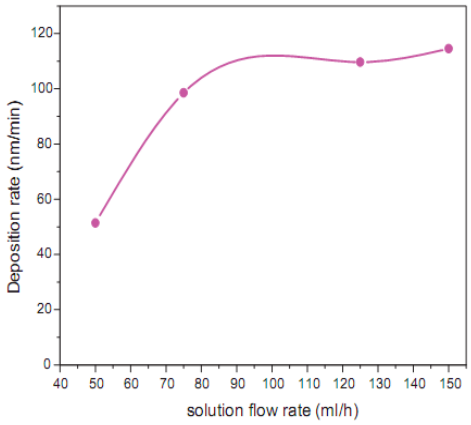

Fig. 3. Deposition rate as function of solution flow rate.

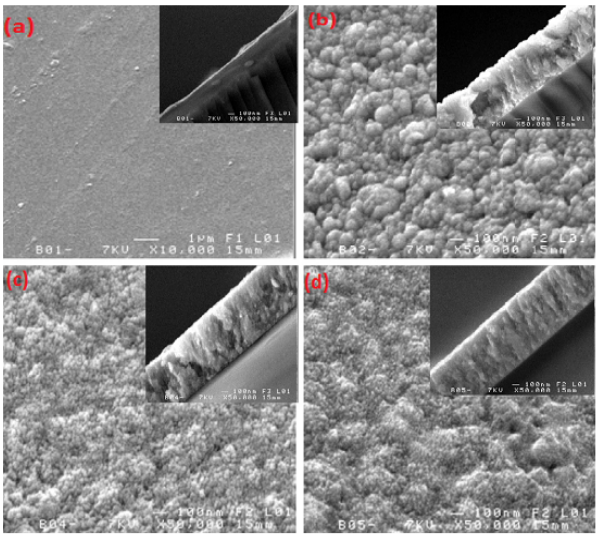

Fig. 4. The SEM images for our samples of ZnO thin films prepared at different values of solution flow rate: (a) 50 ml/h, (b) 75 ml/h, (c) 125 ml/h and (d) 150 ml/h.

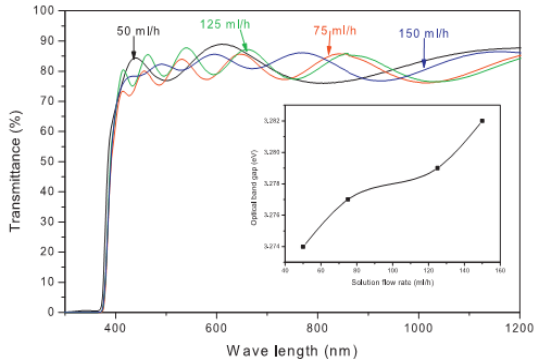

Fig. 5. Transmittance spectra and optical band gap of ZnO thin films as function of solution flow rate.

conduction bands. The value of optical band gap can be found by extrapolation of the linear region to $(\alpha h\upsilon)^2 = 0$ [14].

The optical band gap energy increases with increasing the solution flow rate (Fig. 5). It could be explained by decreases of the crystallite size [15,16] and increases of film thickness [17].

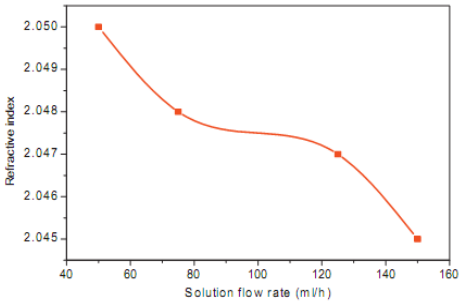

Fig. 6. Refractive index of ZnO thin films as a function of solution flow rate.

Table 1
The resistivity of ZnO thin films at different solution flow rate.

Solution flow rate (ml/h)	Crystallite size D (nm)	Resistivity ρ (Ω cm)
50	36.79	1.59×10^{-2}
75	29.44	2.6×10^{1}
125	19.97	2.7×10^{1}
150	20.11	4.3×10^{1}

The refractive index of ZnO thin films elaborated at different solution flow rate is calculated using Ravindra relation [18,19] given by:

$$n = 4.08 - 0.62 \times E_g \quad (4)$$

The values of refractive index of our samples decrease when the solution flow rate increases (Fig. 6). This decrease is attributed to increase of grains boundaries due to the decrease of the crystallite size [20].

3.5. Electrical properties

The electrical resistivity of ZnO thin films elaborated at different values of solution flow rate is illustrated in Table 1. As seen the resistivity increases with increasing the solution flow rate. This increase in electrical resistivity could be explained by reduction of crystallite size which increases the probability of grain boundary scattering [21].

4. Conclusion

In summary, we have grown ZnO thin films using ultrasonic spray at different values of solution flow rate. We found that the films are polycrystalline. The crystallite size decreases with increasing the solution flow rate. The optical transparency of our films in visible rang depending on solution flow rate.

The optical band gap increases with the solution flow rate. Finally, we conclude that the solution flow rate is the interesting factor for control the quality of the thin films deposited by ultrasonic spray.

References

[1] F. Paraguay D., W. Estrada L., D.R. Acosta N., E. Andrade, M. Miki- Yoshida, Growth structure and optical characterization of high quality ZnO thin films obtained by spray pyrolysis, Thin Solid Films 350 (1999) 192–202.
[2] S.O. Kucheyev, J.S. Williams, C. Jagadish, J. Zou, C. Evans, A.J. Nelson, A.V. Hamza, Ion-beam-produced structural defects in ZnO, Phys. Rev. B 67 (2003) 094115.
[3] B.Y. Oh, M.C. Jeong, T.H. Moon, W. Lee, J.M. Myoung, J.Y. Hwang, D.S. Seo, Transparent conductive Aldoped ZnO films for liquid crystal displays, Appl. Phys. 99 (2006) 124505–124509.
[4] H.T. Wang, B.S. Kang, F. Ren, L.C. Tien, P.W. Sadik, D.P. Norton, S.J. Pearton, JenshanLin, Hydrogen-selective sensing at room temperature with ZnO nanorods, Appl. Phys. Lett. 86 (2005) 243503.

[5] V.R. Shinde, T.P. Gujar, C.D. Lokhande, LPG sensing properties of ZnO films prepared by spray pyrolysis method: Effect of molarity of precursor solution, Sens. Actuators B 120 (2007) 551–559.
[6] Y.C. Kong, D.P. Yu, B. Zhang, S.Q. Feng, Ultraviolet-emitting ZnO nanowires synthesized by a physical vapor deposition approach, Appl. Phys. Lett. 78 (2001) 407–409.
[7] S.E. Demian, J. Mater, Optical and electrical properties of transparent conducting ZnO films prepared by spray pyrolysis, Sci. Mater. Electron 5 (1994) 360–363.
[8] Joint Committee on Powder Diffraction Standards Powder Diffraction File. 1988 International Center for Diffraction: Swarthmore, PA (card 36-1451).
[9] R. Jayakrishnan, K. Mohanachandran, R. Sreekumar, C. SudhaKartha, K.P. Vijay kumar, ZnO thin Films with blue emission grown using chemical spray pyrolysis, Mater. Sci. Semicond. Process. 16 (2013) 326–331.
[10] K. Venkateswarlu, A. Chandra Bose, N. Rameshbabu, X-ray peak broadening studies of nano-crystalline ydroxyapatite by Williamson–Hall analysis, Physica. B 405 (2010) 4256–4261.
[11] A. Ashour, M.A. Kaid, N.Z. El-Sayed, A.A. Ibrahim, Physical properties of ZnO thin films deposited by spray pyrolysis technique, Appl. Surf. Sci. 252 (2006) 7844–7848.
[12] M. Mekhnache, A. Drici, L. Saad, Hamideche, H. Benzarouk, A. Amar, L. Cattin, J.C. Bernède, F.M. Guerioune, Properties of ZnO thin films deposited on (glass, ITO and ZnO:Al) substrates, Superlatt. Microstruc. 49 (2011) 510–518.
[13] C.M. Mahajan, M.G. Takwale, Intermittent spray pyrolytic growth of nanocrystalline and highly oriented transparent conducting ZnO thin films: Effect of solution spray rate, Alloys Comp. 584 (2014) 128–135.
[14] A. Bouraiou, M.S. Aida, O. Meglali, N. Attaf, Potential effect on the properties of $CuInSe_2$ thin films deposited using two electrode system, Curr. Appl. Phys. 11 (2011) 1173–1178.
[15] A. Mosbah, S. Abed, N. Bouhssira, M.S. Aida, E. Tomasella, Preparation of highly textured surface ZnO thin films, Mater. Sci. Eng. B. 129 (2006) 144–149.
[16] M. Caglar, S. Ilican, Y. Caglar, F. Yakuphanoglu, Electrical conductivity and optical properties of ZnO nanostructured thin film, Appl. Surf. Sci. 255 (2009) 4491–4496.
[17] T. PrasadaRao, M.C. Santhoshkumar, Effect of thickness on structural, optical and electrical properties of nanostructured ZnO thin films by spray pyrolysis, Appl. Surf. Sci. 255 (2009) 4579–4584.
[18] N.M. Ravindra, V.K. Srivastava, Variation of refractive index with energy gap in semiconductors, Infrared Phys. 19 (1979) 603–604.
[19] V.P. Gupta, N.M. Ravindra, Comments on the Moss Formula, Phys. Stat. Sol. B 100 (1980) 715–719.
[20] M. Mazilu, N. Tigau, V. Musat, Optical properties of undoped and Al-doped ZnO nanostructures grown from aqueous solution on glass substrate, Optik. Mater. 34 (2012) 1833–1838.
[21] H.L. Maa, Z.W. Liua, D.C. Zenga, M.L. Zhonga, H.Y. Yua, E. Mikmekovaa, Nanostructured ZnO films with various morphologies prepared by ultrasonic spray pyrolysis and its growing process, Appl. Surf. Sci. 283 (2013) 1006–1011.

Résumé ***Elaboration et caractérisation des couches minces d'oxyde de zinc(ZnO) déposées par spray ultrasonique en vue d'applications photovoltaïques et optoélectroniques.***

Dans ce travail nous avons élaboré des couches minces d'oxyde de Zinc (ZnO) par la technique de spray ultrasonique (SPU). Nous avons modifié quelque paramètres tels que, le débit de la solution, la concentration de la solution, la température du substrat (Ts), la concentration d'étain et la température de recuit. Le résultat obtenu démontrées que nos films de ZnO ont été cristallisées selon la structure hexagonale de type wurtzite. Pour les couches non-dopées déposes dans déférent valeurs du débit de 50 ml/h jusqu'à 150 ml/h. la taille des grains diminué de 36.79 nm jusqu'à 20.11 nm. La transmittance est environ 80% dans le domaine de visible. La résistivité varié de $1.59 \times 10^{-2} \Omega.cm$ jusqu'à 43 $\Omega.cm$. pour les couches minces élaborées dans déférent valeur de concentrations. La valeur maximale de transmittance est égale à 88 % (l'épaisseur du film est égale à 580 nm). La résistivité varié de 1.1 x 10^{-1}Ω.cm jusqu'à 8.1 x 10^{-1}Ω.cm. Pour les couches minces élaborées dans déférent valeur de la température du substrat varié de 250 ºC to 500 ºC. On a trouvées la taille des grains augmente de 27.56 nm à 71.09 nm. La transparence optique est environ de 85%. La résistivité a été diminuée de 20 Ω.cm à 8.2 x 10^{-1}Ω.cm. Pour les couches minces déposées à partir de changer la concentration d'étain, la taille des grains varié de 12.85 nm à 39.18 nm. La transmittance est environ de 80 %. La résistivité électrique variée de 43 Ω.cm à 1.2 x 10^{-2}Ω.cm. L'étude de la température de recuit a été indiquée que l'état cristallin de nos couches minces va améliorer avec l'augmentation de température du recuit. La taille des grains variée entre 12.9 nm et 46.94 nm. La résistivité électrique variée de 2.75 Ω.cm à 15 Ω.cm.

Mots clées : Oxyde de Zinc (ZnO) - spray ultrasonique - concentration de la solution - temperature de substrat - percentage d'étain - temperature de recuit.

ملخص:

تحضير وتشخيص الشرائح الرقيقة لأكسيد الزنك الموضعة بتقنية الرش فوق الصوتي من أجل التطبيقات الضوئية الكمونية والضوئية الإلكترونية.

في هذا العمل قمنا بتحضير الشرائح الرقيقة لأكسيد الزنك بتقنية الرش فوق الصوتي. غيرنا بعض العوامل مثل تدفق المحلول، تركيز المحلول، درجة حرارة المسند، نسبة القصدير ودرجة حرارة التلدين. النتائج المتحصل عليها أثبتت أن كل الشرائح قد تبلورت وفق البنية السداسية. من أجل الشرائح المحضرة بتغيير في قيم تدفق المحلول من 50 مل / سا إلى 150مل / سا. يتناقص مقاس الحبيبات من 20.11 نانو متر إلى 36.79 نانو متر. النفاذية في المجال المرئي تقارب 80 %. المقاومية تتغير من1.59×10^{-2} أوم. سم إلى 43 أوم. سم. من أجل الشرائح المحضرة بتغيير في قيم تركيز المحلول تكون القيمة الأعظمية للنفاذية 88 %. المقاومية تتغير من1.1×10^{-1} أوم. سم إلى 8.1×10^{-1} أوم.سم. من أجل الشرائح المحضرة بتغيير في درجة حرارة المسند من 250 م° إلى 500 م ° تتزايد مقاس الحبيبات من 27.56 نانو متر إلى 71.09 نانو متر وتصل قيمة النفاذية إلى 85 %. المقاومية الكهربائية تتناقص من 20 أوم. سم إلى 8.2×10^{-1} أوم. سم. عند التغيير في نسبة القصدير نجد أن مقاس الحبيبة يتغير من 12.85 نانو متر إلى 39.18 نانو متر. أما قيمة النفاذية فتصل إلى حوالي 80%. المقاومية تتغير من43 أوم. سم إلى 1.2×10^{-2}أوم.سم. دراسة تأثير درجة حرارة التلدين بينت ان الحالة البلورية لأكسيد الزنك تتحسن مع الزيادة في درجة حرارة التلدين أما مقاس الحبيبة فيتغير من 12.9 نانو متر إلى 46.94 نانو متر. المقاومية تتغير من2.75 أوم. سم إلى 15أوم.سم.

كلمات مفتاحية أكسيد الزنك، رش فوق صوتي، تركيز المحلول، درجة حرارة المسند، نسبة القصدير، درجة حرارة التلدين